DERMAL APPLICATION OF PROTEINS:

DEVELOPMENT AND CHARACTERISATION OF AN APPLICATION SYSTEM

DOCTORAL THESIS

SUBMITTED IN FULFILLMENT OF THE REQUIREMENTS

FOR THE DEGREE OF

DOCTOR IN NATURAL SCIENCES

AT

KIEL UNIVERSITY, GERMANY

BY

DOROTHEA MARIE ALBOLD

KIEL 2017

Reviewer:	Prof. Dr. Hartwig Steckel
Co-Reviewer:	Prof. Dr. Thomas Kunze
Date of exam:	14.07.2017
Accepted for publication:	14.07.2017

sgd. Prof. Dr. N. Oppelt

Conference contributions:

Albold D., R. Scherließ (2016): Suitability of Microemulsions as Vehicle System for Dermal Protein Application, DPhG Annual Meeting

Albold D., R. Scherließ et al. (2015): Phospholipid-based Microemulsions for the Dermal Application of Proteins, 4th Symposium on Phospholipids in Pharmaceutical Research

Albold D., R. Scherließ et al. (2015): Evaluation of Microneedle Devices for the Application of Dermal Protein Formulations, 8th Polish-German Symposium on Pharmaceutical Sciences

Albold D., R. Scherließ et al. (2015): Evaluation of Microneedle Devices for the Application of Dermal Protein Formulations, 4th Galenus Workshop “Drug Delivery to Human Skin”

Albold D., Proksch E. et al. (2014): Formulation Development and Dermal Penetration of Biomolecules, Skin Forum

It doesn't matter if you fall down

as long as you pick something up

from the floor when you get up.

Efraim Racker

Für Edith & Albin

Erklärung gemäß § 8 der Promotionsordnung

Hiermit erkläre ich gemäß § 8 der Promotionsordnung der Mathematisch-Naturwissenschaftlichen Fakultät der Christian-Albrechts-Universität zu Kiel, dass ich die vorliegende Arbeit, abgesehen von der Beratung durch meinen Betreuer, selbstständig und ohne fremde Hilfe verfasst habe. Weiterhin habe ich keine anderen als die angegebenen Quellen oder Hilfsmittel benutzt und die den benutzten Werken wörtlich oder inhaltlich entnommenen Stellen als solche kenntlich gemacht. Die vorliegende Arbeit ist unter Einhaltung der Regel guter wissenschaftlicher Praxis entstanden und wurde bei keiner anderen Universität zur Begutachtung eingereicht.

Kiel,

_____

Dorothea Marie Albold

Table of Contents

ABSTRACT (GERMAN)

Die Entwicklung einer Zubereitung zur dermalen Applikation von Proteinen eröffnet einerseits neue therapeutische Möglichkeiten, stellt andererseits allerdings auch neue Herausforderungen an den Prozess der Formulierungsentwicklung. Neben dem hohen Molekulargewicht erschwert die hydrophile Struktur sowie die Sensibilität äußeren Einflüssen gegenüber die Verarbeitung von Proteinen und führt häufig zu einer kürzeren Haltbarkeit des Produktes. Zum Beispiel kann die hohe Hydrolyseanfälligkeit einiger Proteine zu Instabilitäten im Produkt führen und wurde exemplarisch in dieser Studie für die Familie der Kollagenasen untersucht. Um erfolgreich ein System zur dermalen Gabe zu entwickeln, muss außerdem eine gute Verträglichkeit auf der Haut gewährleistet werden können.

Mikroemulsionen (ME), oder genauer gesagt Prä-Mikroemulsionskonzentrate, wurden als sehr vielversprechende Darreichungsformen für die Verarbeitung hydrolytisch anfälliger Proteine ausgewählt. ME entstehen spontan, direkt nach der Vereinigung aller Inhaltsstoffe ohne dass zusätzlich ein hoher Energieeintrag nötig ist. Diese Eigenschaft wird genutzt, um das Protein getrennt von der hydrophilen Phase zu verarbeiten. Lipophile und hydrophile Inhaltsstoffe befinden sich in zwei voneinander getrennten Kammern, wobei das Protein suspendiert in der lipophilen Phase vorliegt. Die Vereinigung der beiden Prä-Mikroemulsionskonzentrate zur finalen ME und damit auch das Lösen des Proteins, finden erst kurz vor der Applikation auf die Haut statt. Dadurch wird die Kontaktzeit zwischen Protein und Wasser und somit auch die Gefahr der hydrolytischen Zersetzung deutlich minimiert. Für die Bildung und Stabilisierung eines ME-Systems erwies sich das Phospholipid Lipoid® S LPC 80 (Lip80) als besonders gut geeignet. Neben den selbstemulgierenden Eigenschaften verfügt es über eine gute Hautverträglichkeit und kann die Penetration von Wirkstoffen in die Haut verbessern. Lip80 ermöglichte die Ausbildung von hydrophilen ME mit einem hohen hydrophilen Anteil von 60 %. Die Stabilität der Formulierung und ihre Eigenschaften als Trägersystem für Proteine wurden mithilfe eines Modelenzyms (Katalase) im Vergleich zu einer Referenzformulierung evaluiert. Als Referenz diente dabei eine ME, die mithilfe von PEGylierten Emulgatoren stabilisiert wurde.

Da Proteine über ein hohes Molekulargewicht verfügen, sind sie nicht dazu in der Lage durch Diffusion in die Haut einzudringen. Die äußerste Schicht der Haut, die Epidermis und hier insbesondere das Stratum corneum, fungieren als Schutzschicht, die es zu überwinden gilt. Dafür können z.B. Mikronadelsysteme verwendet werden, die die obere Hautschicht durchstechen. In dieser Arbeit wurde der Dermastamp® mit einer Nadellänge von 500 µm verwendet. Der Dermastamp® wurde gemeinsam mit der Lip80-ME und der Referenz-ME in einem 3D-Hautmodell auf Verträglichkeit geprüft. Evaluiert wurde die Verträglichkeit anhand immunologischer Faktoren wie der Zytokinausschüttung (IL-1α, IL-6, IL-8), der Zellviabilität (LDH) und anhand von morphologischen Veränderungen. Da bereits die Behandlung der Haut mit dem Mikronadelsystem lokal zu minimalen Verletzungen und damit zu Reizungen führt, ist der Einsatz einer milden Formulierung umso wichtiger.

Bereits bei den Untersuchungen der Proteinstabilität und -aktivität zeigte die Lip80-ME deutlich überlegene Ergebnisse. Dieser Trend konnte auch durch die bessere Verträglichkeit im Hautmodell gegenüber der Referenzprobe bestätigt werden. Außerdem konnte durch Lip80-ME eine Abschwächung der durch das Nadelsystem zuvor erzeugten lokalen Irritation erreicht werden.

Das entwickelte System aus Dermastamp® und Lip80-ME ist somit ein vielversprechender Ansatz für die dermale Applikation von (empfindlichen) Proteinen.

ABSTRACT

The development of a dermal formulation containing a protein drug offers novel therapeutic options, but also comprises new challenges regarding the formulation development. Aspects to consider are the high molecular weight of proteins, the polarity and their sensitivity to external conditions which most often result in a short product shelf-life. Hydrolytic sensitivity can be one critical property of a protein that causes a decreased stability and hence has been examined exemplary for the family of collagenases in this study. To ensure the successful development of a vehicle system for the dermal delivery it must be tolerated well on human skin.

Microemulsions (MEs) or more precisely pre-microemulsion concentrates were chosen as promising topical formulations for hydrolytic sensitive proteins. Due to their spontaneous formation after mixing the ingredients, MEs enable a separated storage of the aqueous and the lipophilic phase in a two-chamber-system. This special composition is utilised for the protein stability as the protein is suspended in the lipophilic phase during storage and only dissolved in the aqueous part of the ME shortly before the application. Therefore, the contact time between protein and water is reduced to a minimum. For the ME formation Lipoid® S LPC 80 (Lip80) was chosen as surfactant due to its high self-emulsifying power besides the enhanced skin penetration effects and good tolerability. Formulation stability and the ability to serve as protein vehicle system were analysed with a model enzyme (catalase) in comparison to a reference ME stabilised by PEGylated surfactants.

Since proteins are high molecular weight drugs, a microneedle device supported the penetration to overcome the skin barrier. Dermastamp® (500 µm needle length) was selected and applied in combination with Lip80-ME as well as with the reference ME in tolerability studies with a 3D-full-thickness skin model. The immunological response was measured by the release of cytokines (IL-1α, IL-6, IL-8), the cell viability (LDH) and morphological changes. Microneedling is a minimal invasive procedure, stimulating a local irritation. Thus, the need for mild and well-tolerated formulations is even increased.

The stability and activity of model protein in Lip80-ME were more favourable than the reference ME. The superiority of Lip80-ME was confirmed by a lower irritation potential on reconstructed human skin. Moreover, this formulation showed the property to reduce the local irritation caused by the needle device.

To sum up, the developed combination of Dermastamp® and Lip80-ME is a promising approach in the dermal application of hydrolytically sensitive proteins.

1 INTRODUCTION AND OBJECTIVES

1.1 Introduction

Peptides and proteins have become the drugs of choice for the treatment of numerous diseases. Advances in recombinant DNA-technology, improvements in large scale fermentation, purification processes and analytical characterisations widened the field of biopharmaceutics in the last years [1,2]. Compared to smaller synthetic molecules, protein-based therapeutic agents are believed to be highly specific and selective in their action besides a great effectiveness at lower concentrations. Furthermore, proteins are degraded into amino acids, without the enhanced risk of toxic metabolites [3].

The number of protein and peptide drugs being placed on the market has been increased since 2000 [4]. Main fields of application are cancer, infections, and autoimmune diseases. To date the most feasible administration route of protein pharmaceuticals is the parenteral route. Drug degradation in the gastrointestinal tract either due to the acidic environment or enzymes and the avoidance of a first-pass effect make injections so effective. Many proteins have a short plasma half-life, thus requiring frequent injections. Therefore, alternative delivery methods that offer a more controlled release have drawn a lot of attention in research and development. Oral, nasal, transdermal and even buccal administrations are noninvasive, more patient-friendly and eliminate the need for medical assistance [5].

This thesis will focus on the administration of proteins on skin with the possibility of a local or systemic therapeutic effect. The skin, being the most accessible organ of the body with a large surface area is an attractive option for the delivery of proteins and peptides for several reasons [6]. First, it avoids first-pass degradation by the liver or gastrointestinal tract and exhibits less enzymatic activity compared to mucosal routes. Second, a sustained or extended release of the drug will provide an option to deliver proteins with short plasma half-lives reducing the application frequency [7]. Dermal delivery improves patient acceptance and compliance because it enables a more convenient as well as painless administration compared to parenteral

administration. Furthermore, it provides an alternative to oral dosing in situations with unconscious or nauseated patients [8,9].

Proteins have a hydrophilic and flexible structure with a large molecular size, which results in a negligible penetration through the intact skin [7]. Tuan-Mahmood *et al.* (2013) emphasise the excellent barrier properties of the stratum corneum (SC) against high-molecular-weight drugs (> 500 Da) [10]. Several penetration enhancement techniques have been developed to overcome the SC and facilitate the transport of proteins into the skin. Commonly used strategies like chemical penetration enhancers and encapsulation in vesicles or nanoparticles, however, are unlikely to be effective for dermal delivery of high-molecular-weight drugs. For the dermal delivery of large molecules, the additional support of physical enhancement technologies e.g. electrically assisted (iontophoresis), mechanical (skin puncture) and miscellaneous methods (laser radiation) are needed [5,11]. Until now, these innovative technologies are not well-established on the world market. Various attempts were already made especially with iontophoresis patches to deliver small molecules such as lidocaine (LidoSite®, Vyteris, US) sumatriptan (Zecuity®, Teva Pharmaceuticals, US, suspended sale and marketing) and fentanyl (Ionsys®, The Medicines Company, US/EU, only dispensed in certified hospitals) [12,12,13].

Zosano Pharma used skin microporation as a minimally invasive procedure for the development of a patch containing drug-coated microneedles capable of delivering a variety of drugs including biomolecules [14]. 3M has been working towards developing a hollow microstructured transdermal system for delivering liquid drug formulations into the skin [7]. Apart from the delivery of small molecules into and across the skin, biotherapeutics such as insulin, parathyroid hormone and vaccines have been delivered across the skin, too [15–18]. The usage of microneedles is versatile and many products are in the development stage as well as in clinical trials [19].

In this thesis, microneedle-based devices will be applied to facilitate barrier penetration, because of the easy handling and high efficacy beneath acceptable costs. The desired method involves a two-step approach, where the needles are used to puncture the skin to create micropores, followed by topical administration of a protein formulation. A topical protein-containing formulation should ensure high drug

stability, enable good solubility as well as spreading and penetration properties on patients` skin. This study will focus on the development of a topical formulation which facilitates the application of proteins with a high tendency for hydrolysis. Due to their instability in water bacterial collagenases appear to be good model proteins and will be utilised as references in this thesis.

Collagenases are endopeptidases with a molecular weight of 70-120 kDa. They play an important role in turn-over processes of connective tissue. Collagens are major fibrous components of connective tissue and are digested by collagenases in the triple helix region. There are already products on the market e.g. for the treatment of wound healing processes (topical, Iruxol®, Smith and Nephew) and Dupuytren`s contracture (i.v., Xiapex®, Pfizer). Further clinical or cosmetic applications could be conceivable as the treatment of scar tissue or to stop aging processes in skin [20,21].

Collagenases are stable as lyophilized powder over many years, whereas dissolved in an aqueous environment they show a significant loss of activity caused by autolysis [22]. Formulation development with collagenases is limited due to high costs of pure enzyme, expensive and time-consuming activity assays as well as stability analysis. To improve the efficiency and effectiveness in an early state of product development, collagenases were replaced by a model protein in this project. A molecular weight of 240 kDa (subunits 60-120 kDa), an easy, rapidly performed activity assay, besides a cheap commercially available quality make catalase a suitable model enzyme for the intended purpose [23].

A “perfect” protein delivery system should ensure a high formulation and drug stability next to a favourable tolerability at the envisaged application site. The present study is based on the dermal application of a protein system which will be supported via a microneedling process. Bernhofer *et al.* (1999) stated that products designed for topical administration need to be safe and nonirritating. So-called skin tolerability tests are often included in first development steps of pharmaceutic and cosmetic dermal products to verify a product´s mildness [24]. To examine the irritation potential of developed application system on human skin these tolerability tests will be performed in the present study, too.

Since the early 1990s engineering initiatives have been started, focusing on producing 3D *in-vitro* reconstructed human skin models. Driving force was the demand to replace animal tests in skin tolerability studies. Skin equivalents composed of human-derived epidermal keratinocytes and dermal fibroblasts are fully immunocompetent systems capable of initiating and down-regulating an inflammatory reaction in response to external stimuli [25]. For the purposes of this thesis the presence of both epidermis and dermis is essential. On the one hand the higher skin thickness facilitates the formation of microchannels, on the other hand the interplay of keratinocytes and fibroblasts is necessary for the up-regulation and production of inflammatory mediators, especially cytokines. As consequence of the absence of visible symptoms *in vitro* (erythema and oedema) it is inevitable to investigate biomarkers to assess the irritant potential of a formulation system. In addition, the release of inflammatory markers is followed by morphological alterations, representing the beginning of typical symptoms of contact dermatitis on a cellular level [26].

In short, protein drugs with their high target specificity and broad applicability have the potential to revolutionise medical therapy. Nevertheless, there is still a need for simple, reproducible strategies for the development and characterisation of protein formulations, e.g. facilitating the dermal application. Optimally, findings from this thesis can be adopted in the development of further systems and application sites. As protein stability in the vehicle system and the tolerability on human skin are first encompassing issues of dermal protein formulations, overcoming these challenges will likely lead to pharmaceutical formulations with great therapeutic potential.

1.2 Objectives

This thesis focuses on the development of a topical formulation, which enables the application of hydrolytic sensitive enzymes. Furthermore, this study is an approach to address the challenges going along with dermal protein delivery, taking a look at special requirements of these drugs regarding the vehicle system and the application route (overcome the skin barrier) besides a formulation that is well tolerated on human skin. The development of an innovative dermal application system for proteins provides new treatment options in the field of dermatology.

In order to obtain a skin-friendly formulation, mild excipients will be used. This is especially important because reducing skin barrier properties, e.g. by microneedling increases the irritation potential already. Reconstructed organotypic skin equivalents are a novel strategy to demonstrate the safety and non-irritating potential of topical products and will be utilised in this project.

To realise the objectives, three target values have to be elaborated:

The first part of this work will focus on the development and characterisation of a stable dermal formulation. Excipients have to be selected regarding their ability to form a suitable environment for the hydrophilic sensitive enzyme, enhance the penetration process and present a good tolerability on skin. The formulation will be characterised with analytical methods to demonstrate the stability of system beneath a high therapeutic activity of the incorporated protein drug.

Second, a suitable microneedle device has to be evaluated. It will be chosen based upon its effectiveness and reproducibility forming microchannels through skin *in vitro*.

In the final section of this thesis, the protein formulation will be applied in combination with the selected microneedle device on a reconstructed human skin model. Immunological markers and histological examinations will be evaluated to predict the *in vivo* tolerability on human skin.

2 PROTEINS FOR DERMAL APPLICATION

2.1 Human Skin

The skin, largest organ of the human body, comprises a surface area of approximately 1.5 m² to 2 m². It is a robust, flexible, and self-repairing barrier that protects the body from surrounding influences, harmful molecules as well as microbes. Its low permeability limits excessive water loss and helps to regulate body temperature. The skin forms an extensive sensory surface, permitting senses such as heat, cold, touch, pressure and pain [27,28].

2.1.1 Structure and Function

The ability of the skin to carry out multiple functionalities is related very closely to its structure. The skin can be divided into three main histological layers: the epidermis, the dermis and underneath the hypodermis (Figure 1).

The hypodermis or subcutaneous fat layer is characterised by irregular arranged loose connective tissue with a high proportion of adipose cells and elastin. Due to the high content of adipose tissue it acts as heat isolator and shock absorber. The hypodermis carries most blood vessels as well as nerves within the skin, and contains sensory organs. In addition to the physical support, one further function is the provision of nutrients to upper skin layers [29].

The dermis is located on top of the hypodermis with a thickness of approximately 3-5 mm, depending on its location in the body [30]. It is divided roughly into an upper "papillary" and a lower "reticular" layer. Their names reflect the composition of connective tissue besides the supply of blood vessels and nerves, respectively. Despite the greater volume, the dermis contains fewer cells than the epidermis (Figure 1).

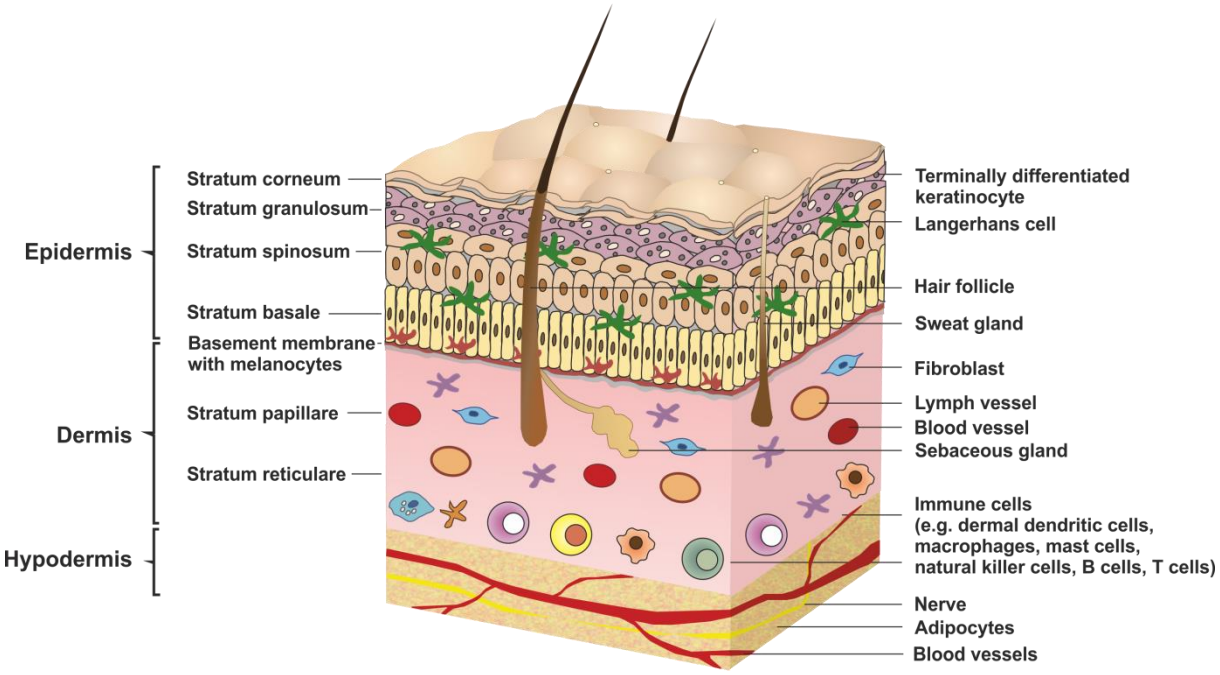

Figure 1. Schematic illustration depicting the structure of human skin. The skin is primarily composed of three layers: the epidermis, the dermis and the hypodermis. Different structures are composed of various cell populations e.g. keratinocytes, fibroblasts or immune cells. (Adapted from [11,29])

The main cell types that can be found within the skin are fibroblasts which produce and degrade extracellular matrix components. The extracellular matrix is a highly complex mixture of bioactive macromolecules which consists mainly of collagens but also of other components like elastin, fibrillin and proteoglycans. Embedded within this matrix are various structures, including nerve tissues, vascular/lymphatic systems and the base of skin appendages [31].

Collagen fibres offer a mechanical and structural stability to the skin, whilst the elastic properties are associated with the presence of elastin. As presented in Figure 1 several types of appendages are associated with the skin, e.g. hair follicles and their sebaceous glands as well as sweat glands. Sebaceous glands are formed as outgrowths of the hair follicle and secrete an oily material, the sebum, onto the skin surface. Sebum, a combination of various lipids, is a plasticiser for the stratum corneum (SC), maintaining an acidic protective mantle of pH 5 [32]. Sweat glands play an important role in the regulation of body temperature. They are responsible for the secretion and evaporation of sweat, stimulated by an increase of external temperature or emotional factors [31].

The blood vessels in the skin form a network which is responsible for the removal of toxins and waste products as well as the assistance in wound repair processes. This natural clearance can be utilised for percutaneous absorption of drugs into the systemic circulation and is additional supported by a lymphatic system [29].

The contact with an exogenous substance (e.g. microbes, chemicals) can stimulate an immune response in the skin. Immune responses originating in the skin are mounted and executed by cells and molecules of either the innate or the adaptive immune system, whereby both are consecutive events influencing each other. The innate immunity presents the first line of defence, consisting of physical (stratum corneum as two-compartment system) and chemical barriers (epithelial and antimicrobial substances or an acidic pH value of five on the epithelial surfaces), phagocytic cells (neutrophils and macrophages), natural killer cells, the complement system and cytokines. In contrast, the adaptive immunity creates immunological memory after an initial response to a specific pathogen. In case of a secondary exposure to this known pathogen (antigen) the release of specific T cell or B cell derived antibodies is heightened [27]. Good examples for the cooperation of innate and adaptive immune system are dendritic cells. They are able to take up the antigen, process it and present it to T-lymphocytes in the draining lymphoid organs. Predominantly, two types of dendritic cells can found in human skin: epidermal Langerhans cells and dermal dendritic cells (Figure 1). Subcutaneous and muscle tissue contain only few dendritic cells, whereas the dermis and the epidermis are populated by a rich network. Due to the closed network residing in dermal and epidermal layers the human skin is an ideal target for the administration of antigenic agents [18,33].

The basement membrane, a non-cellular layer separates the dermis from the outermost epidermis (Figure 1). The deepest layer of the epidermis is the basal layer or stratum germinativum, which is connected by hemidesmosomes to the basement membrane. Throughout the basal layer and higher epidermal layers, cells are connected via desmosomes. Besides basal keratinocytes, typical cells of basal layer are Merkel cells (apparent sensory functions), melanocytes (protection against damages caused by UV radiation) and Langerhans cells (immunological response) [29,31].

The epidermis is the thinnest part of the skin with a thickness ranging from 60 µm on the eyelids to 800 µm on the palms [34]. Despite the extensive vasculature present in deeper skin tissues, the epidermis is avascular and the passage of materials into, through or out of it usually occurs by diffusion across the dermal-epidermal layer [29]. Figure 1 presents the composition of epidermis divided into viable layers (stratum basale, stratum spinosum and stratum granulosum) and a non-viable layer, the stratum corneum. The viable layers are composed of keratin-producing cells, called keratinocytes. Apart from their important role in maintaining the physical barrier of the skin, keratinocytes are an active participant in the innate immunity. They can produce antimicrobial peptides, cytokines, chemokines, and arachidonic acid metabolites [27]. After keratinocyte stimulation via a danger signal, e.g. skin irritation triggered by chemicals, the production and release of cytokines increase, leading to inflammation cascades like T cell activation and modulation of Langerhans cells. The cytoplasm of keratinocytes of all epidermal layers contains the pro-inflammatory cytokine IL-1α. Upon damage it leaks from the cells and induces the expression of secondary cytokines (e.g. IL-6 and IL-8). Furthermore, neighbouring keratinocytes respond to the damage with an increased production of IL-1α, as well as IL-1β, TNF-α and IL-6 to amplify the immune response. This cellular cascade is followed by morphological alterations and may lead to typical symptoms such as oedema, erythema, itching or pain [26,35].

Keratinocytes of the basal layer have stem cell-like properties and differentiate towards the skin surface (cornification). Cell regeneration or differentiation is a complex process in the epidermis, including dehydration and polymerisation of the intracellular material, that finally produces the cells of the SC [31].

The SC or horny layer is the outermost layer of the skin. It mainly consists of dead, keratinised cells, called corneocytes. These cell layers are non-viable, yet flexible and biochemically active [30]. Classically, the SC structure can be described using a "bricks and mortar" model, the bricks representing the tightly packed corneocytes which are embedded in a mortar of lipid bilayers. The most important components of the lamellar structured lipid phase are polar ceramides. Especially the lipophilic nature and the unique architecture are responsible for the effective barrier properties of the skin against foreign substances including APIs. The permeation rate of a drug

through the SC strongly depends on its molecular weight (< 500 Da) and an adequate lipophilicity expressed as partition coefficient preferably between 1-3.5 [10,11]. Transport into or through this layer primarily occurs by two known passive diffusion processes. Firstly, the molecule passes through keratinocytes and lipids in a straight way (transcellular route). Secondly, the molecule stays in the lipid bilayer and permeates around the keratinocytes into deeper layers (intercellular route) [36]. For large molecules (> 500 Da) with a hydrophilic nature like proteins and peptides both ways are impassable. Some of these limitations, however, can be overcome by skin permeability-enhancing techniques, which will be discussed in the following section 2.1.2.

2.1.2 Strategies to Enhance Transdermal and Dermal Delivery

There are large numbers of published studies describing the perfect barrier properties of skin and the problems associated with the delivery into and through it. Transdermal delivery describes the transport of an API through the various layers of skin into the blood circulation leading to a systemic therapeutic effect, e.g. treatment of pain with fentanyl. A local effect within the skin is described with the dermal delivery of a drug, in this case systemic absorption must be kept to a minimum. It is important in the treatment of dermatological conditions such as skin cancer or psoriasis [37].

The need for strategies to overcome the SC barrier to facilitate a rapid and effective penetration of a broader range of molecules, including macromolecules is heightened. Such strategies that have emerged over the last years are summarised in Figure 2 and divided in passive and active methods [11].

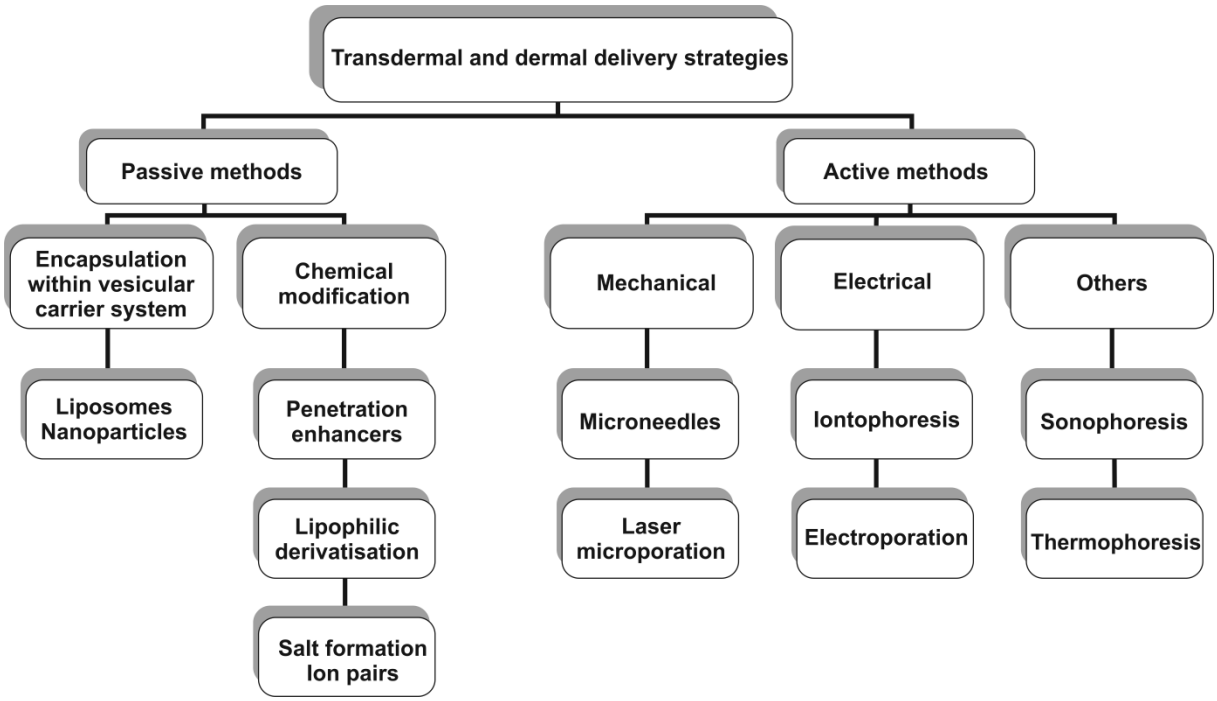

Figure 2. Overview of several strategies for enhancing transdermal and dermal delivery of macromolecules across the skin. (Adapted from [5,11])

Passive methods include the conventional way of drug application in a semisolid dosage form like a cream or gel. More recently these vehicles have been developed and modified for the transport of macromolecules such as proteins and peptides. This approach includes the encapsulation in vesicular carrier systems, e.g. liposomes, the use of penetration enhancers or chemical modifications and more lipophilic analogues [11,38]. However, the amount of drug that can be delivered is still limited because these modifications do not significantly disrupt the skin barrier. Passive delivery strategies might be only effective for the transport of small molecules (< 500 Da). Alternative enhancement technologies named as active methods, increase the penetration of the drug using physical energy or physical abruption of the SC. Prominent examples are presented in Figure 2, they use different sources of energy, e.g. small voltage constant current to push charged molecules into the skin (iontophoresis), ultrasound waves (sonophoresis) or the effect of elevated temperature (thermophoresis) to enhance the drug delivery [5].

Apart from the mentioned techniques above, an enhanced API delivery into the skin can also be achieved using microneedles (MNs). This minimal invasive procedure is

utilised in the present study to support the dermal penetration of proteins and will therefore be explained in more detail.

MNs are tiny micronised structures that pierce the SC and create microchannels for delivery of low and high molecular weight drugs. Typically, MNs range in their height from 100-1000 µm, shorter needles are not effective, because of the elastic nature of skin [29]. In case of longer MNs the risk of bleeding and pain increases, while patients` compliance decreases. Furthermore, MNs have been produced and examined in various geometries (e.g. sharp-, tapered-, conical- or bevel-tipped) as well as needle materials. Different materials exhibiting a range of properties, including metal, silicon, carbohydrates and polymers were processed for the production of MNs [10]. Figure 3, A depicts a microneedle array with 16 stainless steel needles, arranged in two rows (sample for research purposes, Dermaroller GmbH, Wolfenbüttel, Germany). Each needle has a length of 500 µm and a conical shape, tapering towards the tip (Figure 3, B).

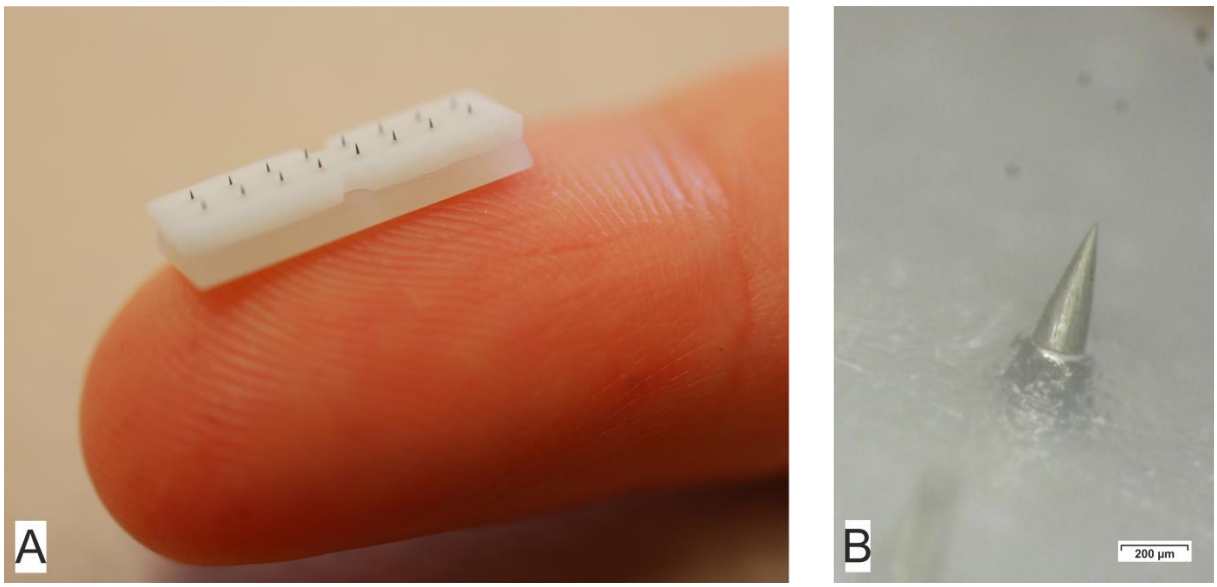

Figure 3. Sample of a microneedle array for research purposes. 16 needles (500 µm in height) are arranged in two rows (A). Image (B) presents a microscopic magnification of one microneedle with a conical shape, tapering towards the tip. (Scale bar = 200 µm)

The application of each material and shape depends on the chosen design of MN device. Generally, there are two main categories, solid or hollow MNs, with the possibility of further modifications. The use of solid MNs is also termed as "poke with patch" approach, which means upon removal of MNs, transient microchannels are

created in the skin and a drug formulation can subsequently be applied (Figure 4, A) [39]. The drug penetrates through the microchannels via passive diffusion into the skin, typically out of a reservoir like a patch or topical formulation. Ding *et al.* (2009) investigated immune responses in mice following MN-mediated transcutaneous immunisation with diphtheria toxoid as model antigen [40]. Stainless steel MNs (4 x 4, 300 µm in height) were used to pierce the mouse skin and diphtheria toxoid was administered as solution afterwards. The immune response (measured as IgG titres) was significantly higher after MN treatment [40]. Although solid MNs are versatile and easy to use there are limitations, e.g. the two-step application process which may lead to practicality issues for the end-user [10].

Figure 4, B shows solid MNs coated with a drug formulation. This modification is termed "coat and poke" and enables after piercing the deposition of drug in the skin upon dissolution of the coating material [39].

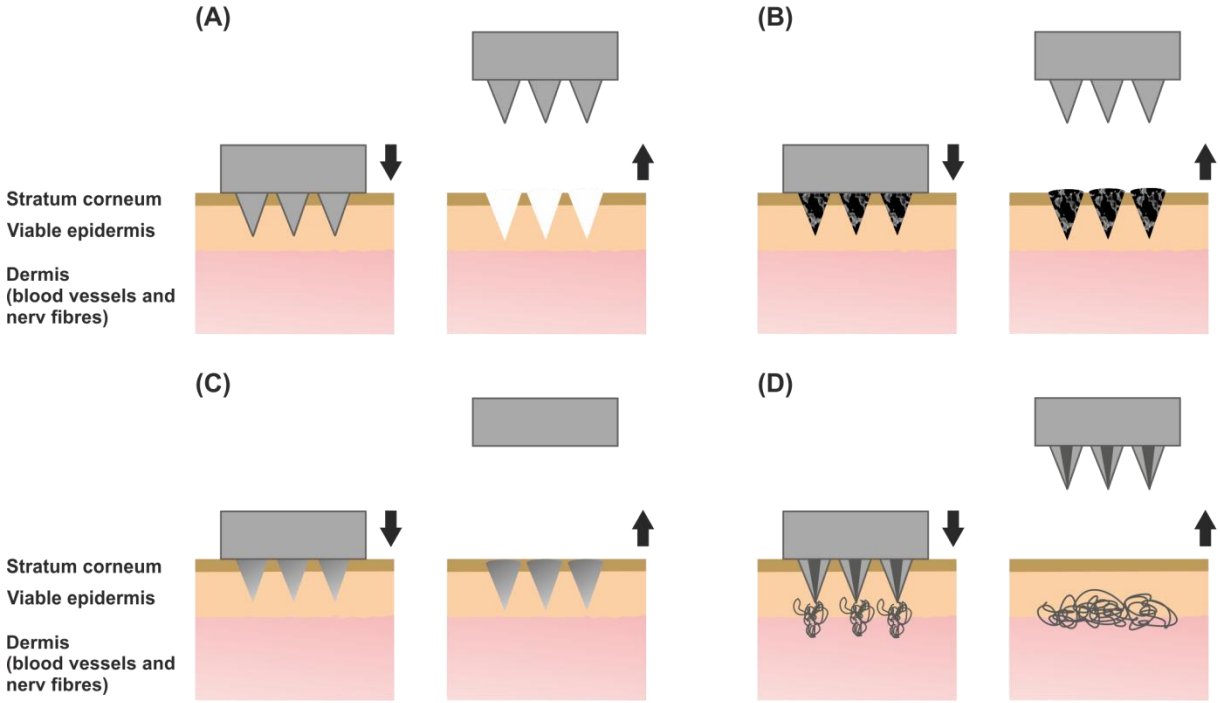

Figure 4. Schematic representation of four different MN designs. Picture (A) shows solid MNs create micro-holes into the skin, (B) MNs are coated with a drug solution, (C) MNs are dissolvable and the drug is incorporated within the needles and finally (D) depicts hollow MNs which create microchannels and facilitate an active transport of the drug solution into the skin through needle bores. (Adapted from [10,19])

Zosano Pharma (Fremont, US) developed the Macroflux® delivery system composed of titanium needles that can be coated with diverse drugs and vaccines [41,42]. This MN modification is restricted by the amount of protein/drug that can be coated onto the microneedles. Furthermore, parameters of the coating formulation such as viscosity and surface tension should be determined carefully to avoid on the one hand protein aggregation and to facilitate on the other hand an adhesion to the needle surface [43].

Another possibility to modify the type of solid MNs is the use of soluble needle materials (Figure 4, C). So-called dissolving MNs include an encapsulated API and have been fabricated primarily from polymers which are biocompatible, biodegradable and exhibit an established safety profile in medical tools [44]. Examples of materials that might be processed are polylactic acid, polyglycolic acid and carbohydrates (sugars, carboxymethyl cellulose) [44,45]. Depending on the chosen material the needles can be utilised for prolonged release of the drug. Similar to the coated MNs the use of dissolving MNs is limited to a maximum of incorporated API as well. Increasing the drug load might in turn compromise the mechanical strength of the needles. A critical point in case of incorporating thermosensitive drugs, e.g. proteins, might be the manufacturing process which might involve high temperatures (> 60 °C) necessary for melting the sugars or polymers [46,47].

Infusion of liquid drug formulations is a promising feature in the MN technology and presented in Figure 4, D [19]. Hollow MNs containing bores that offer the possibility of transporting API solutions through the needles by diffusion or by a pressure-driven flow. They facilitate the transport of higher amounts of drug compared to coated or soluble MNs. However, the volume of formulation that can be infused is limited by the back pressure from the densely packed layers of skin [48]. Tuan-Mahmood *et al.* (2013) emphasised that most studies using hollow MNs have been focused on their fabrication aspects and less on their potential in delivering compounds across the skin. The transdermal delivery of insulin into diabetic rats might be one promising example for the use of hollow MNs [49].

In general, MNs have a good patient compliance because there are less painful compared to hypodermic needles. Due to their small size, MNs are less likely to reach nerve endings in the dermis that perceive pain [19]. A frequently discussed

safety consideration regarding the puncturing of skin is the possibility that microorganism could gain access and potentially lead to infections. Channels created by hypodermic needles were reported to induce greater microbial penetration than those by MNs. Donnelly *et al.* (2009) emphasised the need for more exhaustive *in vivo* studies to conclusively demonstrate the low infection risk of MNs [50]. Additional approaches to enhance patient safety will be established by sterile or aseptic manufacture and by fabricating MNs from dissolving or biodegradable materials to prevent reuse [50].

This technology serves as an important and exciting advance in dermal and transdermal delivery techniques. The delivery of a broad range of molecules from small molecular weight drugs to large hydrophilic biopharmaceuticals such as vaccines and proteins is possible. MN devices are potential drug delivery systems that have been made by many pharmaceutical companies to line up their product portfolio as better options instead of an existing delivery systems. MN based systems like Soluvia™ by BD or Fluzon Intradermal® by Sanofi Pasteur received FDA clearance for the delivery of influenza vaccination [19]. There are still more products on the market, in clinical trials or under development. The shape and design of MN devices are versatile just as their field of application, underlining the potential as dermal/transdermal delivery systems.

2.2 Protein Stability

Protein stability is a particularly relevant issue in the pharmaceutical field and will continue to gain more importance as the number of therapeutic protein products increases. Proteins are large biomolecules of a complex architecture. They consist of one or more polypeptide chains from the serial condensation of various amino acid monomers. Amino acids are covalently bonded together in chains by peptide bonds between the amino nitrogen and the carboxyl carbon. Sequences with fewer than 20 amino acids are generally referred to as peptides, while the term polypeptide or protein is used for longer chains [51].

There are four levels of protein structure, namely primary, secondary, tertiary and quaternary. The primary structure describes the linear arranged amino acids in a

polypeptide chain. The secondary structure includes the folding of polypeptide chains into huge substructures. The structural conformation of secondary structure depends on the formation of hydrogen bonds and leads to the two main substructures, α-helix, and the β-sheet. Tertiary structure of protein is its native or functional 3D-structure. Many stabilising forces fashion the 3D-shape of a protein such as hydrophobic interactions, disulphide bridges, hydrogen bonds, and Van der Waals forces. These interactions are weak, short range and sensitive to external influences as pressure, temperature, pH and ionic strength [51].

Some proteins are made up of multiple polypeptide chains, often referred to as subunits. These protein subunits interact with each other (via hydrogen bonds, disulphide bridges, salt bridges etc.) and arrange themselves to form a larger aggregate protein complex termed as quaternary structure [52].

In living organism proteins act as transporter for ions and other molecules regulating most chemical reactions. Proteins that can catalyse biological reactions are called protein enzymes. Enzymes have a high specificity to the reaction they catalyse. This might be one property that makes them so important as diagnostic and research tools [52,53].

A protein´s structure is directly related to its function, thus anything that severely disrupts the natural structure will also disrupt the function or activity. Many proteins are structurally unstable especially in solution and are susceptible to conformational changes during manufacturing, storage, handling steps or shipping. Instabilities can be divided into chemical or physical instabilities and are mostly concomitant acting in a synergistic way, e.g. an oxidation or deamidation can increase the sensitivity to aggregation [53,54].

2.2.1 Chemical Instability

Chemical degradation involves processes that create or break covalent bonds. Chemical modifications of a protein include reactions, such as oxidation, reduction, deamidation and hydrolysis [53].

Deamidation is one of the most common chemical degradation pathway of proteins and peptides which particularly involves the hydrolysis of side chain amides

asparagine and glutamine [54]. Generated degradation products can lead to impurities and increase the immunogenicity, while they likewise decrease the bioactivity, e.g. the deamidation of peptide growth-hormone-releasing factor caused a 500-fold inactivation. Possibilities to reduce the deamidation rate in a solution might be the optimisation of the pH (generally minimised at pH 3-5) and the decrease of dielectric strength (addition of organic solvents). Furthermore, in lyophilised formulations the deamidation is reduced, because of the absence of free water where the reaction can occur [55].

Another primary chemical degradation process of proteins and peptides is the oxidation. Proteins that contain methionine, cysteine, histidine, tryptophan or tyrosine are particularly at risk to get damaged by reactive oxygen species [54]. The oxidation can alter the physicochemical characteristics of proteins like folding, subunit association and leads to physical instabilities (fragmentation or aggregation). There are several methods to minimise the oxidative degradation e.g. to control the enhancing factors (pH, temperature, light exposure, buffer conditions etc.) or to add antioxidants (ascorbic acid) and metal chelating agents (EDTA) to the protein formulation [54].

2.2.2 Physical Instability

Physical degradation includes protein unfolding, surface adsorption, aggregation and precipitation. Protein aggregation is the most common physical instability because it is encountered routinely during manufacturing, processing, storage, and shipping. For protein therapeutics, the presence of aggregates is undesirable as they may lead to an immunogenic reaction and decrease of bioactivity [56]. The impact of aggregation depends on the physicochemical attributes of each protein relative to its functional domains and natural activity. Enzymes such as catalase and urease can lose up to 50 % of their activity just after shaking due to the mechanical stress [55].

Protein aggregation is often irreversible and accompanied by large changes of secondary as well as tertiary structure which result in the loss of native structure. Physical degradation processes can influence each other. External stress including temperature, pH, removal of water, high shear and the presence of metal ions can lead to an irreversible disruption of native state of a protein and finally cause a

denaturation or unfolding. Partially unfolded protein molecules are especially prone to aggregation [53,57].

In general, protein formulations, e.g. in a dissolved state, can be stabilised against physical destabilisations by optimising the pH, ionic strength, adding sugars, amino acids and/or surfactants [55]. In many cases, nonionic surfactants such as Polysorbate 20 and Polysorbate 80 can prevent the formation of aggregates if used in concentrations below the critical micelle concentrations. Via a protein-surfactant interaction these compounds stabilise proteins by lowering the surface tension and binding to their hydrophobic sites, reducing the possibility of protein-protein interactions, which could lead to aggregations, too [58].

There are several more techniques to improve the stability of proteins in solid or dissolved state. The choice of the "right" mechanism depends on the requirements of the formulation and the nature of protein.

3 MATERIALS AND METHODS

3.1 Materials

3.1.1 Surfactants

1.1.1.1 Natural Surfactants

The group of natural surfactants is not univocally defined. Surfactants taken directly from a natural source as well as those synthesised from natural raw materials like sugars, sterols or amino acids are usually categorised as “natural”. Holmberg *et al.* (2001) emphasised that lecithin obtained from a natural source (either soybean or egg yolk) is probably the best example of a truly natural surfactant [59]. This project focused on the use of lecithins because of their versatile applications (drug and food industry) as well as their property to be well-tolerated on skin (approved as penetration enhancer and surfactant) [60].

The U.S. Pharmacopeia defines lecithins as a “complex mixture of acetone-insoluble phosphatides, which consists chiefly of phosphatidylcholine, phosphatidylethanolamine, phosphatidylinositol, and phosphatic acid, present in conjunction with various amounts of other substances such as triglycerides, fatty acids, and carbohydrates (...)” [61]. Typical for natural phospholipids is the composition of fatty acids with a polar head group (schematic representation in Figure 5, B). Lecithins are also determined by the composition of the natural starting material and the applied purification. Moreover, the chemical composition determines the properties and their application field.

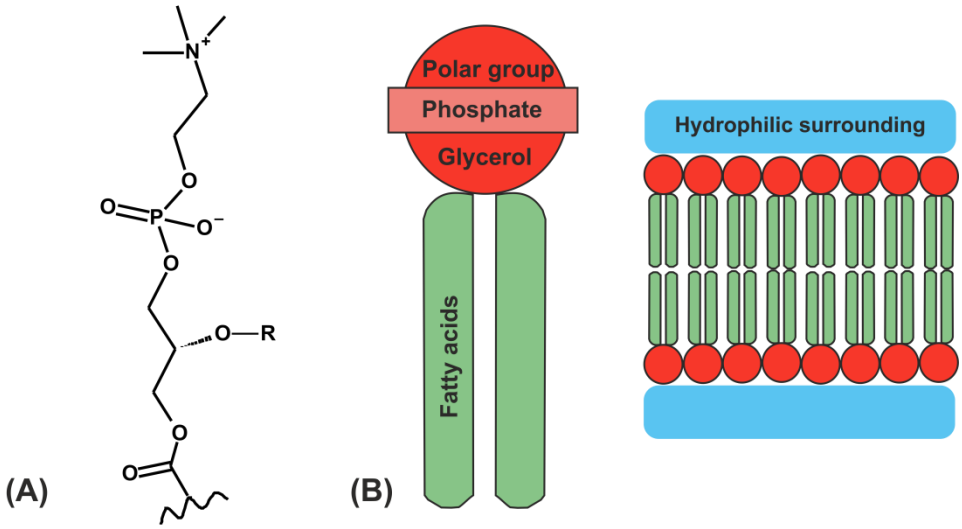

Figure 5. General lecithin structure. (A) shows a part of monoacyl phosphatidylcholine (MAPL), which is linked to one fatty acid chain (R = H) compared to diacyl phosphatidylcholine (DAPL; R = fatty acid). (B) shows a simplified model of lecithins (left) next to their arrangement in biological membranes (right).

Next to the simplified lecithin structure in Figure 5, B section A shows a part of monoacyl phosphatidylcholine (MAPL). This thesis focused on phospholipids with a higher content of MAPL besides the diacyl phosphatidylcholine (DAPL) content in the formulation development. As shown in Figure 5, A MAPL is linked to only one fatty acid chain (R = H) compared to DAPL (R = fatty acid). Hence, MAPL has a higher polarity. The higher the polarity, the higher is the self-emulsification power [62]. In present investigations, Lipoid S LPC 80 (Lip80, Lipoid GmbH, Ludwigshafen, Germany) was applied as hydrophilic representative of a phospholipid containing 80 % of MAPL.

As endogenous substances phospholipids are structural and functional components of all cell membranes (Figure 5, B). This might be the reason for their good tolerability, and the drug penetration enhancing effect on skin making phospholipids a popular group of emulsifying ingredients.

1.1.1.2 PEGylated Surfactants

The abbreviation PEG stands for polyethylene glycol which is an important structural part of many nonionic surfactants. In more detail, the term PEGylated means the covalent coupling of a PEG structure to another large molecule. Such a molecule

could be a therapeutic protein or, as in this study, a hydrophobic molecule to produce non-ionic surfactants [63]. Polyoxyl castor oil (USP/NF Polyoxyl 15 castor oil) and polyoxyethylene-20-sorbitan monooleate (USP/NF Polysorbate 80) are two representatives of the huge family of nonionic surfactants and of importance in the following experiments.

Polyoxyl 15 castor oil, also known under the trade name Kolliphor® EL (BASF SE, Ludwigshafen, Germany), is an oil-in-water emulsifier or solubiliser with a hydrophilic-lipophilic balance (HLB) value between 12 and 14. Kolliphor® EL is used in many different branches of industry. It is particular suitable as solubiliser in liquid fat-soluble vitamin solutions or hydrophobic active pharmaceutical ingredients [64].

Polysorbate 80 (Caesar & Loretz GmbH, Hilden, Germany) is reported as a very common non-ionic oil-in-water surfactant [65]. Because of its high HLB value of 16.0 it is suitable as a solubiliser for poor water-soluble drug substances in either liquid or solid dosage forms. Furthermore, Polysorbate 80 is a popular emulsifier or coemulsifier in pharmaceutical preparations like semisolids and foams [66].

Kolliphor® EL and Polysorbate 80 are promising surfactants for dermal formulation systems due to their versatile application fields and good skin tolerance [64,66].

3.1.2 Lipophilic Ingredients

In the present study, several lipid excipients from the portfolio of Gattefossé (Saint-Priest, France) were selected. Plurol Oleique® CC 497 (USP/NF Polyglyceryl-3 dioleate), Labrafac™ PG (USP/NF Propylene glycol dicaprylocaprate), Labrafac™ Lipophile WL 1349 (USP/NF Medium chain triglycerides), Peceol™ (USP/NF Glyceryl monooleate, Type 40) and Maisine™ 35-1 (USP/NF Glyceryl monolinoleate) are known examples and were utilised in the following experiments [67].

Plurol Oleique® CC 497 (PO CC 497) is classified as water-in-oil surfactant with an HLB value of 6. It is a viscous lipophilic liquid that improves the stability of emulsions as well as the solubility of drugs [68].

Labrafac™ PG, Labrafac™ Lipophile WL 1349, Peceol™ and Maisine™ 35-1 are defined as oily vehicles. In general, they are used as oily phase for topical formulations, but can also solubilise lipophilic active pharmaceutical ingredients

(APIs). Essential for this property is their surface activity with HLB values of 2 (Labrafac™ PG) and 1 (Labrafac™ Lipophile WL 1349, Peceol™ and Maisine™ 35-1), respectively [69–71].

To sum up, all these lipid excipients are high performance liquid solubilisers that can be used to improve the drug delivery in a variety of formulations (oral, topical and partly parenteral). In addition, they are characterised by a good tolerability especially on human skin [72–74].

3.1.3 Catalase

Catalase is an ubiquitous existing globular protein that can be found in almost all aerobic and anaerobic organisms, such as mammalians, plants or bacteria. It is an antioxidative enzyme which decomposes hydrogen peroxide into water and oxygen. Therefore, it plays an important role in protecting cells against reactive oxygen species [75].

Within this study, a lyophilised catalase from bovine liver (Sigma Aldrich, St. Louis, MO, US) with an activity of 2000-5000 U/mg was used. Bovine liver catalase is a tetramer (240 kDa) composed of four identical tetrahedrally arranged subunits (Figure 6). Each 60 kDa subunit contains a haeme group and NADPH in its own active side [76,77]. The secondary structure of catalase is composed of two globular domains (β-barrel and α-helical domain). The β-barrel is anti-parallel eight-stranded and includes at least six inserted α-helices in the central area, as indicated in Figure 6 [78].

All haeme-containing catalases perform the degradation of hydrogen peroxide in a two-stage catalytic mechanism. First, a molecule of hydrogen peroxide binds and oxidises the haeme to an oxyferryl species. A porphyrin cation radical is generated when one oxidation equivalent is removed from iron and, generally, one from the porphyrin ring. Then, a second hydrogen peroxide molecule binds and acts as reducing agent to regenerate the resting state enzyme, with the concomitant production of oxygen and water [78,79].

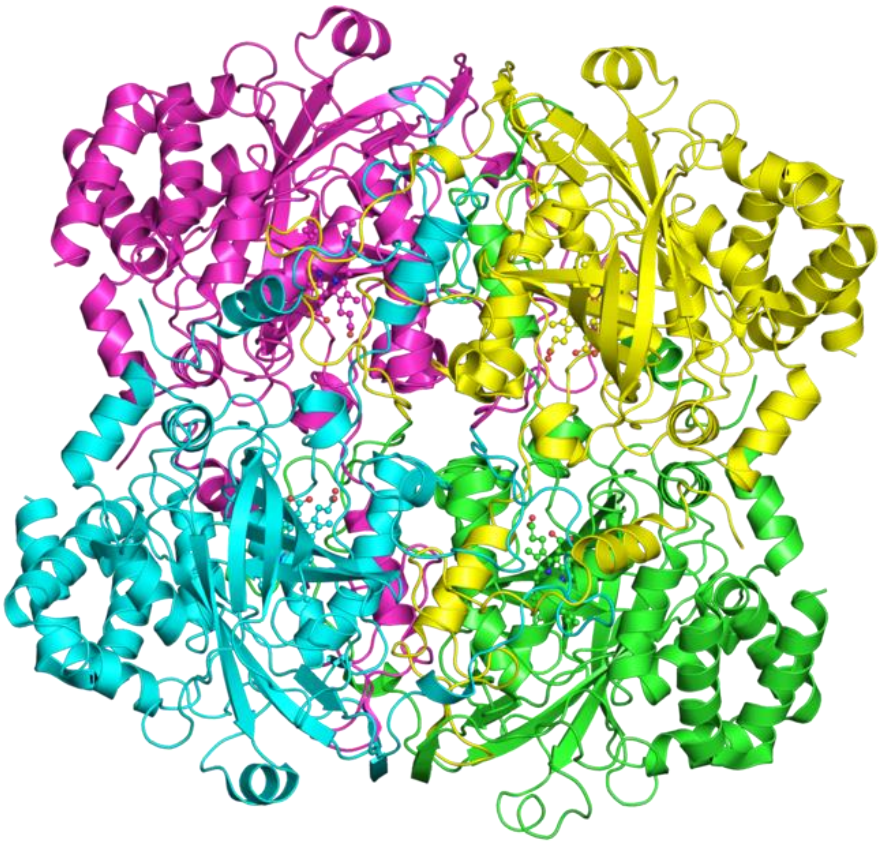

Figure 6. Crystal structure of bovine liver catalase without NADPH. The tetrameric structure is well defined by the differently coloured four subunits. (Adapted from [80])

Bovine liver catalase is insoluble near its isolelectric point of pH 5.4, and soluble outside this pH range. It is most stable in a 50 mM phosphate buffered saline (PBS) at pH 7.0. Below a pH value of four or higher than a pH of nine the three-dimensional structure changes and the enzymatic activity is considerably inhibited [81,82].

3.1.4 Microneedle Devices

Microneedling is a minimal invasive treatment of skin texture. It is already established in cosmetic and medical applications to tighten or improve skin texture as well as in scar therapy [83]. Three commercially available needle devices Dermaroller®, eDermastamp® and Dermastamp® (Dermaroller GmbH, Wolfenbüttel, Germany) were examined.

The different design of applied needle devices is shown in Figure 7 and results in a deviating handling of piercing process.

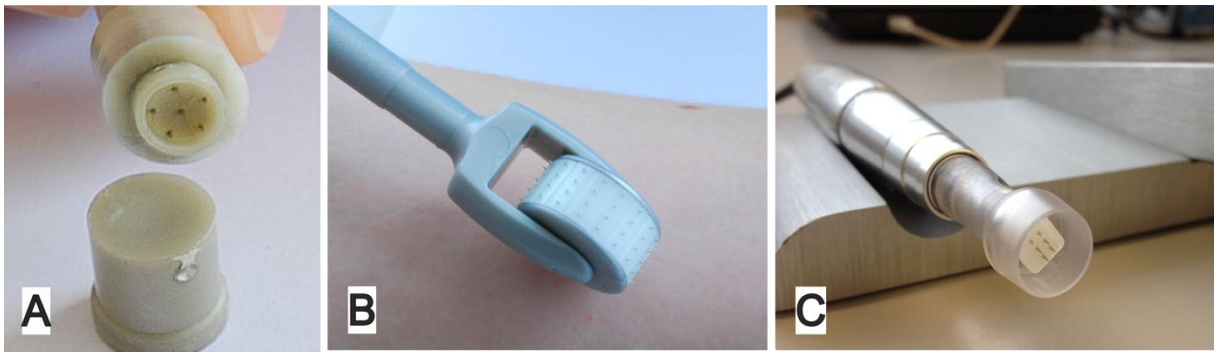

Figure 7. Overview of the three evaluated needle devices. The image (A) shows Dermastamp®, (B) Dermaroller® MC405 and (C) the electrically driven eDermastamp®. Each device has the same conically shaped needles, used with 500 µm needle length.

However, the three devices have the same conically shaped needles, made of stainless steel. In the current study, uniform needle dimensions were used (500 µm in height, 350 µm diameter at the base and 84 µm at the tip) [84]. Further technical data are summarised in Table 1.

Table 1. Summary of technical information of three applied needle devices.

Model	Available needle length	Number and arrangement of microneedles	Application
Dermaroller® MC405	fixed	72 needles, rows	rolling process
eDermastamp®	variable, adjustable by user (0-1.5 mm)	6 needles, rows	automatically driven, 50-150 pricks/min
Dermastamp®	fixed	6 needles, radial	stamping process

3.1.5 Full-Thickness Human Skin Models

The term "full-thickness human skin model" means a reconstructed skin equivalent engineered in a tissue culture insert. Full skin equivalents consist of human keratinocyte cultures grown on fibroblasts containing collagen matrices with an underlying microporous membrane ensuring contact to the cell culture media [26].

To date three commercially available reconstructed human skin models are on the market: EpiDerm™ FT (MatTek Corporation, Ashland, US), AST2000-FT (CellSystems Biotechnologie Vertrieb GmbH, Troisdorf, Germany) as well as Phenion®-FT (Henkel AG & Co. KGaA, Düsseldorf, Germany). These skin models are promising tools in versatile research topics. Furthermore, they are used by pharmaceutical, chemical and consumer product companies for a broad range of applications such as skin corrosion, -irritation and sensitisation tests are only a few examples [85].

EpiDerm™-models are most often cited, hence the user benefits from extensive experience. Therefore, in this thesis EpiDerm™ FT 400 from MatTek Corporation (Ashland, US) was utilised for the performances of tolerability studies. The presence of fibroblast-keratinocyte cell interactions is necessary for the release of inflammatory biomarkers like secondary cytokines. Epiderm™ FT consists of organised basal, spinous, granular and cornified epidermal layers analogous to those found *in vivo* [86]. An example of the skin histology of the chosen model is shown in Figure 8.

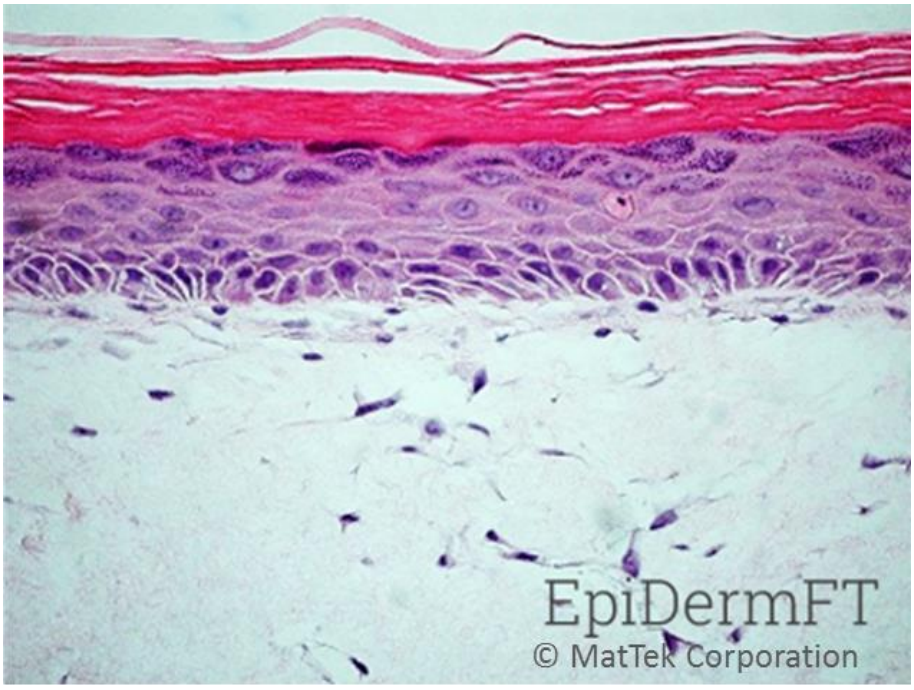

Figure 8: Microscopic image of skin histology samples of Epiderm™ FT representing the epidermis containing basal, spinous as well as granular keratinocytes and stratum corneum. The underlying, dermis contains numerous viable fibroblasts and is displayed brightly (H & E staining, 400x magnification). Reprinted with permission of MatTek Corporation [87].

The reconstructed full-thickness skin tissues have a surface area of 1 cm^2 with a total thickness of 700 µm and are shipped as transwell system in 6-well plate units [88]. Surface area and thickness of EpiDerm™ FT 400 match the intended needle application.

All tissues need constant contact to culture media based on Dulbecco`s Modified Eagle`s Medium supplemented with growth factors, antibiotics, anti-fungal agents and other additives (EFT-400-MM, MatTek Corporation, Ashland, US). Skin tissues are screened and tested negative for pathogens such as HIV and hepatitis B. It is necessary to handle this biological material under aseptic conditions in a laminar flow hood [89].

3.2 Methods

3.2.1 Multiple Light Scattering

Multiple light scattering (MLS) is the underlying technology of Turbiscan LAB^{TM} (Formulaction SAS, L`Union, France), which was utilised in the current experiments. The Turbiscan LAB^{TM} allows the physical properties analysis of emulsions or suspensions, especially size measurements, detection of concentration variations, and changes in physical properties such as sedimentation, creaming as well as flocculation or coalescence.

The measurement is performed by sending a light beam (λ = 880 nm) through a cylindrical glass cell containing the liquid sample. Two synchronous optical sensors, detect the transmitted or backscattered light. The transmission detector receives the light going through the sample (at 180° from the incident light beam), whereas the backscattering detector receives the light scattered backwards by the sample (at 45° from the incident light beam). Transmission and backscattering values directly depend on the particle diameter and their volume fraction [90].

Based on recommendations of the manufacturer this study was focused on the detection of transmission values enabling the differentiation between clear and turbid dispersions, however, backscattering is suggested for the analysis of more opaque and concentrated systems [90].

Figure 9 shows the chosen experimental setup for the Turbiscan LAB^{TM}. Samples were filled in a cylindrical glass vial and equilibrated at 25 °C for 30 min.

After the equilibration time, variations in optical transparency were measured over time (Figure 9). First, a fixed transmission value in % was recorded at a fixed height of 15 mm directly after the preparation. Second, cumulative transmission curves were taken, indicating time-dependent stability changes of formulations with one measurement per hour over 24 h. For the detection of time-dependent variations the laser evenly scanned the glass vessel along 20 mm height (Figure 9).

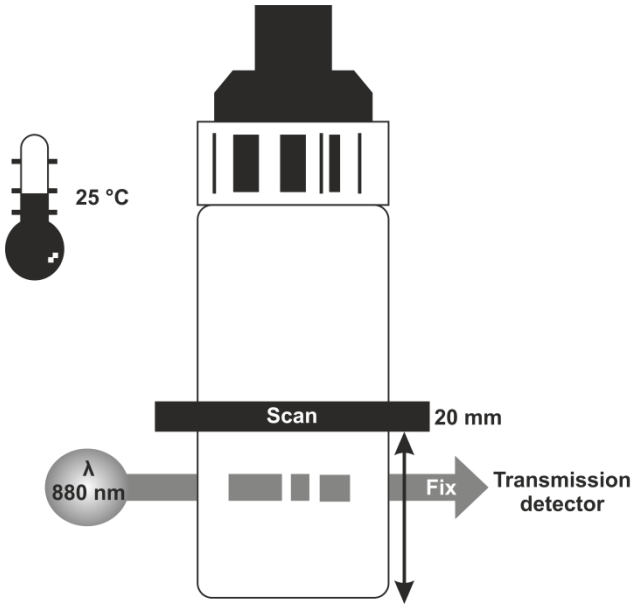

Figure 9. Setup of Turbiscan LAB™ with a typical cylindrical sample vessel. The optical transparency of each formulation was controlled via transmission values in %, at 25 °C. Transmission values were taken at a fixed height of 15 mm or scanned along 20 mm. (Adapted from [90])

3.2.2 Dynamic Light Scattering

Information about the inner structure of developed colloidal formulations were determined with dynamic light scattering (DLS). DLS, also known as photon correlation spectroscopy, measures changes in light scatter intensity over time due to Brownian motion of molecules or particles in dispersion [91]. Particles are constantly moving based on their random collision with fast-moving molecules of the liquid surrounding (Brownian motion) [91]. An essential factor of this phenomenon for DLS is that small particles move faster than large particles. In case of illumination of a sample via laser (λ = 633 nm) the intensity of scattered light (detected at an angle of 173°) from small particles will fluctuate quicker than for larger particles showing slower fluctuations The relationship between the size and the speed of a particle due to Brownian motion is defined in the Stokes-Einstein equation *(1)* [92].

$$D = \frac{k \times T}{6 \times \pi \times \eta \times r_h} \quad (1)$$

D = diffusion coefficient
k = Boltzmann constant
T = absolute temperature
η = dynamic viscosity
r_h = hydrodynamic radius

The fluctuation of scattering intensity is detected over time intervals, plotted as correlation curves, and is used to extract information about the diffusion coefficient of particles or droplets in a solution. Based on the measured diffusion coefficient the hydrodynamic radius of the particles or droplets can be calculated using Stokes-Einstein equation *(1)* (in the present study given as z-average). The size distribution generated by DLS is an intensity distribution, not a number or a volume distribution, because it is calculated from the signal intensity [92].

In the present study, DLS measurements were performed using the Zetasizer Nano ZS (Malvern Instruments, Worcestershire, UK). Nano ZS series can be used for the detection of particle sizes between 0.3 nm to 10 µm as maxima. The most important and reliable values produced by this technique are the z-average diameter and the polydispersity index (PDI). Both parameters were used for the characterisation of developed formulations. The z-average also known as "cumulants mean" is the mean hydrodynamic diameter calculated from signal intensity, whereas the PDI describes the width of cumulants analysis giving values between zero and one. Calculations for both parameters are defined in the ISO 13321:1996 E and 22412 [92]. All DLS measurements were performed with undiluted, particle free filtered (cellulose acetate membrane, 0.2 µm pore size) samples.

3.2.3 Advanced Differential Scanning Fluorimetry (nanoDSF)

nanoDSF is an advanced Differential Scanning Fluorimetry method measuring the intrinsic fluorescence of proteins containing aromatic amino acids like tryptophan. The measurable fluorescence of tryptophan strongly depends on its position in the protein and the closed surrounding. Because of its hydrophobic character it is usually located in the hydrophobic core of proteins isolated from the surrounding hydrophilic solvent [93]. Intrinsic protein fluorescence can mainly be attributed to the

fluorescence of tryptophan. The fluorescence of tryptophan is excited at 280 nm and emitted at 330 nm in non-polar environment and 350 nm in polar environment [94].

The measuring principle of nanoDSF is an increasing temperature profile followed by changes in the intrinsic fluorescence of a protein. Figure 10, (A) depicts the process of protein unfolding upon heating steps. Therefore, changes of tryptophan fluorescence at 350 nm and 330 nm wavelength can be monitored and used to determine the unfolding transition temperature T_m (°C). T_m is defined as temperature at which half of the protein is unfolded and acts as important parameter for the conformational stability of a protein [95].

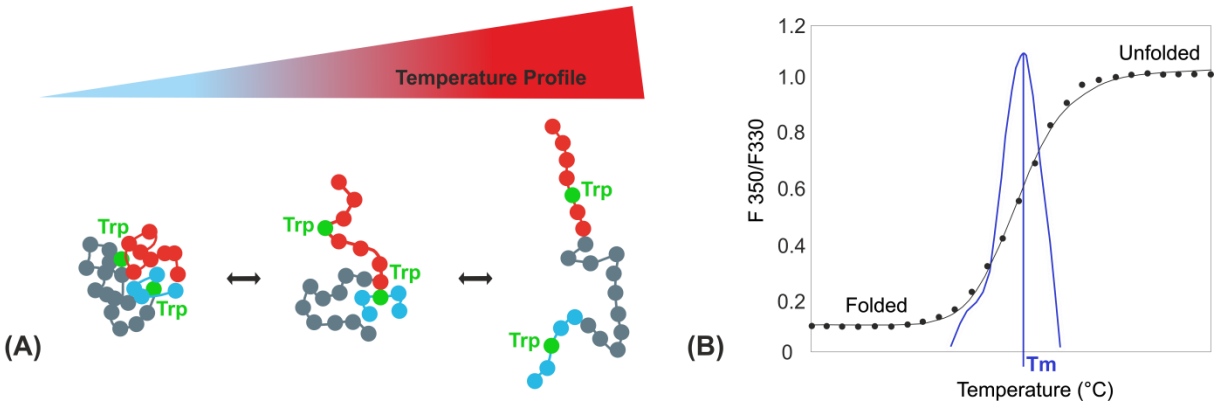

Figure 10. Measuring principle of nanoDSF. Increasing temperature causes protein unfolding and changes in tryptophan fluorescence (A). The transition from folded to unfolded status of a protein is plotted as ratio of two wavelengths 350 nm and 330 nm against increasing temperature (B, black line) next to its first derivative (blue line). (Adapted from [95,96])

The data at emission wavelengths of 350 nm and 330 nm are plotted as ratio (Figure 10, B black line) against the temperature. Additionally, their first derivative was calculated, displaying as peak at the point of maximal slope, which corresponds to T_m (Figure 10, B blue line). Destabilising chemical or thermal influences might lead to changes in a protein and hence to changes in fluorescence intensities as well as shifts in T_m [93].

In most cases the loss of protein stability correlates with a reversible or irreversible unfolding often followed by an aggregation process. nanoDSF technology also enables the determination of aggregation behaviour (colloidal stability) of proteins via backreflection optics. Protein aggregates scatter the incident light similar to particles and the intensity of reflections is quantified by a detector [97].

In the present study nanoDSF measurements were performed with Prometheus NT.48 in laboratories of nanoTemper technologies GmbH in Munich. For the measurement 10 µL of each lipophilic protein formulation were loaded undiluted into standard treated Prometheus NT.48 capillaries and subjected to a thermal ramp from 20 °C to 95 °C at a heating rate of 1 °C/min. A closer look at the described technical setup is shown in Figure 11.

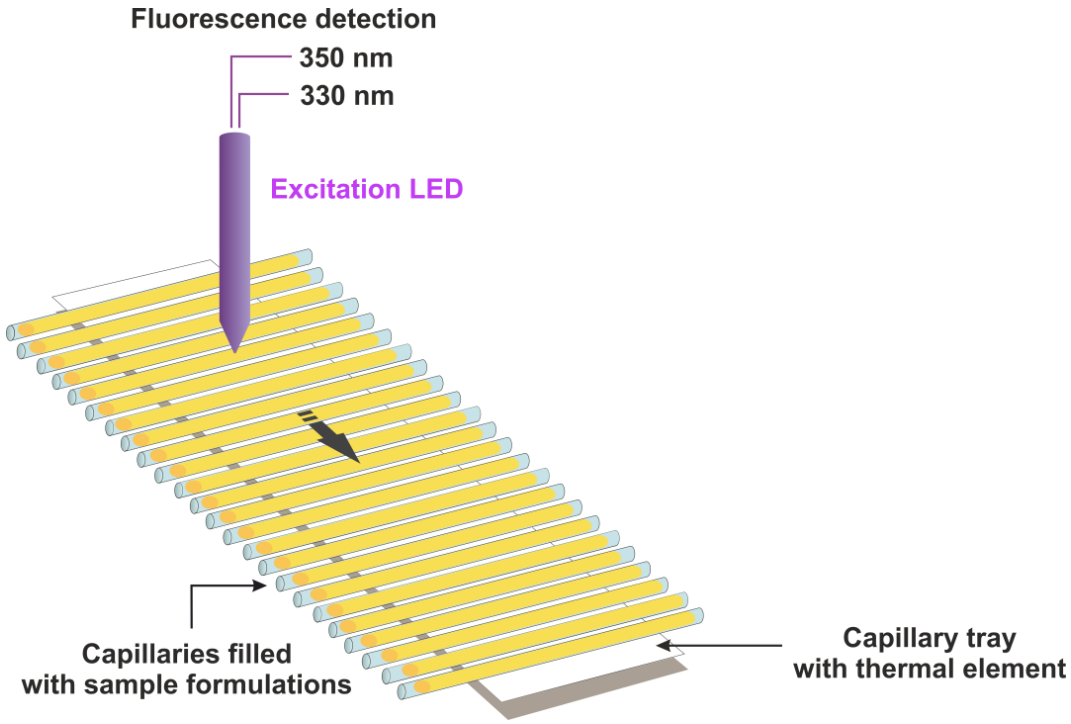

Figure 11. Technical setup of Prometheus NT.48. The lipophilic protein formulation is heated in capillaries with a thermal gradient from 20 °C to 95 °C. The protein is excited by a LED laser (280 nm) and changes of intrinsic tryptophan fluorescence emission are detected [98]. (Adapted from [95])

3.2.4 Size Exclusion Chromatography

Size exclusion chromatography (SEC) is a liquid column chromatographic technique that separates biomolecules according to their molecular weight or hydrodynamic volume. The stationary phase consists of porous particles with a defined pore size through which the molecules diffuse based on their molecular weight and hydrodynamic volume (Figure 12) [99].

Basically, SEC works by trapping small molecules in the porous material of the stationary phase resulting in a larger accessible volume and a longer retention time. Hence, larger molecules will pass the column material faster and elute first.

SEC separates on the basis of enthalpic interactions with a stationary phase, in contrast to other liquid chromatography separation techniques. In liquid chromatography generally used secondary interactions like adsorption partition or ion exchange are in SEC unwanted and must be avoided [99,100]. Figure 12 presents an overview of described SEC setup.

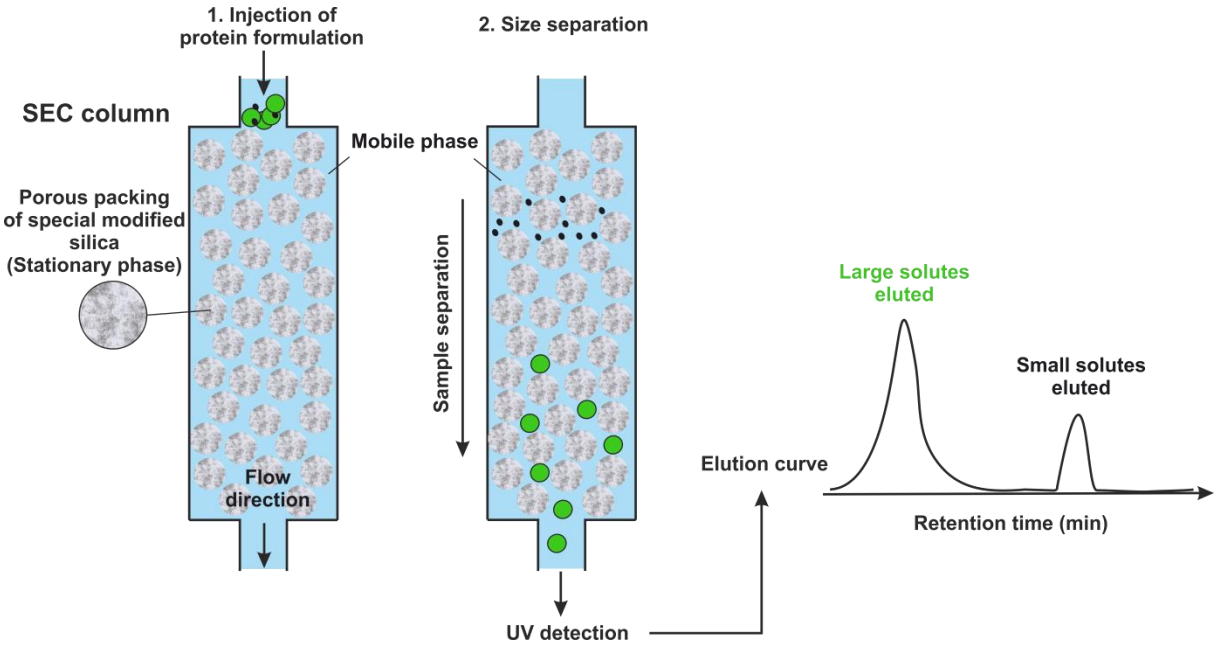

Figure 12. SEC separation technique. Small molecules can freely diffuse into and on porous packaged stationary phase, thus they elute at a later time. Molecules which are too large to penetrate the pores elute earlier.

In the present study an aqueous 50 mM phosphate buffered saline pH 7.0 modified with 200 mM L-arginine hydrochloride (Arg-HCl, Appendix chapter 8.1.2) was used as isocratic mobile phase. As typical for an aqueous SEC a silica-based stationary phase packaging was used [101]. The applied 5 µm PSS PROTEEMA analytical 300 Å (8 x 300 mm) SEC column (PSS Polymer Standards Service GmbH, Mainz, Germany) consisted of a special modified silica and is well-suited for a separation range between 10-1200 kDa. All experiments were performed with a Merck-Hitachi D 7000 system (Merck-Hitachi, Darmstadt, Germany) coupled to a UV detector at 280 nm.

SEC is frequently used for analysis and quality control of proteins, studying their aggregation or degradation products [102]. This study focused on the detection of

changes in protein stability within the formulations as an important quality parameter next to the investigations with nanoDSF (chapter 3.2.3).

Protein formulations were diluted with mobile phase to get a concentration of approximately 1 mg/mL. Sample volumes of 50 µL were injected as triplicate into SEC and run at a flow rate of 0.7 mL/min (Appendix, chapter 8.2).

3.2.5 Catalase Activity Assay

The catalase activity was examined with a method modified after Beers and Sizer (1952) utilising the ability of an active enzyme to degrade hydrogen peroxide (H_2O_2) to water and oxygen. One unit of catalase can decompose one micromole of H_2O_2 per minute at pH 7.0 and 25 °C.

Figure 13 shows the rate of H_2O_2 decomposition which can be measured by the decrease in absorption at a wavelength of 240 nm over time. In the current study the measurements were performed with a Varian Cary® 50 UV-Vis Spectrophotometer (Agilent Technologies, Santa Clara, US) enabling one absorbance reading per second over a time range of 180 seconds [103].

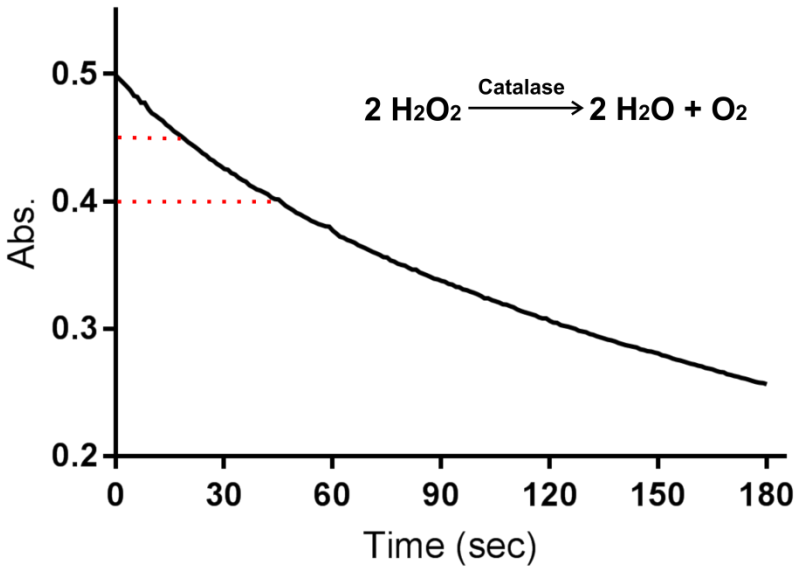

Figure 13. Typical degradation curve of H_2O_2. Catalase is catalysing the decomposition of H_2O_2 to water and oxygen. The disappearance of H_2O_2 can be measured as function of absorbance at 240 nm against time. Red dotted lines label the area of linearity between absorbance and time which are crucial for the activity calculations.

Lipophilic samples, containing 1 % (m/V) catalase, were diluted just before use to approximately 100 U/mL in 50 mM potassium phosphate buffer pH 7.0 at 25 °C. 100 µL of sample solution were mixed with 2900 µL of a 0.045 % (V/V) H_2O_2 solution in a cuvette. The degradation reaction was monitored for 180 seconds as ΔA_{240}/second. To calculate the enzyme activity of catalase in U/mg the decrease of time in the linear range between 0.45 to 0.40 (red dotted line in Figure 13) was determined and used in the following equations *(2)* and *(3)* [103]:

$$\text{U/mL enzyme} = \frac{3.45 \times \text{df}}{\text{time} \times 0.1} \qquad (2)$$

$$\text{U/mg solid} = \frac{\text{U/mL enzyme}}{\text{mg enzyme/mL formulation}} \qquad (3)$$

df = dilution factor

time = minutes, required for A_{240} to decrease from 0.45 to 0.40

3.2.6 Skin Preparation Techniques

Human, abdominal, female skin (42 years) obtained after a plastic surgery (Dr. med. A. Häring, esthesis-Kiel, Kiel, Germany) was used in subsequent analyses. Patients' identities were kept anonymous and they were informed about the experimental use.

For later skin preparations it was necessary to completely remove the fat tissue and to clean the surface with PBS pH 7.4 (Dulbeccos Phosphate Buffered Saline without $CaCl_2$ and $MgCl_2$, Sigma Aldrich, St. Louis, US). Afterwards, the skin was dried with a cotton swap, cut into 5 x 5 cm pieces at least and wrapped into aluminium foil. Stored at -30 °C skin is stable with regard to its barrier function for up to six month [104].

1.1.1.3 Heat-Separation of Epidermis Sheets for Scanning Electron Microscopy studies

Heat-separation is a simple and fast technique to obtain pure epidermal sheets. Generally, the epidermal layers are used as barrier in permeation studies with Franz diffusion cells, however, in the current study they were utilised for microneedle device characterisation experiments [104].

The cadaver skin pieces were thawed at room temperature and carefully fixed between two aluminium plates. Heating the fixed full-thickness skin at 60 °C in purified water for 120 s resulted in a clear separation of the epidermis from the dermis. With blunt forceps the epidermis was carefully peeled off from the underlying dermis and hydrated in PBS pH 7.4 for 30 min. The hydration step ensures a complete unfolding of the epidermis.

Afterwards, the epidermis sheet was ready for perforation steps with a microneedle device (chapter 3.1.4). To visualise formed micro channels on skin surface, scanning electron microscopy (SEM) was utilised.

For this purpose the perforated sheet was fixed with a 4 % (m/m) buffered formalin solution overnight. After at least 16 h the sample was rinsed with purified water and dehydrated in alcoholic solutions with increasing ethanol content every 30 min (50 %, 70 %, 96 %, 99 %, V/V) [104]. The membrane was mounted on an aluminium sample holder (Plano GmbH, Wetzlar, Germany) with a special glue of conducting carbon particles (Plano Leit-C nach Göcke, Plano GmbH, Wetzlar, Germany) and sputter coated using a SCP 005 Sputter Coater (BAL-TEC AG, Balzers, Liechtenstein). Finally, the coated sample was transferred into the SEM chamber and imaged with an acceleration voltage of 2 kV. Skin surface images were measured with a SE-2 detector as part of the Zeiss Ultra 55 Plus SEM (Carl Zeiss NTS GmbH, Oberkochen, Germany) setup.

1.1.1.4 Paraffin Embedding and Sectioning

In this procedure, tissue is dehydrated through a series of graded ethanol baths to displace the water, and then infiltrated with liquid paraffin wax. The infiltrated tissues are then embedded into wax blocks. Once the tissue is embedded it is stable for many years [105].

The present study used for the dehydration step of fresh skin samples an automatically controlled Leica ASP300 Tissue Processor (Leica Mikrosysteme GmbH, Wetzlar, Germany). Finished samples were embedded in paraffin and manually sectioned into 5 µm slices with a Microm HM355 microtome (Thermo Fisher Scientific GmbH, Schwerte, Germany).

Most cells are colourless and transparent, therefore, the sections were stained with a non-specific, commonly used staining system called H & E (Haemotoxylin and Eosin). The basic principle is a colouring of acidic (with Haematoxylin) next to basic (with Eosin) components in cells which results in characteristic pink and purple images [105].

Advantages of H & E staining combined with paraffin sections are high contrast images going along with long storage stability. However, detrimental effects are the high number of alternating dehydration and incubation steps which may lead to a swelling of skin layers, thus changing the tissue structure.

With regard to the evaluation of tolerability studies with human skin models, this preparation technique was an essential part of histological studies. The assessment for pathohistological changes was performed in cooperation with the group of Professor E. Proksch at the Department of Dermatology, Kiel University.

1.1.1.5 Cryo-Embedding and -Sectioning

Cryosections are rapidly and easily performed prior to paraffin fixation. They provide overview images as a snapshot of cell status, without tissue changes that might occur as consequence of various incubation steps. Therefore, this procedure was applied in the present study for visualisation of microchannels as cross section in cadaver as well as in EFT-400 skin samples.

Freshly pierced human skin samples were placed in a microcentrifuge tube and frozen in liquid nitrogen. It is necessary to pay attention on rapid freezing procedures to reduce ice crystal formation as well as morphological damages. Frozen samples were embedded in a freezing medium (Tissue-Tek, Sakura Finetek, Torrance, US) on metal sample stubs (Figure 14, A).

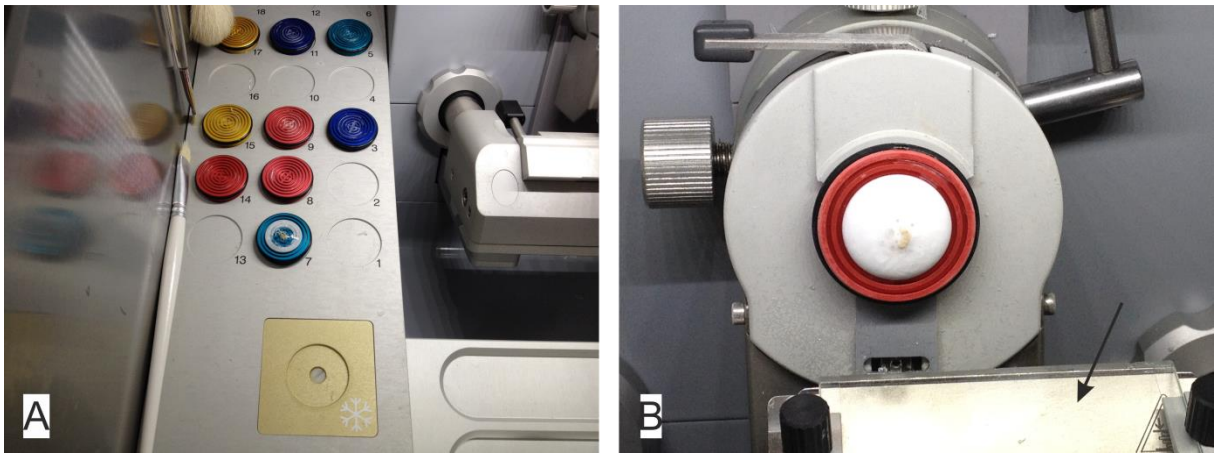

Figure 14. Setup of CryoStar NX 70. Image (A) shows yellow, red and blue coloured sample stubs used for tissue embedding. (B) Presents a detailed view on the chuck holding the stub with a complete embedded, frozen sample. The arrow marks the anti-roll plate for tissue slices and the subjacent knife-holder.

Afterwards the stub was fixed on a chuck, as shown in Figure 14, B, and cut in 5 µm thick slices in a cryostat (CryoStar NX 70, Thermo Fisher Scientific GmbH, Schwerte, Germany) at -20 °C. For the following microscopic examination skin slices were transferred on a microscope slide and analysed with an Axioskop 40 light microscope (Carl Zeiss Microscopy, Oberkochen, Germany). Without further fixation steps the skin slices are stable for 24 h [106].

3.2.7 Transepidermal Water Loss Measurements

Measurements of transepidermal water loss (TEWL) detect the water evaporation from the skin as an important parameter for the evaluation of skin water barrier function. Already slight damages of outermost skin layers disturb the natural water homeostasis and increase the water loss [107].

TEWL is typically used to evaluate *in vivo* effectiveness and/or tolerability of several dermal formulations [108]. In the present study, this technique was used to characterise the efficiency of three needle devices to form microchannels into *in vitro* cadaver skin samples. Contrary to clinical tolerability evaluations, that usually aim a low water loss, in the current investigations an increased TEWL was intended.

For the assessment of the TEWL the Tewameter® TM 300 (Courage+Khazaka electronic GmbH, Cologne, Germany) was applied (Figure 15).

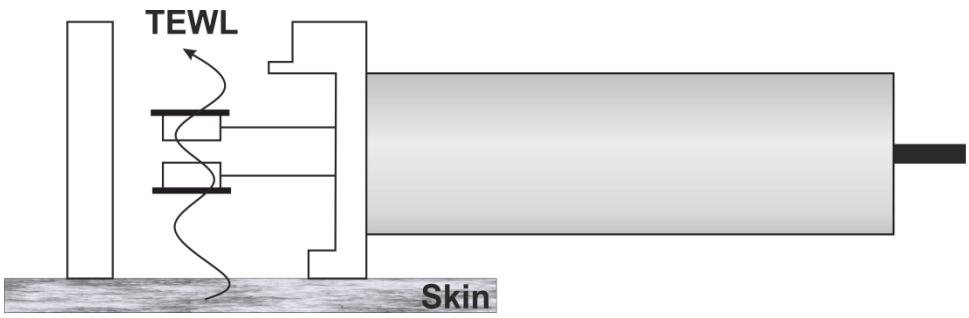

Figure 15. Schematic drawing of Tewameter® TM 300 probe. The Tewameter® probe is a hollow, cylindrically formed open chamber with two pairs of sensors (temperature and relative humidity). (Adapted from [108])

The Tewameter® probe measures the density gradient of the water evaporation from the skin indirectly by two pairs of sensors (temperature and relative humidity) located in a hollow cylinder (schematically shown in Figure 15). A microprocessor analyses the results and expresses them as evaporation rate in g/h/m^2.

The hollow, open cylinder facilitates the expansion of a homogenous diffusion zone above the skin surface and thus allows continuous TEWL measurements without any influences of the microclimate of the skin. Nevertheless, the so-called "open chamber method" is exposed to interfering influences like air temperature, ambient relative humidity (rH), and anatomical sites. To ensure a high accuracy all TEWL analyses were performed on the same day, at 22 °C and 33 % rH.

To avoid unnecessary dehydration of skin, thawed samples were removed from the aluminium foil directly before measurements were performed. The probe was placed on the skin surface in a fixed position. Continuous detections of TEWL values were started and stopped automatically after reaching a constant standard deviation of < 0.2 g/h/m^2 [107].

3.2.8 Tolerability Studies with a Full-Thickness Human Skin Model

Upon arrival of EFT-400 tissues, the inserts were placed in fresh 6-well plates, fed with 2.5 mL of culture media (EFT-400-ASY, MatTek Corporation, Ashland, US) and equilibrated at 37 °C; 5 % CO_2. Following 16-18 h pre-incubation, the culture medium was replaced with fresh medium. Tissues were now ready within 24 h for the experiment [109].

60 µL of liquid sample volume were dispensed and gently spread atop the tissue surface using a pipette (Figure 16, A). In case of a perforation with Dermastamp® 500 µm, the tissue inserts were taken out of the well plate and pierced 10-fold evenly through the surface (Figure 16, B).

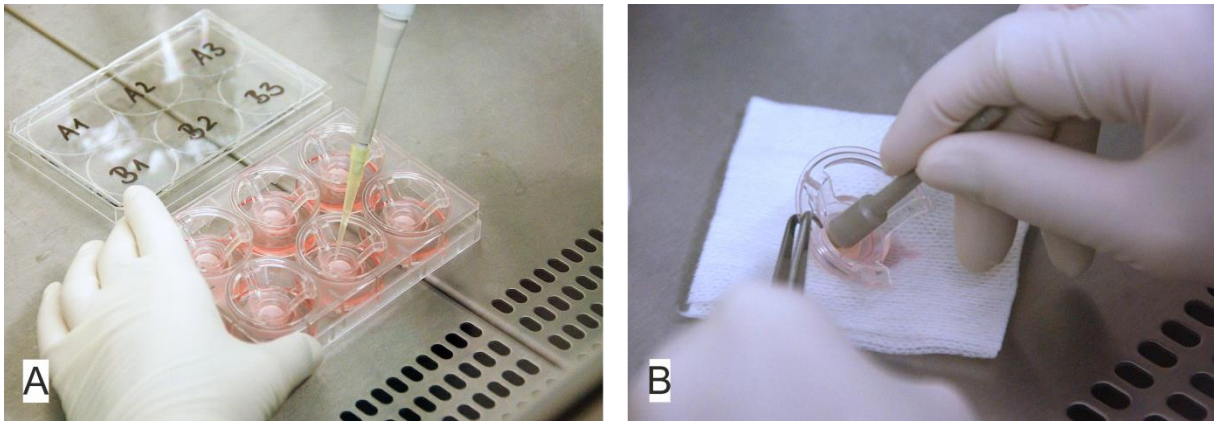

Figure 16. Treatment of EpiDerm™ FT 400. The application of liquid samples using a pipette is shown in image A. In case of a perforation with Dermastamp® 500 µm, the tissues were pierced outside their well plate (B).

According to the experience of Badran *et al.*, this study utilised the most effective application order; first piercing followed by applying the test formulation [104]. Each skin treatment was performed in triplicate.

After 3, 8 and 24 h culture medium was collected for analysis and replaced with fresh medium. The collected culture media were quantitatively analysed using assay kits for IL-6, IL-8 (BioLegend, San Diego, US) and LDH (Sigma Aldrich, Saint Louis, US) according to manufacturer`s protocol [110–112]. For the detection of IL-1α the supernatant of a skin tissue lysate was used. For this, each tissue was completely immersed in 0.5 mL cold lysis buffer-protease inhibitor mix (for detailed composition see appendix), homogenised with a pellet pestle for 40 s at 425 rcf and centrifuged (20817 rcf, 10 min, 4 °C) to pellet debris [113]. The supernatant as well as the culture media samples were aliquoted and frozen at -80 °C until use. The detection of IL-1α was performed after 24 h incubation time because of total tissue destruction following the instructions from manufacturer`s protocol [114]. All samples were analysed in duplicate. One EFT-400 tissue of each test formulation was collected after 8 h and prepared as paraffin embedded and H & E stained samples (chapter 3.2.6).

4 RESULTS

4.1 Formulation Development and Characterisation

The development of a dermal formulation containing protein drugs comprises some obstacles. On the one hand their high molecular weight and hydrophilic character complicate the penetration into skin; on the other hand the flexible and sensitive structure which is prone to external conditions is oftentimes responsible for a short shelf-life [4]. This study focused on the development of a topical formulation which facilitates the application of proteins with a high tendency for hydrolysis like the family of bacterial collagenases.

Nevertheless, in case of containing an instable protein, a topic formulation must ensure high drug stability, solubility as well as good penetration and spreading properties on the patients` skin. Kogan *et al.* (2006) presented microemulsions as promising systems with the previously mentioned characteristics [65]. In comparison to emulsions and creams they have an advantageous thermodynamic stability beneath an easy preparation because of their spontaneous formation without any energy input [115]. Due to this spontaneous formation upon mixing the ingredients, it was envisaged to create an application system based on two separated phases within this project. A water-free pre-formulation (microemulsion concentrate) offers the opportunity to suspend the protein in the lipophilic phase separated from the aqueous phase. The mixing of those two phases should be performed directly before the application on skin, hence the contact time between protein and water, which is critical regarding the protein stability, is minimised.

It is envisaged to combine the application of the formulation with a microneedling step (chapter 1.1). The resulting superficial damages increase the sensitivity of human skin. Therefore, it is crucial in the process of formulation development to select ingredients with a low potential of skin irritation.

The process of formulation development including the formulation characterisation and *in vitro* tolerability studies will be described in following sections. A detailed discussion of obtained results will be held in the subsequent chapter 5.

4.1.1 Microemulsion Development

The term "microemulsion" (ME) has been defined diversely by various authors [65]. This study follows the definition of Danielsson and Lindman in 1981 [116]: “(...) a microemulsion is a single, optically isotropic structured solution of surfactant, oil, and water.”

Kogan *et al.* (2006) emphasised the versatile properties of ME such as thermodynamic stability, easy formation and a low viscosity with Newtonian behaviour [65]. The pronounced stability of these systems generally depends on the high content of surfactants. Quite a number of well-known non-ionic surfactants raise, however, skin irritations, especially in the chronical treatment, thus alternatives for the present investigations need to be found [117].

Mild production processes and high environmental compatibility along with low irritation potential are frequently named reasons for the application of natural surfactants [65,115,117,118]. According to Paolino *et al.* (2002) natural surfactants of choice are phospholipids due to their good skin tolerability next to penetration enhancing effects [119]. The ability of phospholipid-based surfactants to stabilise microemulsions is already well reported in literature [62,115,118]. This study focused on the application of Lip80 (DAPL with 80 % of MAPL). The high amount of MAPL leads to a high polarity of the phospholipid and promises self-emulsifying properties with a great emulsification power (chapter 1.1.1.1).

To exploit Lip80-based microemulsions for dermal protein delivery it was desired to produce systems that form stable microemulsions over a wide range of oil and water concentrations. Of particular importance was a high hydrophilic concentration range, to facilitate a complete solubility of water-soluble catalase. In addition, variations over a wide hydrophilic range mean superior microemulsion stability besides better application stability on skin, e.g. changes in water content as consequence of hydration and dehydration processes could be balanced easier.

50 mM PBS pH 7.0 was set as hydrophilic phase instead of purified water because of its positive effect on model proteins solubility and stability [120]. Lip80 was determined as surfactant. Furthermore, a suitable additive to dissolve the

phospholipid as well as a lipophilic phase had to be selected to finally create a ME with the desired properties.

4.1.1.1 Screening of Cosolvents

Lip80 consists of yellow wax-like agglomerates. For processing this emulsifier in MEs a dissolving step is necessary. Short chain alcohols, e.g. 2-propanol, were already mentioned in literature to be suitable cosolvents [62,121].

Due to their low irritation potential on skin and dissolving properties for Lip80, the following alkyl alcohols next to a polyethylene glycol were screened in ratios of 1:1, 2:1 and 1:2 (surfactant:cosolvent):

- Propylene glycol
- Ethanol 99.9 % (V/V)
- 2-Propanol
- Macrogol 400

Regarding the predefined ratios, Lip80 and a cosolvent were weighed in and stirred for 12 h at 22 °C. At the end, all agglomerates must be dissolved completely.

Macrogol 400 was not able to dissolve the surfactant in either of the tested ratios. For the alkyl alcohols, the ratio of 2:1 (surfactant:cosurfactant) resulted in incompletely dissolved samples. The reverse ratio with higher cosolvent amount (1:2), resulted in a dissolved surfactant but no subsequent ME formation was observed. Surfactant and cosurfactants in a ratio of 1:1 lead to completely dissolved samples. Moreover, a formation of ME systems could be achieved for all alkyl alcohols. This ratio was most promising and used accordingly for further investigations.

In order to find the concentration range of components (Lip80/alkyl alcohol:lipophilic phase:PBS) where they form ME, a pseudoternary phase diagram was constructed. As shown in Figure 17 he components are plotted on an x-, y- and z-axis, respectively. Together, they build a triangular shaped diagram, with 100 % of one component in each vertex. As predefined in the pseudoternary diagram the ingredients were calculated in fixed ratios (%, m/m) and combined in 10 % steps for a first cosolvent screening.

At ambient conditions, Lip80 was completely dissolved under stirring in a cosolvent. Afterwards, oil and PBS were added in parts as predefined in the pseudoternary diagram. These final mixtures were gently shaken as ME formation should occur spontaneously and inspected visually. A slightly to strongly turbid sample indicates the presence of a two-phase system whereas a ME is a clear to opalescent coloured, single-phase formulation such as defined by Danielsson and Lindman [116].

Figure 17 presents the titration results of Lip80 dissolved in propylene glycol combined with two different lipophilic phases. The combination with Labrafac™ Lipophile WL 1349 (Figure 17, A) and Labrafac™ PG (Figure 17, B) showed small ME areas (labelled grey).

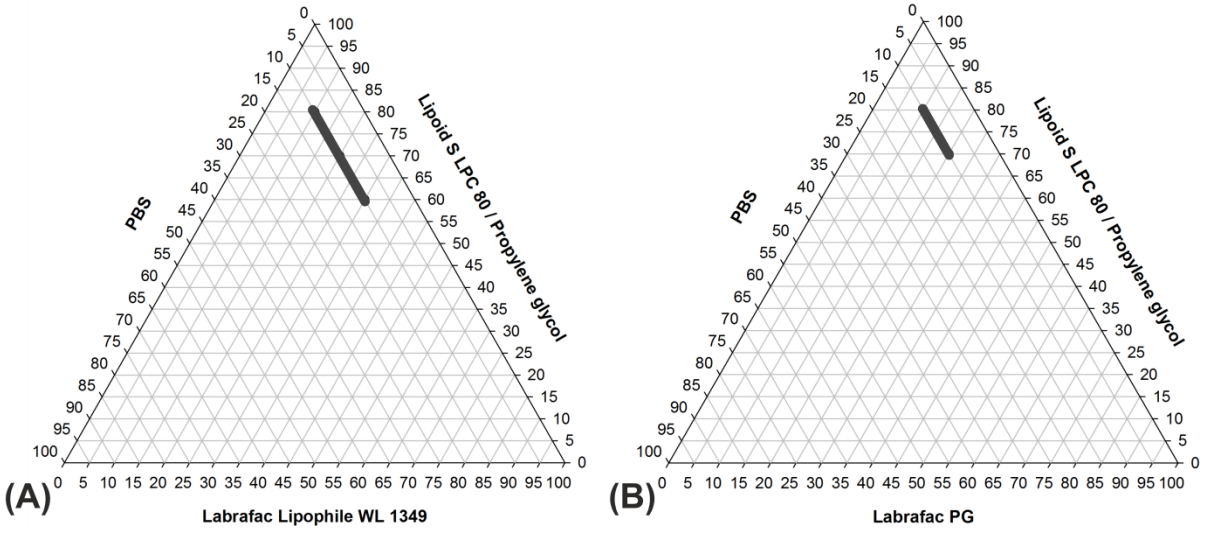

Figure 17. Pseudoternary phase diagrams show ME areas with Lipoid S LPC 80 (Lip80), propylene glycol and as lipophilic phase (A) Labrafac™ Lipophile WL 1349 or (B) Labrafac™ PG. The grey areas label the formation of isotropic microemulsions.

Formulations with Labrafac™ Lipophile WL 1349 (shown in Figure 17, A) required at least 60 % of surfactant/cosolvent whereas the mixtures with Labrafac™ PG (Figure 17, B) need a minimum of 70 % to stabilise a ME. Formation of ME systems in this experimental setting was enabled at 10 % of PBS.

Using ethanol 99.9 % (V/V) as cosolvent ME areas changed (Figure 18). The formation of isotropic areas was more pronounced with Labrafac™ PG (Figure 18, B) than Labrafac™ Lipophile WL 1349 (Figure 18, A).

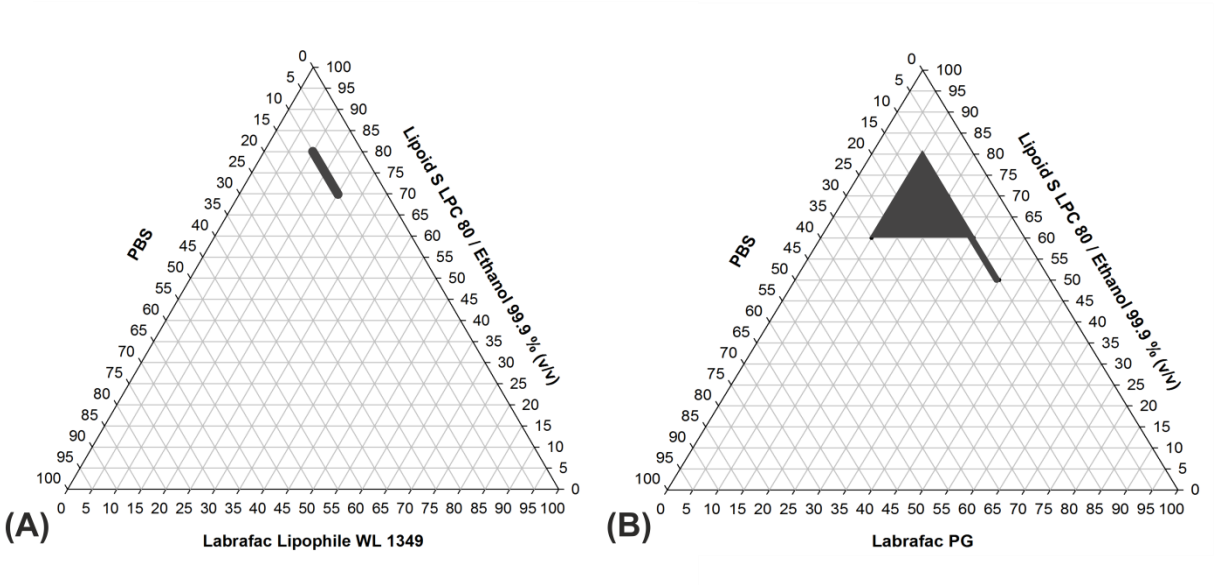

Figure 18. Pseudoternary phase diagrams show ME areas with Lipoid S LPC 80 (Lip80), ethanol 99.9 % (V/V) and as lipophilic phase (A) Labrafac™ Lipophile WL 1349 or (B) Labrafac™ PG. Isotropic areas (highlighted in grey) are most pronounced in diagram (B).

The combination with Labrafac™ PG facilitated more variations of ingredient concentrations, especially of the hydrophilic phase with 10 % to 30 %. Using ethanol 99.9 % (V/V) enabled the stabilisation of 30 % PBS with 60 % surfactant/cosurfactant.

Less suitable was the utilisation of Labrafac™ Lipophile WL 1349 for the formation of isotropic areas (Figure 18, A). Variations of the three phases were more limited compared to Figure 17, A.

The efficiency of forming ME increased by dissolving Lip80 in 2-propanol. As shown in Figure 19, A even the combination with Labrafac™ Lipophile WL 1349 led to the formation of larger isotropic areas compared to the other alkyl alcohols.

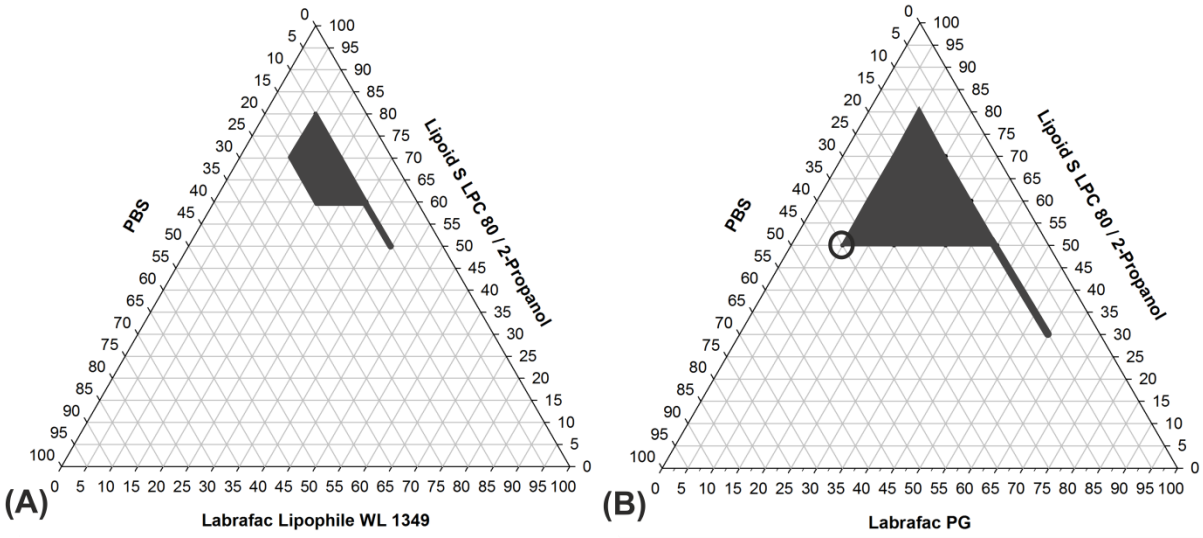

Figure 19. Pseudoternary phase diagrams show areas of ME formation with Lipoid S LPC 80 (Lip80), 2-propanol and as lipophilic phase (A) Labrafac™ Lipophile WL 1349 or (B) Labrafac™ PG. Isotropic areas are highlighted in grey. The composition with the highest PBS content 50 %:10 %:40 % (m/m, Lip80/2-propanol:Labrafac™ PG:PBS) is encircled black.

Regarding to the application of 2-propanol in Figure 19, A the PBS concentration was twice as high as in Figure 17, A and in Figure 18, A. More variations in the content of lipophilic and surfactant phase were possible. The exchange of the lipophilic phase increased the ME area even further (Figure 19, B). The application of 10 % Labrafac™ PG and 50 % surfactant/cosurfactant enables the stabilisation of 40 % hydrophilic phase. Therefore, this composition was used for dissolution experiments with 1 % catalase.

Catalase was suspended in a mixture of 50 % Lip80/2-propanol and 10 % Labrafac™ PG, 40 % of PBS were added and the suspension was shaken carefully. Nonetheless, the content of hydrophilic phase was not big enough for a complete dissolution of 1 % of enzyme as envisaged in the aims.

4.1.1.2 Optimisation of Microemulsion Area

To increase the PBS content in ME formulations and correspondingly the solubility of model protein, the influence of further lipophilic ingredients was examined. Besides Labrafac™ PG, oily vehicles like Peceol™, Maisine™ 35-1 as well as Plurol Oleique CC 497 (PO CC 497) were selected. Starting with the necessary PBS concentration

(for dissolving the enzyme) of 50 % and a reduced oil phase of 5 %, Lip80/2-propanol were added until 100 %.

Figure 20 represents formed ME systems with maximal possible hydrophilic capacity. The oil content was fixed at 5 %, whereas the hydrophilic range was increased in 5 % steps and the content of surfactant/cosolvent decreased correspondingly.

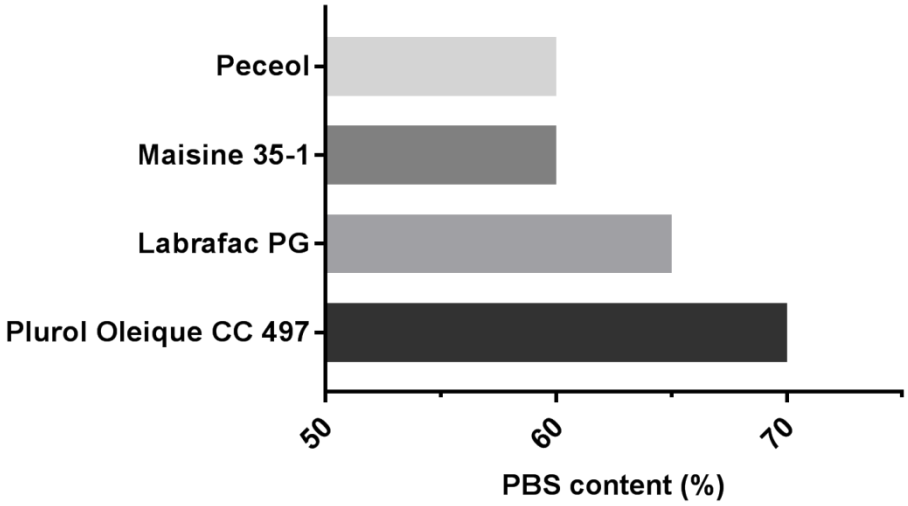

Figure 20. Property of different lipophilic ingredients to form microemulsion systems with an increasing hydrophilic content. The oil content was fixed to 5 %, whereas the PBS concentration was increased, the content of surfactant/cosolvent decreased correspondingly (not shown).

Peceol™- and Maisine™ 35-1-based MEs stabilised 60 % of incorporated PBS (Figure 20). In contrast, Labrafac™ PG contained a maximum of 65 % hydrophilic phase and PO CC 497 70 %.

Labrafac™ PG and PO CC 497 formed MEs with the highest hydrophilic phase content. Figure 21 depicts more precisely titrated (5 % steps) ME areas of Labrafac™ PG in diagram A next to PO CC 497 in diagram B.

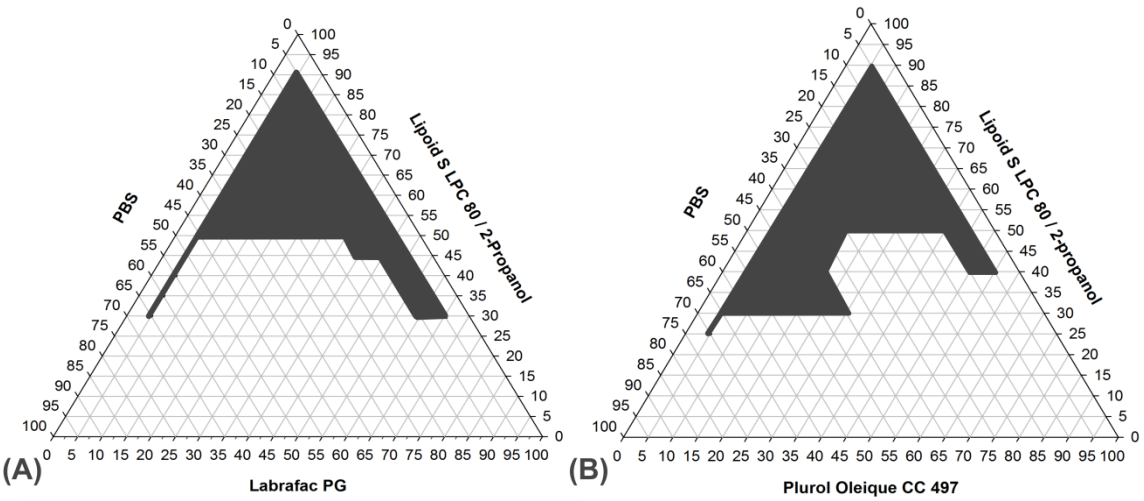

Figure 21. Pseudoternary phase diagram formed with oily vehicles (A) Labrafac™ PG and (B) PO CC 497. The formed isotropic areas are marked in grey.

Figure 21, A presents a small hydrophilic isotropic area. A content of PBS larger than 45 % formed ME systems only with 5 % of Labrafac™ PG. The hydrophilic ME area in Figure 21, B is more distinct. In a concentration range from 45 % to 60 % PBS, the content of PO CC 497 could be varied from 15 % to 30 %.

Both systems stabilised more than 50 % PBS, thus they were suitable for the dissolution of 1 % catalase.

4.1.1.3 PEGylated Microemulsion Systems

It was envisaged to compare the phospholipid based ME to a formulation based on PEGylated surfactants in tolerability studies with reconstructed human skin (chapter 4.3). This system needs to include the same ingredients in a similar composition, only the natural surfactant Lip80 is exchanged.

According to the experience of Kogan *et al.* (2006) forming ME with nonionic surfactants, in this study Polysorbate 80, Span® 20 and Kolliphor® EL were selected and tested in following combinations presented in Figure 22 [65]:

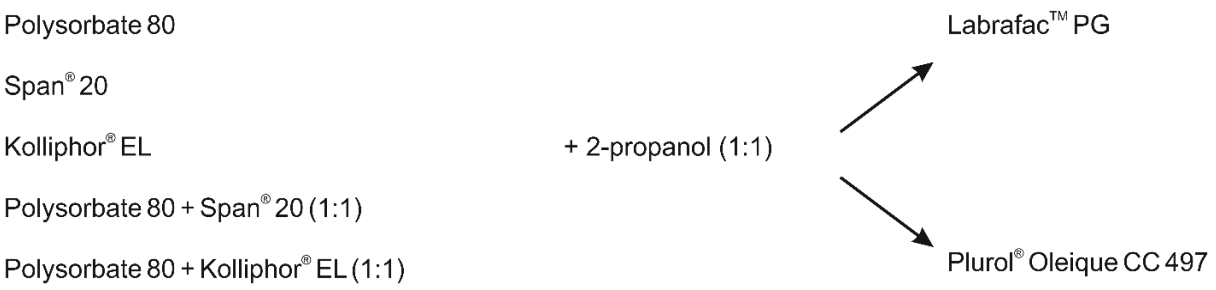

Figure 22. General chosen strategy for combinations of surfactant, 2-propanol and lipophilic phase.

All surfactants or surfactant combinations were dissolved in 2-propanol (in equal proportions) and mixed with the two most promising lipophilic phases Labrafac™ PG and PO CC497, respectively (Figure 22).

Figure 23 represents the titrated isotropic areas of the mixture Polysorbate 80 and Kolliphor® EL (ratio 1:1) combined with Labrafac™ PG (diagram A) as well as PO CC 497 (diagram B). Applying this surfactant combination, ME areas with the highest PBS capacity were formed.

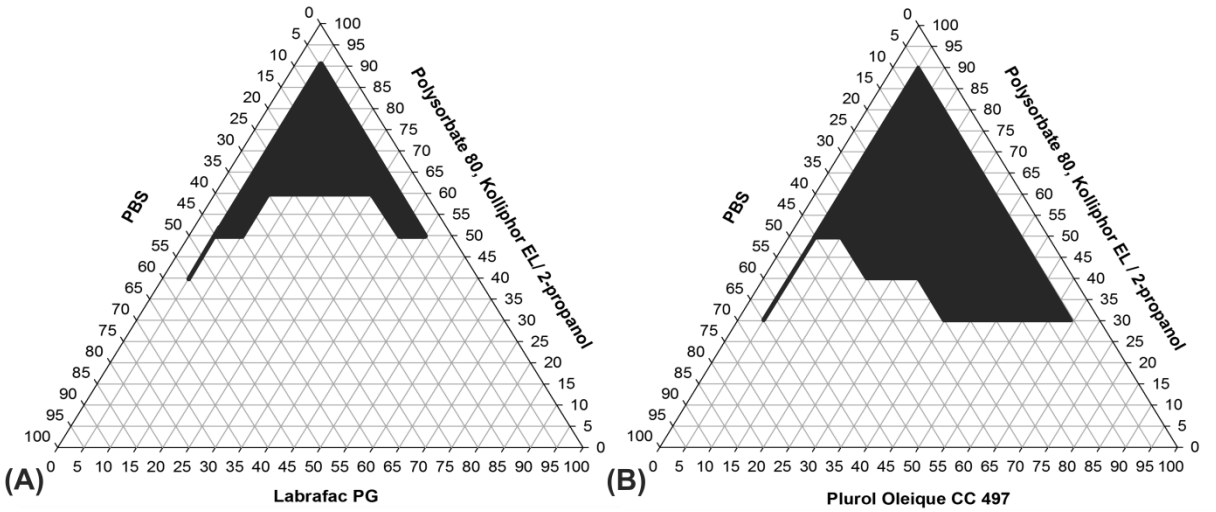

Figure 23. Comparison of two ME areas (marked grey) based on (A) Labrafac™ PG and (B) Plurol® Oleique CC 497 (PO CC 497).

The comparison of both diagrams displays an extended isotropic area for the application of PO CC 497 (Figure 23, B). The superior properties of PO CC 497 confirmed the observations made on the Lip80 system in Figure 21, B. Contrary to the more hydrophilic phospholipid ME (Figure 21, B), the PEG-based system showed

a more lipophilic ME (Figure 23, B). Although, a maximum concentration of 65 % PBS was stabilised by the PEG system, hydrophilic variations were more restricted compared to Lip80 system.

Because of its more promising performance PO CC 497 was chosen as lipophilic phase for both surfactant systems. A composition of 35 %:5 %:60 % (m/m, surfactant/cosolvent:PO CC 497:PBS) was selected for comparison on both ME systems in later investigations. These developed formulations were promising for a good solubility of model enzyme. Figure 24 gives an overview of the PEG-based and Lip80-based ME areas with the selected concentrations (encircled black).

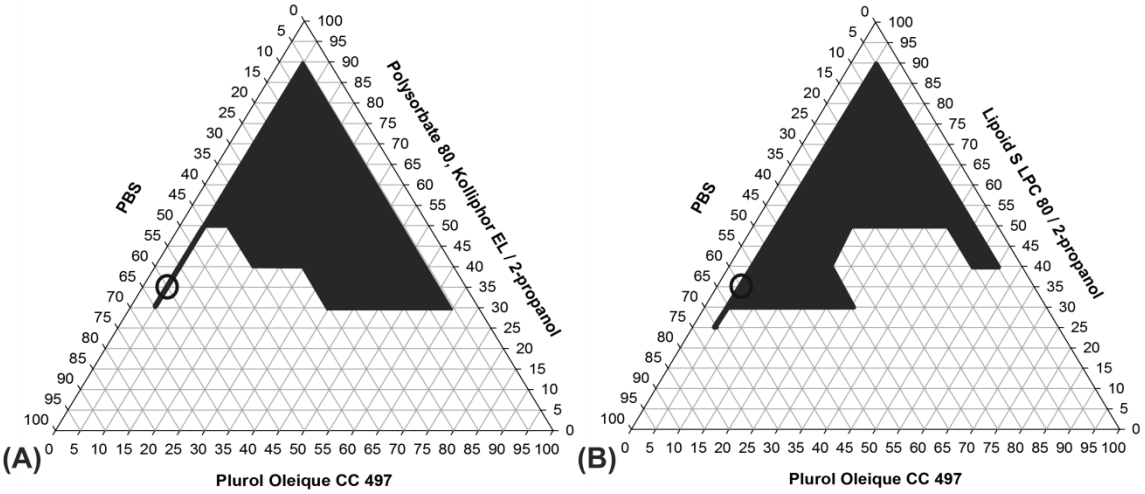

Figure 24. Comparison of the final ME systems. Diagram (A) shows the PEG-based ME area next to diagram (B) with the Lip80 formed area. Compositions resulting in ME formation are marked grey and the final selected compositions are encircled black.

4.1.2 Microemulsion Characterisation

4.1.2.1 Multiple Light Scattering

In order to confirm an optically clear, isotropic nature indicating ME formation (definition by Danielsson and Lindman [116]), transmission values of Lip80-ME and PEG-ME were measured with TurbiScan™ LAB. All investigations with TurbiScan™ LAB were performed with protein-free formulations.

Images in Figure 25 illustrate the gradations between optically clear ME and turbid macroemulsions. Transparent systems like isotropic ME do not interfere with the

laser light, hence transmission values (T-value) are ≥ 80 % (red line Figure 26). Turbid macroemulsions show significant decreased transmission values smaller than 80 %.

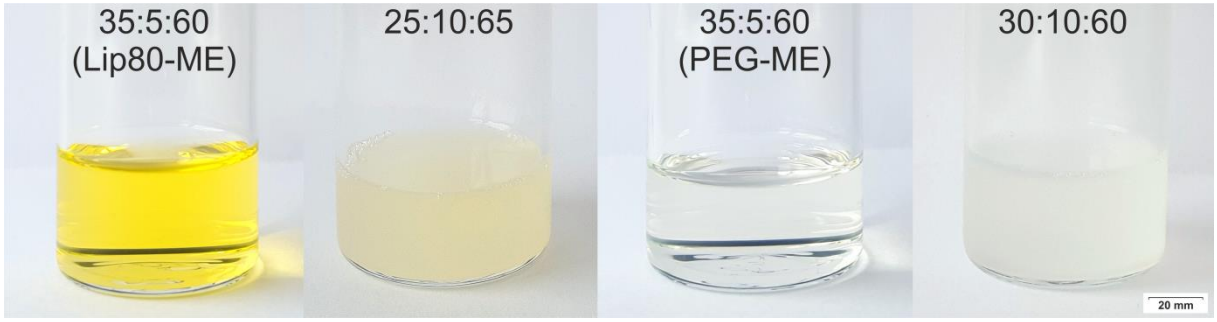

Figure 25. Lip80-ME and PEG-ME are depicted next to macroemulsion systems with slightly different compositions. Each image shows the ratio of ingredients in % (m/m), listed as surfactant/cosolvent:PO CC 497:PBS. (Scale bar = 20 mm)

ME formulation results were compared to T-values of pure ingredients, PO CC 497, and PBS (Figure 26). PO CC 497 slightly deflects the laser light, resulting in the lowest transmission (85.6 %). A T-value of 91.3 % was measured for the more transparent aqueous PBS.

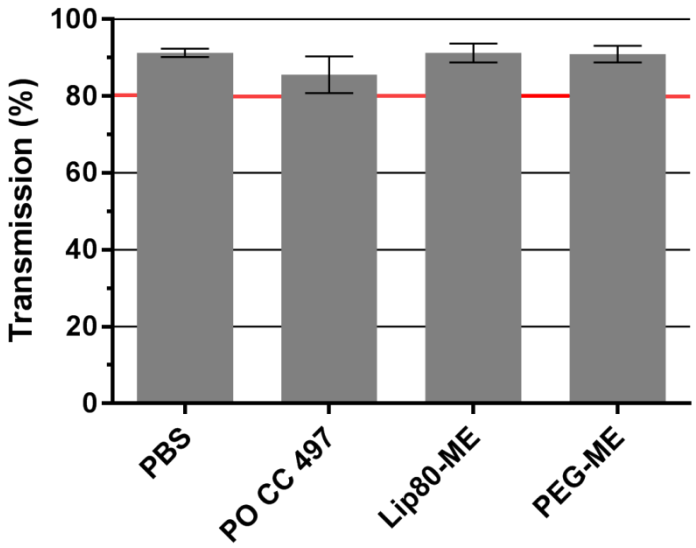

Figure 26. Transmission values of multiple light scattering measurements with TurbiScan™ LAB. The test formulations Lip80-ME and PEG-ME are plotted against pure PO CC 497 and PBS. Each column presents the mean of three measurements and error bars present the standard deviation. All groups were calculated with ANOVA as not significantly different, $p > 0.05$. Red line refers to the determined minimum T-value indicating the presence of an isotropic system.

Measurements of both ME formulations obtained transmission levels higher than 80 %. The optical transparency of Lip80-ME (91.3 %) as well as PEG-ME (91.0 %) was confirmed. Figure 26 demonstrates a similar transmission level of all samples, depicting no significant differences.

The ME systems should be prepared directly before the preparation is administered on the skin. Hence, the product stability must be ensured for the application process and penetration period. In case of destabilisation phenomena e.g. phase separation, a shift in T-values would detect this. The formation of new interfaces is a global phenomenon taking place everywhere in the sample. Therefore, it is important to monitor the whole sample volume. Figure 27 represents the transmission profiles of tested formulations over 24 h.

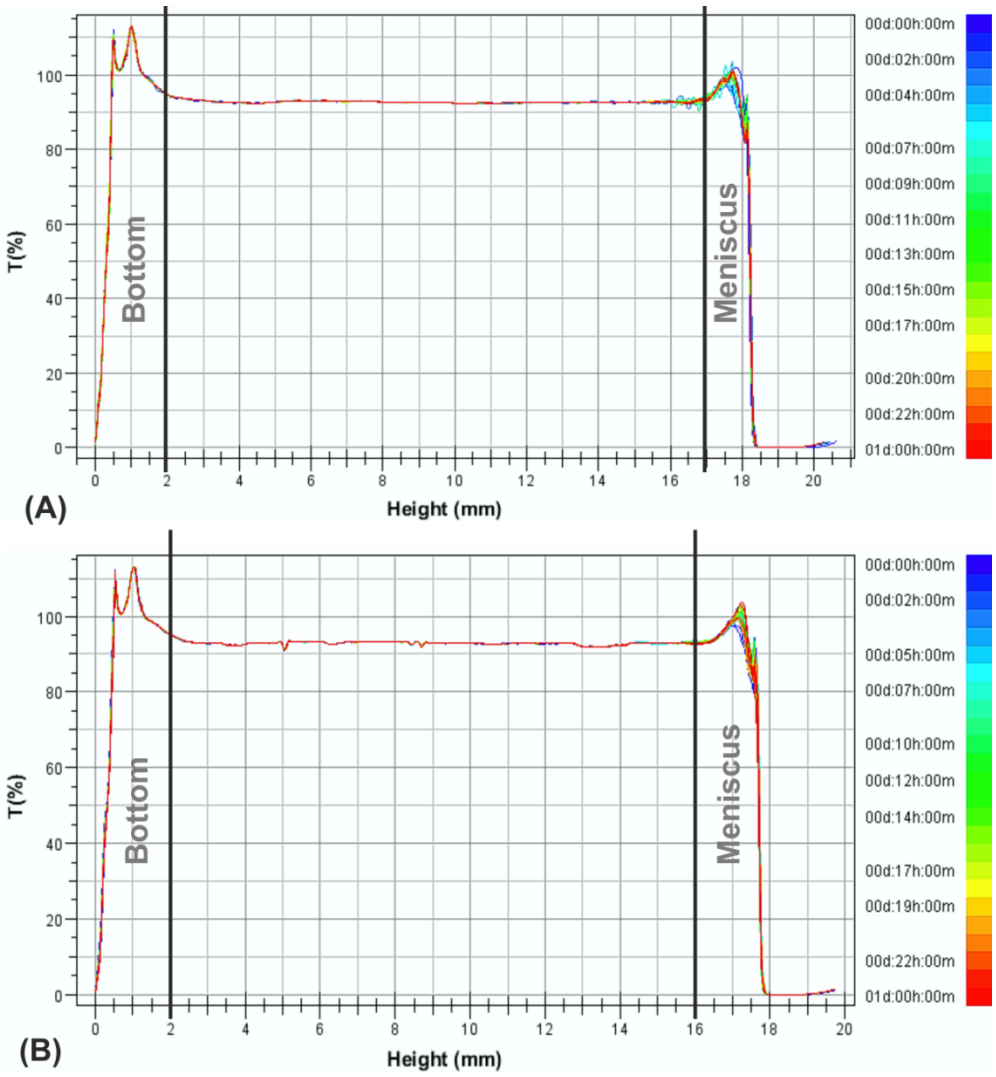

Figure 27. Transmission profiles of PEG-ME (A) and Lip80-ME (B). Data are reported as a function of time (0-24 h) as well as sample height (2-16 mm).

Bottoms of glass vials besides the meniscus of formulations were excluded from the evaluations. Black lines in Figure 27 frame the screened sample area from 2 to 16 mm. It is clearly visible that no increase or decrease in T-values occurred. In Figure 27 diagrams A and B show stable formulations over the complete measurement time.

4.1.2.2 Dynamic Light Scattering

Table 2 lists characteristic physical properties of ME systems like viscosity (Vibro Viscometer SV-10, A&D Company Limited, JPN), refraction index (manual Abbe Refractometer) and density (m/V) which were performed and used for the examination of dynamic light scattering. They are also important for the prediction of application behaviour, e.g. pipetting or spreading on human skin.

Table 2. Selected physical properties of Lip80-ME and PEG-ME. All measurements were performed at 22 °C.

Test system	**Viscosity η (mPa*s)**	**Refractive Index n_T^D (°)**	**Density ρ (g/mL)**
Lip80-ME	11.33	1.37	0.97
PEG-ME	23.53	1.37	0.97

The determined dynamic viscosity of PEG-ME was twice as high as Lip80-ME (Table 2). These deviations are probably based on different surfactant structures and their varying viscosities. Compared to purified water (0.98 mPa*s, 22 °C) and PO CC 497 (2063 mPa*s, 22 °C) the formulations were of rather low viscosity. However, the results of refractive index and density were identical.

The physical parameters in Table 2 are crucial for droplet size calculations via dynamic light scattering technique and subsequent evaluations of ME systems microstructure. Figure 28 shows the intensity distribution of PEG-ME (A) and Lip80-ME (B) obtained in triplicate.

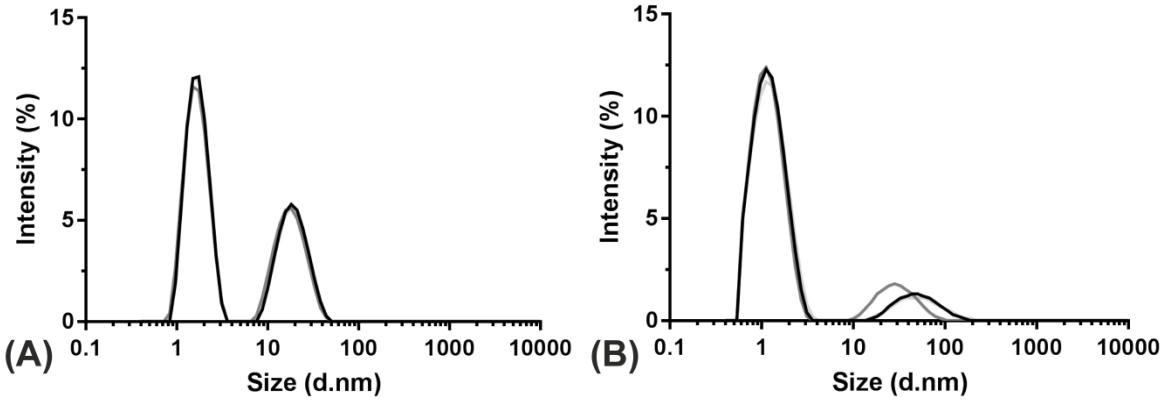

Figure 28. Intensity size distribution of tested ME. (A) shows peaks of droplet size measurements of PEG-ME and diagram (B) of Lip80-ME. (n = 3)

The results presented reproducible intensity patterns with calculated z-average diameters of 1.4 nm (A) and 1.2 nm (B), respectively. PDIs above 0.1 (PEG-ME 0.1 < 0.5 and Lip80 0.1 < 0.3) demonstrated a broad scattering of particle sizes and confirmed the bimodal distribution of both formulations, shown in Figure 28. Distribution curves of diagram A and B are characterised by a decreased intensity pattern to higher droplet sizes (second peak). Despite the property of large particles to scatter the light much more than small particles, the signal intensity is considerably low compared to smaller particles Hence, first peaks around 1 nm represented the dominant droplet sizes of ME formulations.

Stability measurements over 24 h resulted in no changes of droplet sizes as well as intensity distributions (for comparison of z-average 0 h/24 h and PDI 0 h/24 h data see Appendix (chapter 8.3).

Figure 29 shows the intensity size distribution of ME systems obtained by dilution of pre-concentrated lipophilic suspensions with PBS. 1 mg/mL of catalase was suspended in the lipophilic-surfactant/cosolvent pre-formulation. Protein-loaded ME diagrams are overlaid with distributions curves of pure formulations (red dotted lines in Figure 29, A and B).

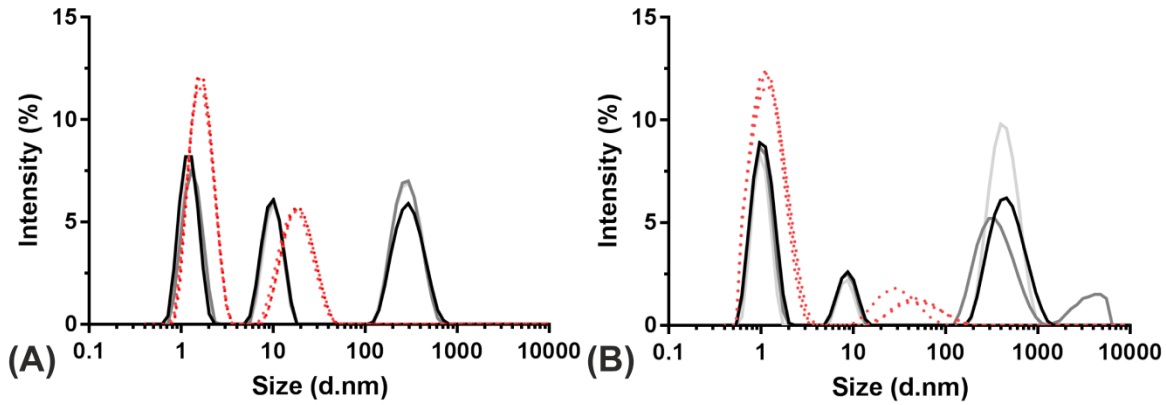

Figure 29. Overlaid plot of the pure ME (red dotted lines) and ME containing dissolved catalase (black/grey). Diagram (A) represents measured particle size distribution of PEG-ME next to diagram (B) with the results of Lip80-ME. (n = 3)

In Figure 29 diagram A and B an additional peak arises at approximately 0.3 microns, caused by the dissolved protein. Compared to the unloaded formulation curves (red dotted lines), protein-loaded ME curves showed a shift to smaller particle sizes as well as a redistribution of peak intensities. Particularly, the intensity profile of PEG-ME (Figure 29, A) presented three peaks with almost the same intensity distribution. The incorporation of catalase in PEG-ME led to an increase of large particles which concurrently weakened the signal intensity of smaller droplets.

In Figure 29, B the shift of second peak is most pronounced. Following the dissolution of protein in Lip80-ME, particle sizes altered from a z-average of 57 nm to 8 nm. Contrary to the evenly distributed intensities of PEG-ME, the signal intensities of Lip80-ME, especially the peaks at highest sizes, displayed strong fluctuations between measurement repetitions.

In consideration of present intensity detections (Figure 29, A and B) protein-loaded MEs showed a bimodal particle size distribution, whereas the dissolution of the model enzyme in MEs led to a multimodal distribution. Both ME systems, protein-loaded and -unloaded, presented very small droplets in a range of 1 nm.

4.1.3 Analysis of Protein Stability in Microemulsion Systems

In this study stability analysis includes not only the assurance of formulation stability during the application period but the control of API stability as well. Characterisations of ME formulations stability were already described (chapter 4.1.2). Following chapters will present various methods to analyse the behaviour of model protein in the ME systems.

4.1.3.1 Catalase Activity Assay

The suitability of photometric determinations to detect changes in catalase activity was examined utilising targeted destabilisation processes.

As positive control 1 % of enzyme was diluted in 50 mM PBS pH 7.0. Figure 30 depicts three single sequent measurements at pH 7.0, 25 °C, while one experiment took approximately 5 min. In the preferable environment, the maximum measurable activity was 3584 U/mg (equation *(2)*, chapter 3.2.5). As shown in Figure 30 even the optimal value was subject to variations (n = 3, 3584 U/mg ± 186 U/mg).

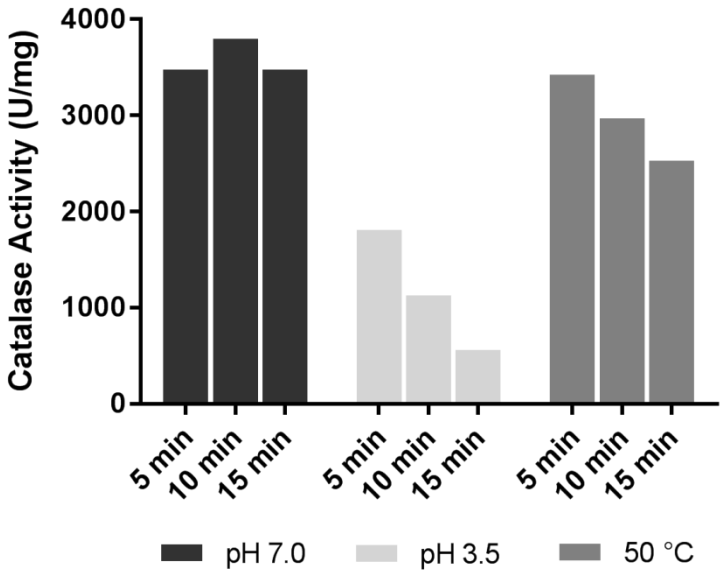

Figure 30. Catalase activity analysis under various conditions; pH 7.0/25 °C, pH 3.5/25 °C and pH 7.0/50 °C Single data of sequent performed measurements are displayed.

An acid-treatment of the 1 % catalase solution induced a first destabilisation. The enzyme was diluted in 50 mM PBS pH 7.0 and afterwards acidified with phosphoric

acid to pH 3.5. In an acidic environment catalase showed an immediately started inactivation of 50 % after 5 min (1812 U/mg, Figure 30). After 10 min and 15 min contact time the activity decreased from 1127 U/mg to 563 U/mg, continuously. In comparison to a stable solution at pH 7.0, the total loss of enzyme activity after 15 min acid-treatment was 84 %. Between 10 min to 15 min catalase started to precipitate from the acidic solution. This visible enzyme degradation process confirmed the loss of activity.

A slower reduction of catalase activity was examined for heating of the stable 1 % catalase solution pH 7.0 up to 50 °C (Figure 30). Monitored in 5 min steps also, the substrate turnover started at 3423 U/mg and was calculated to 2529 U/mg, finally after 15 min. Under these conditions a total loss of activity of about 29 % and no enzyme precipitation were observed.

ME formulations stabilised with Lip80 or PEGylated surfactants were prepared, including 1 % of model enzyme. Activity values were calculated in % with respect to 100 % activity of an unchanged 1 % phosphate-buffered catalase solution pH 7.0 (positive control, Figure 31 and Figure 32). Figure 31 demonstrates the decrease of enzyme activity in Lip80-ME over 24 h at ambient conditions. Changes were detected directly after mixing the final protein-loaded ME (0 h) and frequently every hour for the first 3 hours storage time and then again after 18 h and after 24 h, respectively.

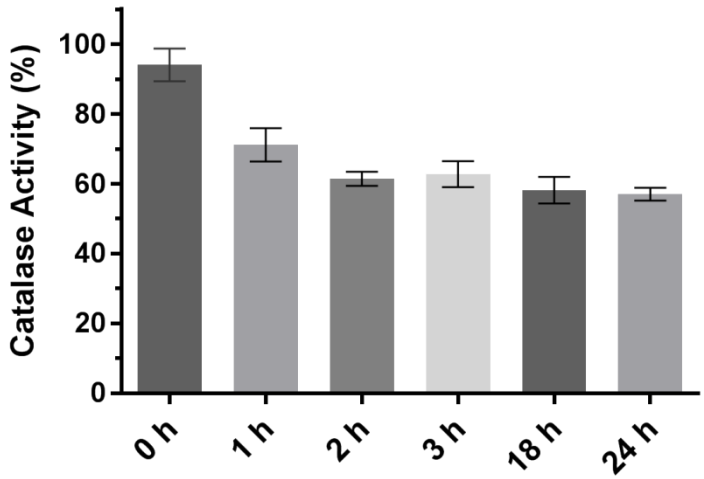

Figure 31. Time-dependent changes of catalase activity in Lip80-ME. The activity is calculated in comparison to a positive control, set as 100 % activity. n = 3, error bars indicate the standard deviation.

The most pronounced decrease of 24 % was observed during the first hour after preparation. In the subsequent monitored storage time, catalase activity varied around an activity of 60 %.

In following experiments the influence of the PEGylated ME on model enzymes activity was examined at ambient conditions (Figure 32). Compared to the phospholipid-based system this formulation showed a strong inactivation of 62 %, directly after the preparation (0 h).

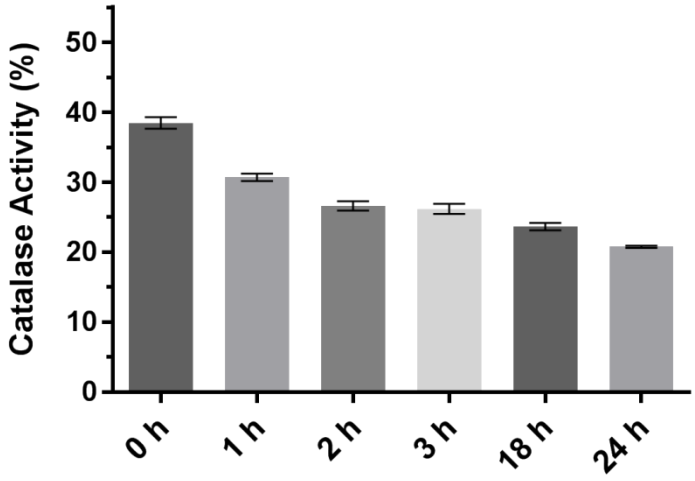

Figure 32. Time-dependent changes of catalase activity in PEG-ME. The activity is calculated in comparison to a positive control, set as 100 % activity. n = 3, error bars indicate the standard deviation.

During the following 24 h catalase continuously lost its activity from 1497 U/mg (0 h) to 812 U/mg (24 h). The overall loss of enzyme activity in PEG-ME after 24 h was 79 % compared to the positive control.

Enzyme precipitations from both ME formulations were not observed. It was assumed that the detected decrease of the substrate turnover of catalase was due to structural alterations of the enzyme.

4.1.3.2 Size Exclusion Chromatography

Catalase is a tetrameric structured enzyme with a total molecular weight of approximately 240 kDa [23]. In Figure 33 the size exclusion chromatography (SEC) profile of a stable phosphate-buffered catalase solution pH 7.0 is shown.

The chromatogram of catalase is characterised by a major peak with a corresponding peak shoulder at a retention time (R_t) of 16 min. Using calibration standards between 2000 kDa (blue dextran) and 13.7 kDa (ribonuclease A) it was possible to classify the molecular size of the catalase peak.

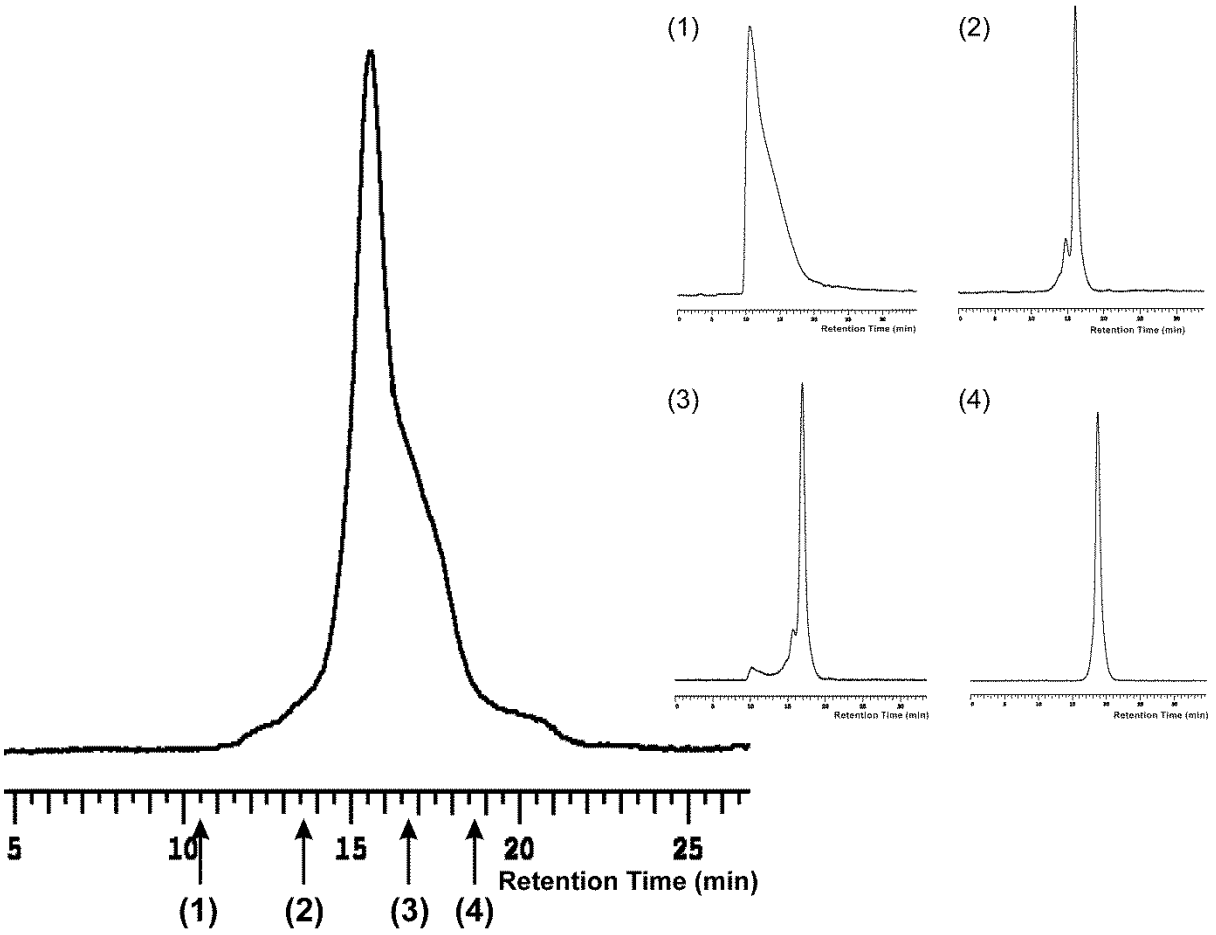

Figure 33. SEC profiles of bovine liver catalase and molecular weight standards (1-4). Arrows in the catalase chromatogram mark the retention time of molecular weight markers: (1) blue dextran 2000 kDa; (2) bovine serum albumin 67 kD; (3) ovalbumin 42 kDa; and (4) ribonuclease A 13.7 kDa. Catalase elutes as monomer with a molecular weight of 60 kDa between (2) and (3).

As shown in Figure 33 the catalase peak eluted between bovine serum albumin and ovalbumin. Thus, catalase was detected as monomer with a molecular weight of 60 kDa (chapter 3.1.3).

Besides the calibration of the measuring range it was required to determine the sensitivity of the chosen setup in detecting 3D-structural changes within the enzyme.

As already conducted in chapter 4.1.3.1, acid and heat stress tests were applied to induce a denaturation and to determine changes in detection signals (Figure 34).

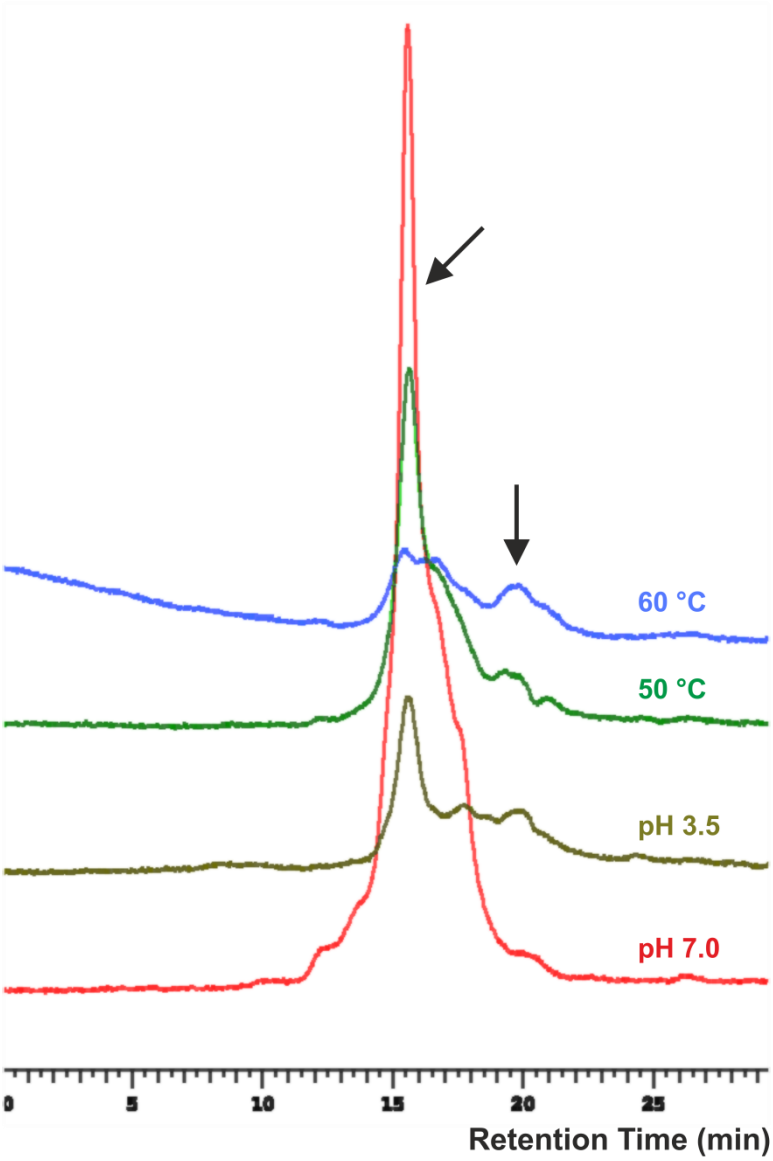

Figure 34. SEC profiles of bovine catalase under various conditions. Arrows mark regions of interest with loss of signal intensity (arrow at R_t 16 min) or the elution of new peaks (arrow at R_t 20 min).

The reduction from pH 7.0 to 3.5 led to protein destabilisation. The major peak is assigned to the catalase monomer and minor peaks correspond to destabilised parts of the protein structure. With longer storage time at pH 3.5 the protein lost its native structure and the solubility in an aqueous environment decreased, thus it started to precipitate. Insoluble, precipitated parts of the protein stayed in the SEC column and caused a decreased signal intensity (chapter 4.1.3.1).

The SEC profile of catalase at 50 °C showed less structural changes of the protein compared to the signal detected at 60 °C. When the temperature was increased the amount of destabilised protein parts increased, too. Concurrently, the intensity of peaks decreased, due to the starting precipitation.

SEC analyses of catalase under various conditions resulted in peaks of degraded protein structures at a similar R_t of 20.3 min. The molecular weight of detected structures must be lower than the molecular weight of ribonuclease A (13.7 kDa), because it eluted approximately 2 min earlier (Figure 33).

These investigations proved the ability of SEC to detect changes in protein structure. Further analyses dealt with the challenges to determine the behaviour of protein in ME formulations. It is essential to differentiate between signals from catalase monomer or its degradation products and those originating from formulation excipients. Figure 35 depicts the chromatograms of Lip80-ME (Figure 35, A) and PEG-ME (Figure 35, B) excipients.

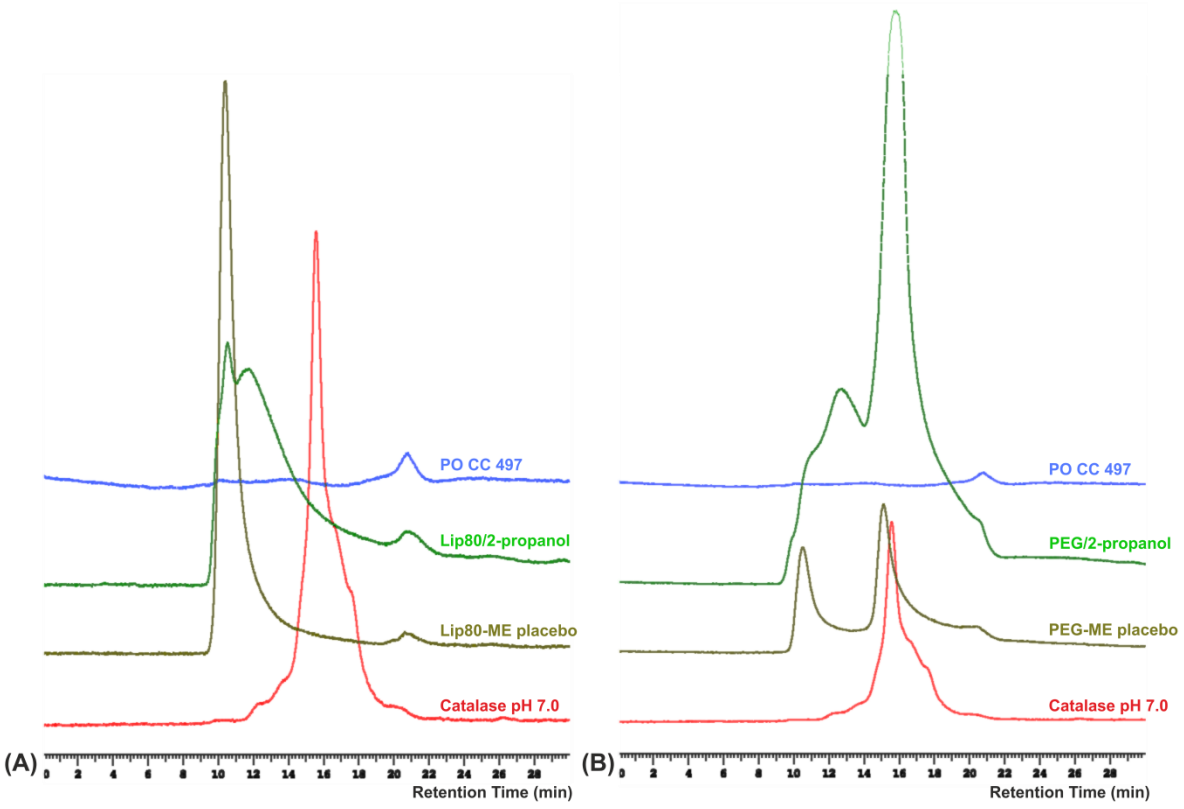

Figure 35. Chromatograms of pure (A) Lip80-ME and (B) PEG-ME excipients. The catalase solution pH 7.0 is plotted in each diagram as comparison.

Both diagrams in Figure 35 (A and B) show that the lipophilic phase PO CC 497 generated a small signal at a R_t of 21 min. The surfactant/cosolvent mixture of each ME formulation induced a high signal with a large peak area. Compared to catalase pH 7.0, Lip80/2-propanol appeared earlier at 10 min with a strong tailing besides a splitted top (Figure 35, A). The signal intensity of the PEG/2-propanol peak was much higher than the Lip80/2-propanol peak (Figure 35, B). The signal of PEG/2-propanol was splitted into two incompletely seperated peaks, whereas the main peak appeared simultaneously with the signal of catalase monomer.

The complete formulation Lip80-ME placebo eluted as a smaller and uniformly shaped peak compared to the single surfactant/cosolvent phase. Despite different peak shapes both signals were detected at the same R_t (10 min). Afterwards, the PO CC 497 signal appeared unchanged at 21 min. The catalase monomer eluted between the surfactant- and lipohilic phase signal, hence there is no risk of an overlapping of signals.

It was shown, that the signals of excipients injected solely differed from the chromatogram of formulated ME. This also holds true for the measurements of PEG-ME in Figure 35, B. While PO CC 497 eluted unchanged at 21 min, the signals of surfactant/cosolvent phase and the final ME were different compared to those detected in diagram A. PEG-ME placebo eluted in two overlayed peaks and a slightly shifted R_t compared to the signal of PEG/2-propanol phase. However, the SEC-chromatogram of PEG-ME placebo overlapped the signal of catalase. This simultaneous elution complicated the identification of changes in the structure of enzyme.

In following experiments, ME formulations were loaded with 1 % catalase and examined regarding their influence on the enzyme structure. Time-dependent analyses of catalase stability in Lip80-ME (diagram A) as well as in PEG-ME (diagram B) are depicted in side-by-side chromatograms in Figure 36.

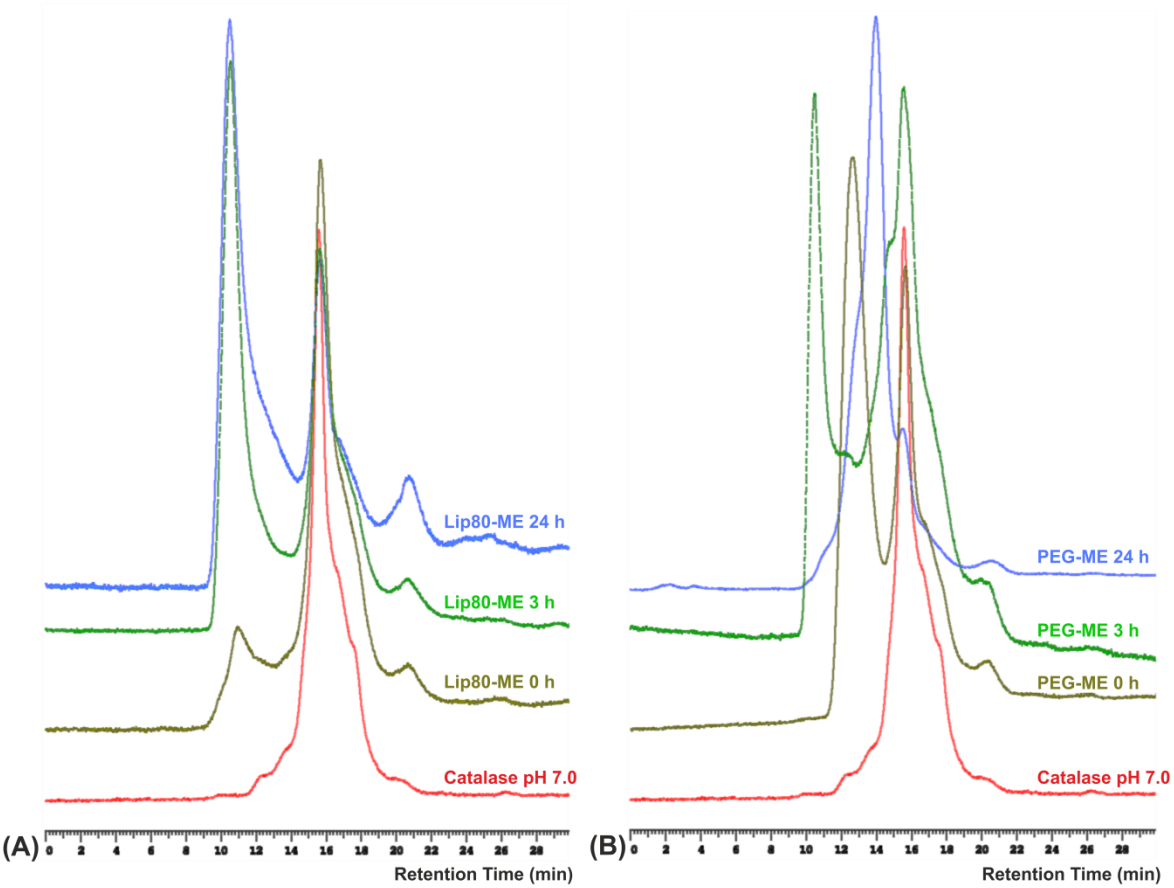

Figure 36. SEC graphs of time-dependent analyses of catalase changes in (A) Lip80-ME and (B) PEG-ME.

Protein-loaded ME formulations were prepared and injected directly (0 h), 3 h later and after 24 h, respectively.

Directly after preparation of the phospholipid-based ME (0 h) the detected chromatogram can be characterised by three incompletely separated peaks (Figure 36, A). Initially, at approximately 10 min, Lip80/cosolvent phase eluted as a small peak before the catalase monomer signal at 16 min. Afterwards, the lipophilic phase appeared with its typical low signal intensity. The sample representing the ME 3 hours after preparation showed an increased surfactant peak, shaped like the signal of pure components (Figure 35, A). The other two signals (catalase monomer, lipophilic phase) appeared in a similar size and R_t compared to Lip80-ME directly after preparation.

Lip80-ME 24 h presented a more pronounced tailing of the first peak and a lower recovery of the catalase peak. Contrary to measuring times at 0 h and 3 h,

the lipophilic phase appeared in an increased peak signal. Changes of enzyme structure with a redistribution of molecular sizes were assumed. One part of destabilised protein formed smaller degradation products next to catalase monomer and eluted later. This shift in R_t led to an overlapping with the PO CC 497 signal and hence an increase in intensity. Instabilities of protein structure caused also the formation of larger protein aggregates, they eluted earlier compared to catalase monomer and overlapped with the signal of surfactant/cosolvent phase increasing the intensity of peak, too.

In comparison to previous analysed Lip80-ME the interpretation of SEC results of protein stability in PEG-ME (Figure 36, B) was more challenging. The examination of SEC signals induced by catalase or its degradation products was complicated by the peaks of PEG-ME which eluted at same retention times.

The chromatogram of protein-loaded PEG-ME 0 h was characterised by two incompletely separated major peaks and a minor peak. The major peak corresponded to two retention times: a signal at 13 min and another one, corresponding to the catalase monomer at a retention time of 16 min. This peak was linked to a minor peak (R_t = 21 min) corresponding to PO CC 497. In Figure 35, B no signal was observed matching the first peak at 13 min. It was assumed that this peak is a combination of the PEG-ME signal and large protein aggregates. The ongoing shift of SEC signals to earlier retention times at 3 h and 24 h after preparation confirmed this hypothesis. However, the catalase peak at 0 h looked like the pure catalase signal at pH 7.0. 3 h later the peak eluted with a larger area and was more irregular shaped. A completely altered separation profile of PEG-ME was detected after 24 h. One major peak at 14 min indicated severe changes of ME formation and enzyme structure.

SEC measurements of protein-loaded Lip80-ME and PEG-ME demonstrated the challenges of protein stability analysis out of "multicomponent" mixtures like MEs with an interfering potential. Overlapping signals were especially observed in the SEC profiles of PEG-ME including 1 % catalase.

4.1.3.3 nanoDSF

To verify changes in protein stability within ME formulations the ratio of fluorescence intensities at 350 nm and 330 nm (conformational stability) as well as the backscattering intensities (colloidal stability) were examined. As performed in previous investigations (chapter 4.1.3.1 and 4.1.3.2), nanoDSF measurements utilised acid and heat stress to induce protein degradation. The F350/F330 ratio of stable (pH 7.0) as well as destabilised (pH 3.5) catalase are plotted in Figure 37, A and B.

In contrast to destabilised catalase at pH 3.5, the sample at pH 7.0 presented a measurable thermal unfolding transition. The inflexion point in the curve of fluorescence ratio (Figure 37, A) and correspondingly the peak of the first derivative (Figure 37, B) are defined as the unfolding transition temperature T_m which was found to be at 56 °C for the stable catalase solution. However, no peak in the first derivative and hence no defined melting temperature could be found for the destabilised protein sample. Figure 37, C shows the tendency of protein aggregation in test solutions. Whereas the sample at pH 7.0 presented a low signal of scattered light (0.108 A.U. at 20 °C), the intensity increased with increasing destabilisation. Already the initial value of 0.158 A.U. (at 20 °C) of protein solution at pH 3.5 was higher demonstrating a loss of colloidal stability.

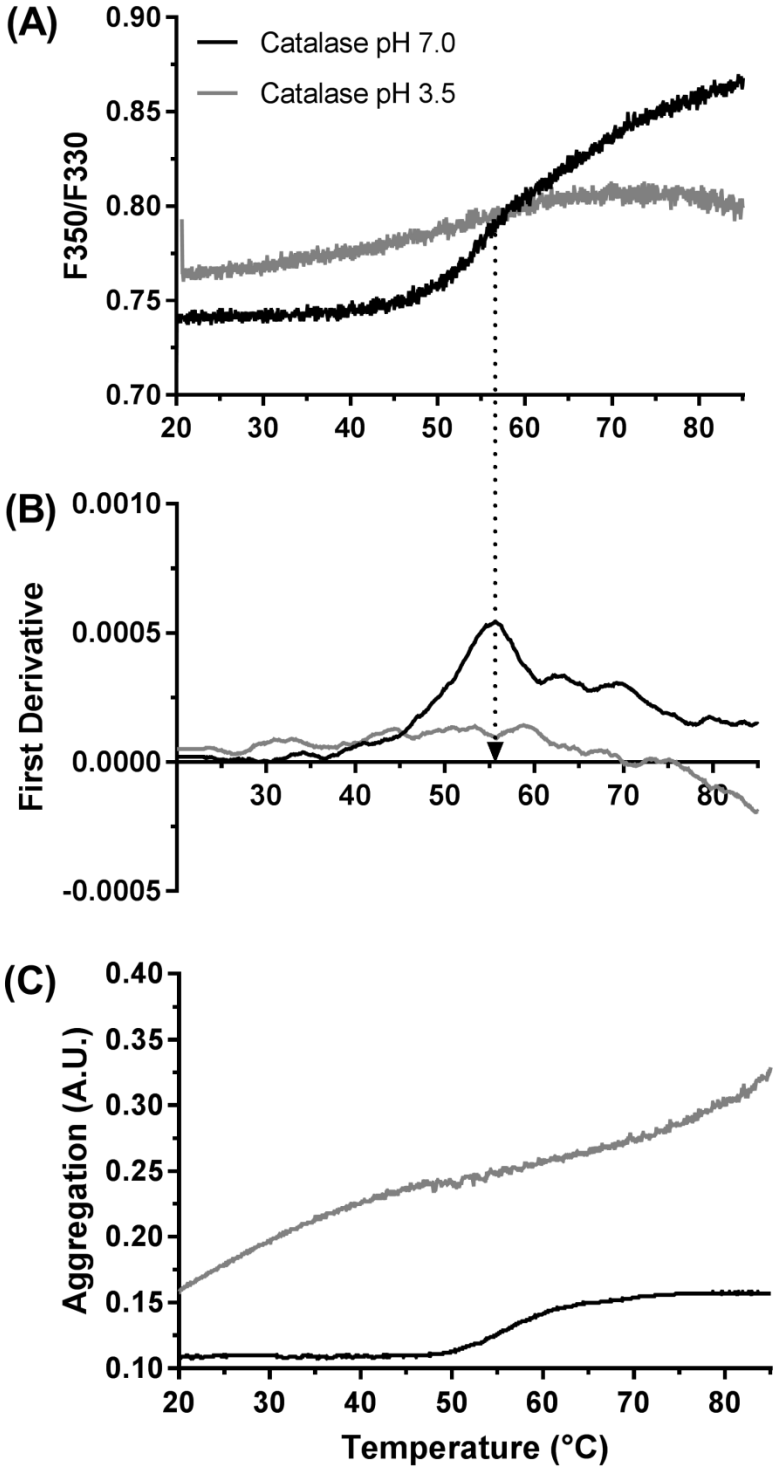

Figure 37. Conformational stability and aggregation of bovine liver catalase at optimal pH 7.0 and destabilising pH 3.5. Diagram (A) shows the ratios of fluorescence intensities at 350 nm and 330 nm of both catalase formulations. (B) presents the first derivative of (A), the arrow indicates T_m at 56 °C of buffered catalase solution. (C) depicts the aggregation detected by changes in backreflection.

Thermal unfolding curves of protein-loaded ME formulations are presented in Figure 38. The resulting unfolding signals in F350/F330 ratio showed two different profiles generated by the ME-systems (Figure 38, A and B).

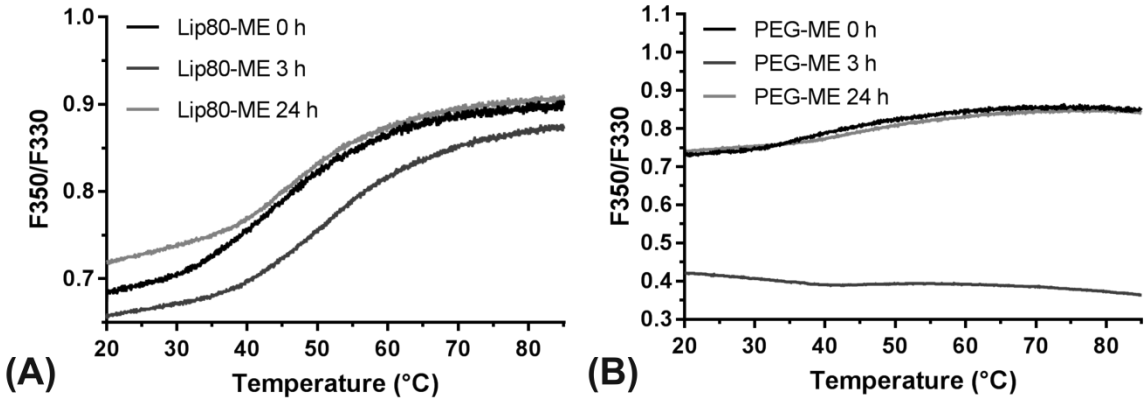

Figure 38. Ratios of fluorescence intensity at 350/330 nm present thermal unfolding curves of catalase in (A) Lip80-ME and (B) PEG-ME. Changes in conformational stability are examined at 0 h, 3 h and 24 h.

A clearly defined transition of Lip80-ME curves was detectable up to 24 h after preparation (Figure 38, A). PEG-ME curves were characterised by transitions with a smooth progression comparable to the destabilised catalase solution at pH 3.5 (Figure 37, A and Figure 38, B).

Calculated T_m values at 0 h, 3 h and 24 h for Lip80-ME are listed in Table 3. The temperature at which half of the protein is unfolded was changed in Lip80-ME compared to the stabile protein structure at pH 7.0. 3 h after Lip80-ME preparation the structure of protein changed to an unfolding at higher temperature, whereas at 24 h a declined T_m was detected. After 24 h the F350/F330 curves as well as the calculated T_m were like 0 h samples. No T_m was calculable for PEG-ME samples because of the smooth progression of fluorescence curves.

Table 3. Unfolding transition temperatures (T_m) and aggregation values (agg.) at 20 °C of catalase. Results are calculated after 0 h, 3 h and 24 h of ME preparation.

	Lip80-ME		PEG-ME	
	T_m (°C)	**Agg. (A.U.)**	**T_m (°C)**	**Agg. (A.U.)**
0 h	44.0	0.321	Unfolded	0.318
3 h	52.0	0.214	Unfolded	0.422
24 h	45.5	0.398	Unfolded	0.445

Results of Lip80-ME and PEG-ME F350/F330 ratios demonstrated differences in conformational stability between the two systems. The loss of conformational stability and likewise the unfolding of enzyme were more pronounced in PEG-ME, presented by the missing transition points of fluorescence curves. Directly after PEG-ME preparation a main part of the enzyme was already unfolded. As shown in Figure 38, B an increase of temperature did not led to further denaturation processes in PEG-ME 0 h.

Changes in colloidal stability of enzyme in both MEs were also examined and are shown in the following section. Single backscattering values in A.U. at 20 °C enable an overview of the initial state of model enzyme in MEs (Table 3). Lip80-ME at 3 h showed a decreased backscattering value compared to the initial status at 0 h. Most pronounced was the colloidal instability after 24 h storage time resulting in the highest backscattering.

PEG-ME showed increased aggregation behaviour with increasing measurement time (Table 3). Higher backscattering values of catalase in PEG-ME indicated a more pronounced colloidal instability compared to Lip80-ME. Figure 39 shows the progression of backscattering intensities with increasing temperature.

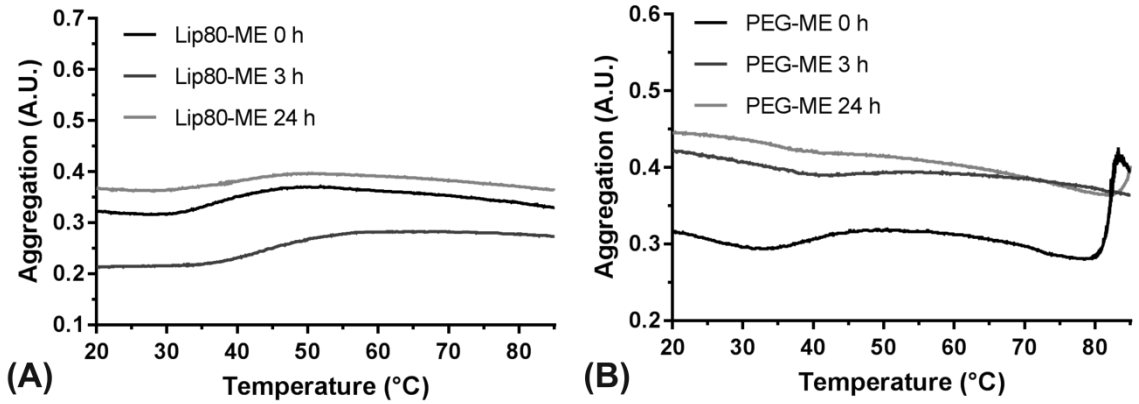

Figure 39. Aggregation behaviour of catalase in (A) Lip80-ME and (B) PEG-ME after 0 h, 3 h and 24 h.

Backscattering curves of Lip80-ME at 0 h, 3 h and 24 h suggest an increase in aggregation with rising temperature (Figure 39, A). Above 50 °C formed enzyme aggregates seemed to dissolve, resulting in declining curves. The aggregation curve of catalase in PEG-ME at 0 h ran irregular, whereas after 3 h and 24 h curves showed a decrease (Figure 39, B) comparable to Lip80-ME curves. However, the highest backscattering values were measured in the initial state at 20 °C and started with rising temperature to decline as Lip80-ME in Figure 39, A. The observed peaks above 80 °C in Figure 39, B can be attributed to measurement artefacts caused for example by air bubbles in sample capillaries.

Lip80-ME and PEG-ME presented changes in colloidal stability. But as already observed for conformational enzyme instabilities, colloidal instabilities in PEG-ME were more pronounced as in Lip80-ME.

4.2 Evaluation of a Needle Device

In this thesis, it is envisaged to combine the application of a protein-loaded ME formulation with a prior microneedling step. Three needle devices (chapter 3.1.4) were examined regarding their reproducibility and efficiency in forming microchannels into human cadaver skin. Furthermore, the needle device should be suitable for the application in tolerability studies with 3D-human skin models. Special requirements here are the small skin surface (1 cm^2) and the lateral boundary of the transwell system.

The measurements were performed in comparison to a reference needle device. As reference a single-use, disposable needle for intramuscular injections (specification 0.90 x 50 mm) was selected due to its strong potential to induce deep channels into the uppermost skin layers.

4.2.1 Microchannel Morphology

Heat-separated epidermis sheets (6.0 mm in diameter, ⌀) were perforated with the different microneedle devices and the morphology of created pores was examined via scanning electron microscopy (SEM). SEM technique enabled the recording of top view images with a detailed view on pore shapes.

SEM images of the reference sample are shown in Figure 40, A. The created pores are characterised by a V-shaped incision, comparable to a lancet cut. Mainly responsible for this was the bevelled needle tip of the used cannula.

In comparison to the almost 100 µm long incision of the reference needle, the Dermaroller® created smaller pores of about 40 µm in diameter (Figure 40, B). A detailed view on the formed channel revealed an almost triangular shape (Figure 40, B detailed view). eDermastamp® and Dermastamp® (Figure 40, C and D) showed this shape as well, which was attributed to the same conical needle shape.

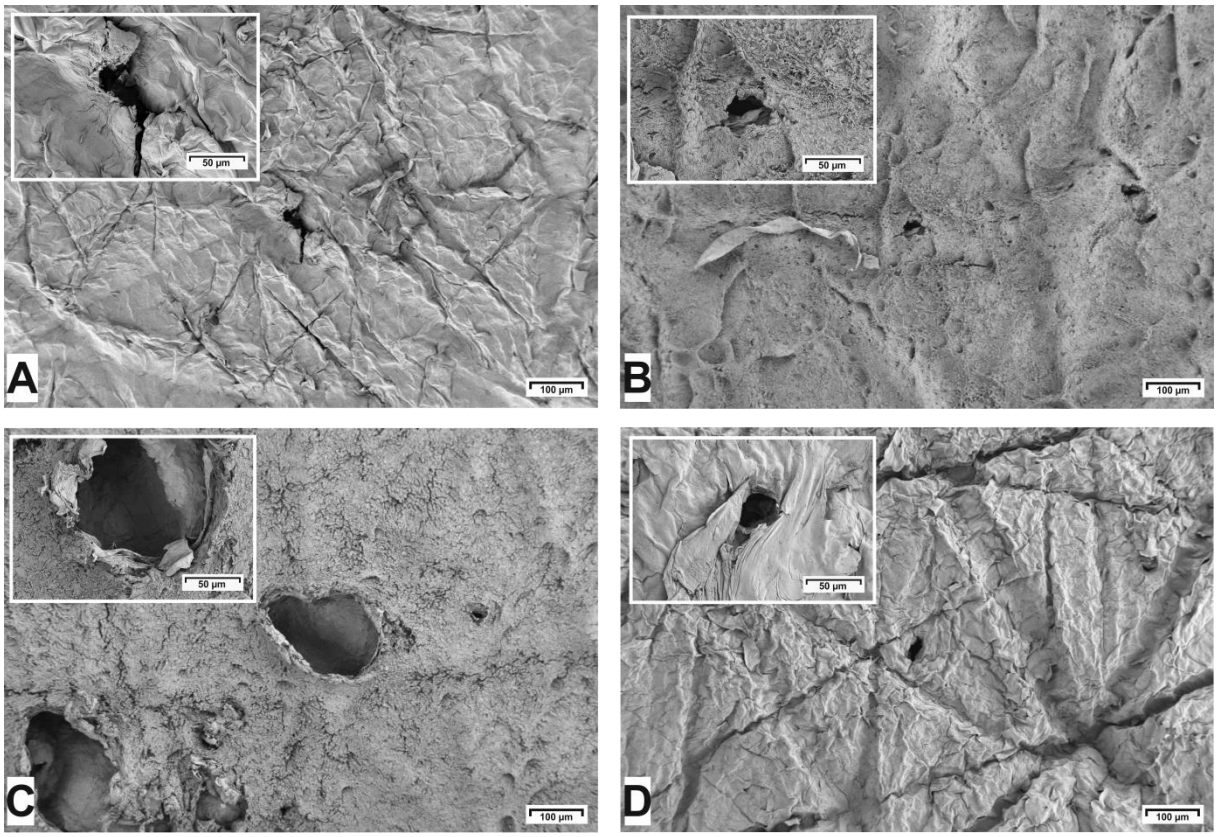

Figure 40. Scanning electron microscope images as top view on skin surface treated with (A) reference device (cannula, dimension 0.90 x 50 mm), (B) Dermaroller®, (C) eDermstamp® and (D) Dermastamp®. Images (scale bar = 100 µm) are depicted with a detailed view on the micropore (scale bar = 50 µm).

Size and shape of microchannels formed by a rolling or stamping process were comparable (Figure 40, B and D). Largest pores were achieved by using the eDermastamp® (Figure 40, C). Responsible for this was the automatic prick-frequency (100 pricks/min) during the piercing process. Besides bigger puncture sites, pores were characterised by frayed edges (Figure 40, C detailed view).

The efficiency in microchannel creation was also examined by analysing channel depth via cross-sectional images (Figure 41). A defined area (5 x 5 cm) of full thickness human skin was treated with the needle devices. Afterwards, histological sections were prepared with a cryo-microtome and analysed by light microscopy without any further staining.

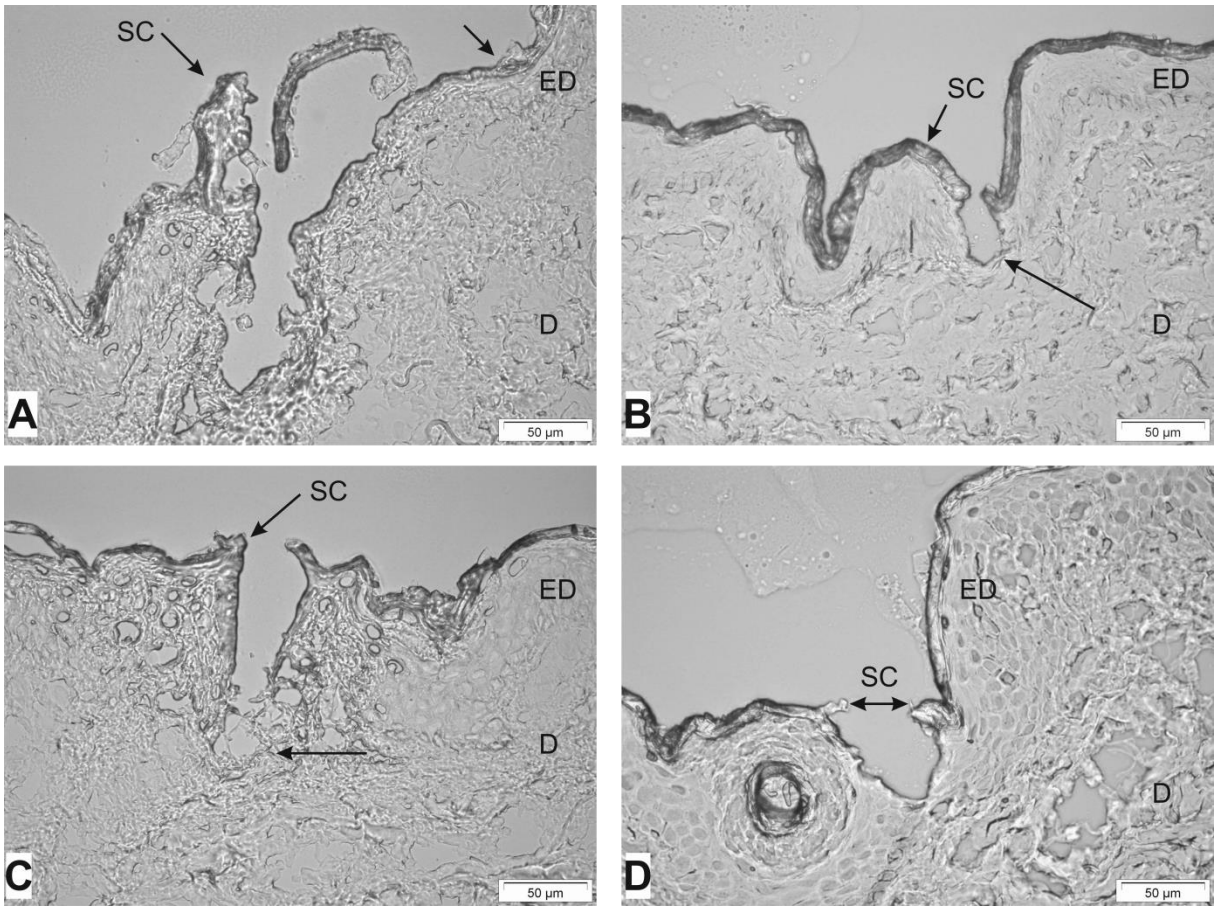

Figure 41. Bright field images of histological cross-sections of human skin treated with (A) reference device (cannula, dimension 0.90 x 50 mm) treated skin, (B) Dermaroller®, (C) eDermstamp® and (D) with Dermastamp®. The microneedles penetrated the skin (EP = epidermis, D = dermis) through the stratum corneum (SC) barrier as indicated by the arrows. (Scale bar = 50 µm)

An image of a pore formed by the reference needle device is shown in Figure 41, A. The channel ranged from the SC to uppermost layers of dermis and was approximately 200 µm deep. The channel is characterised by a rough and frayed shape.

Microchannels created by Dermaroller® were superficial and ranged with about 50 µm only into epidermal layers (Figure 41, B). Compared to the channel formed by cannula, the Dermaroller® created regular shaped pores. Shaped similar, but with a wider puncture site was the microchannel created by Dermastamp® (Figure 41, D). With a pore depth of approximately 60 µm it pierced into the epidermis, too.

The channel formed by the automatically driven eDermastamp® (Figure 41, C) was around 120 µm deep. Compared to images B and D, the uniform shaped channel in C tapered towards the tip and achieved uppermost dermal layers.

All types of microchannel devices had sharp tips and were strong enough to pierce the SC barrier of skin.

4.2.2 Assessment of Skin Integrity

TEWL is a parameter of skin barrier function and was employed to test the efficiency and reproducibility of microneedle devices to disrupt the integrity of SC. As baseline control and for calculation of skin disruption strength, the TEWL of intact skin was tested before device application. All measurements were subjected to statistical analysis to calculate differences between untreated and treated groups. Changed TEWL values were used to classify the strength of skin disruption.

The continuous water loss of intact skin was found to be 19.13 ± 1.02 g/h/m², calculated as mean of all presented measurements (Figure 42).

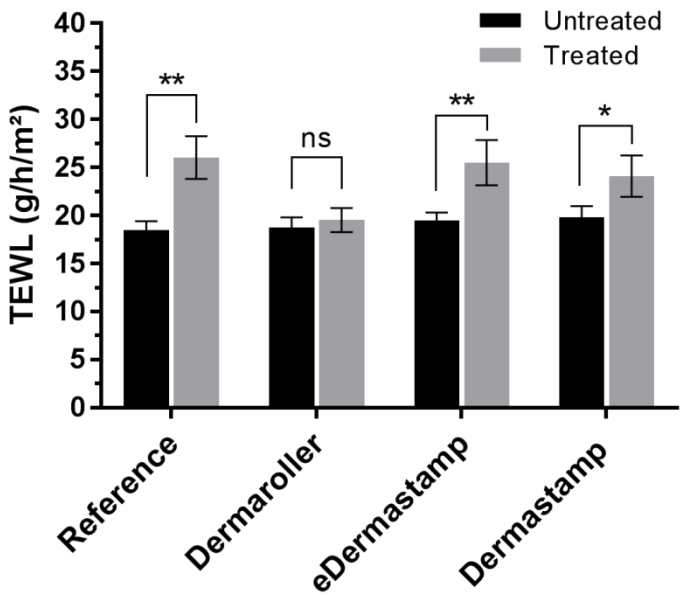

*Figure 42. TEWL values of skin before and after treatment. The cannula (reference), eDermastamp® as well as Dermastamp® showed a significant increase in TEWL values compared to untreated skin samples (one-way ANOVA, not significant (ns) p > 0.05, *p ≤ 0.05, **p ≤ 0.01; n = 5).*

The TEWL values of reference, Dermaroller®, eDermastamp® as well as Dermastamp® were measured immediately after treatment and found to be 26.03 ± 2.20 g/m²/h, 25.50 ± 2.34 g/h/m², 24.10 ± 2.14 g/h/m² and 19.53 ± 1.24 g/h/m², respectively. A significant increase (ANOVA, *p ≤ 0.05, **p ≤ 0.01) in water loss was observed as result of microchannel formation in the skin by reference device, eDermastamp® and Dermastamp®, compared to untreated skin samples. Whereas the automatically and manually driven Dermastamps reached similar TEWL values to the cannula, the Dermaroller® was significant different resulting in the lowest SC disruption.

Small standard deviations indicated a good reproducibility of the piercing by the devices. The best efficiency in forming microchannels (showing highest TEWL values) was achieved by eDermastamp®.

Requirements for the needle device which had to be considered were a high reproducibility and efficiency in forming microchannels next to the use in tolerability studies with a small application area. The Dermaroller® presented an inefficient disruption of SC and needed a large skin area for its rolling application. Hence, this device was unsuitable for the use in tolerability studies.

Best results were achieved by using the eDermastamp®, but its head was slightly bigger (⦰ 1.1 cm) than the transwell system (⦰ 1.0 cm). The Dermastamp® was finally chosen because of the smaller device head (⦰ 0.90 cm), besides a comparable reproducibility and efficiency in forming microchannels to eDermastamp®.

4.3 Skin Tolerability Studies

To examine the tolerability of developed Lip80-ME on human skin, the formulation was tested in combination with the selected needle device Dermastamp®. For comparison, a system based on PEGylated surfactants was applied and treated under equal conditions. The samples were tested on an Epiderm™ FT skin model as described in chapter 3.2.8. The effects of the formulations on skin were characterised by investigating the immunologic response next to histopathological changes. Aim of the investigation was the prediction of *in vivo* skin irritation of the developed ME system combined with a microneedling process. Therefore, Lip80-ME and PEG-ME were prepared and analysed as protein-free systems.

4.3.1 Cytokine and Cell Viability Analyses

For the immunological assessment of Lip80-ME and PEG-ME different ways of application were tested. Table 4 presents an overview of applied test systems and their individual compositions.

Table 4. Overview and compositions of applied samples in the tolerability studies.

Sample Identification	Ingredients/Application
PBS	Phosphate buffered saline pH 7.0 (TC-PBS-100 by MatTek Corp.)
SDS	0.8 % aqueous sodium lauryl sulfate solution
Lip80-ME	Placebo; 35 % Lipoid S LPC 80/2-propanol, 5 % PO CC 497, 60 % PBS
PEG-ME	Placebo; 35 % Kolliphor® EL, Polysorbate 80/2-propanol, 5 % PO CC 497, 60 % PBS
Dermastamp®	Piercing step 10 x
Dermastamp® + Lip80-ME	1. Piercing step 10 x 2. Application of test formulation
Dermastamp® + PEG-ME	1. Piercing step 10 x 2. Application of test formulation

PBS was chosen as a control group to demonstrate the influence of a well-tolerated and mild substance on 3D-human skin model. The opposite was represented by the application of a 0.8 % SDS solution. This control group was selected to induce a remarkably irritating effect on the skin model [122]. Listed samples in Table 4 were applied in triplicate on 3D-human skin and analysed after 3 h, 8 h and 24 h. To simulate extreme conditions, ME formulations were removed after the maximum period (24 h).

In this thesis, IL-1α, IL-6 and IL-8 were selected as immunological markers to characterise the influence of developed application system (microneedle device + ME) on human skin. In response to physical or chemical stresses, keratinocytes and fibroblasts produce and release, *inter alia*, inflammatory cytokines (IL-1α), secondary cytokines (IL-6) as well as chemotactic cytokines (IL-8) [123]. For further information about immune functions of the skin, see chapter 2.1.1.

IL-1α is a primary cytokine, contributively to the onset and maintenance of an inflammatory response. It stimulates the release of secondary mediators including IL-6 as well as IL-8 [124]. Figure 43 shows the IL-1α release after 24 h for all applied formulations.

A comparison between PBS and SDS demonstrated a significant difference between these two control groups. Additionally, Lip80-ME and PEG-ME were significantly different to PBS. They showed an IL-1α concentration like SDS, hence they had a comparable irritating potential after 24 h contact time.

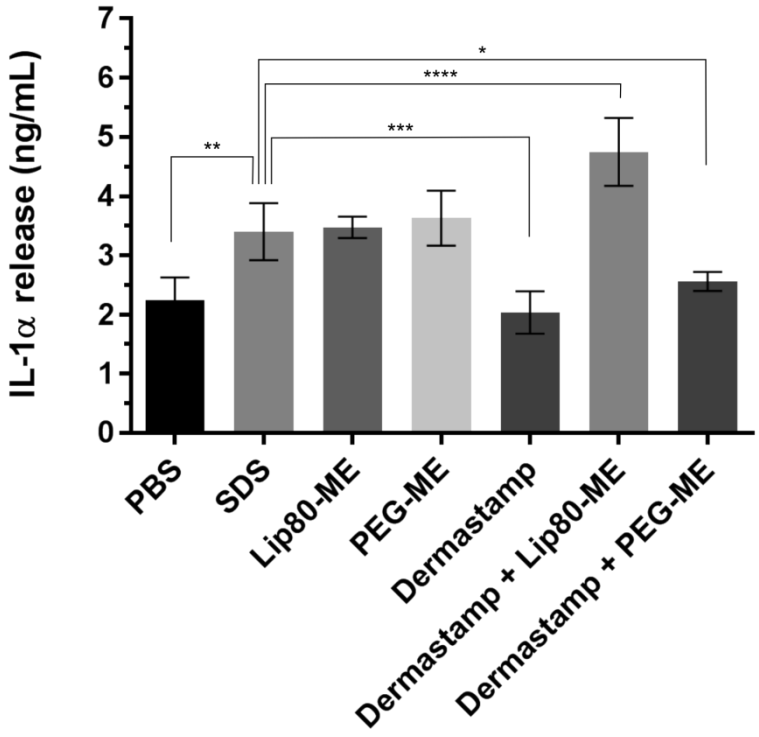

*Figure 43. IL-1α response in ng/mL after 24 h. Each column presents the mean of three obtained single concentrations and bars indicate the standard deviation. Significance levels are shown for selected groups and calculated with a one-way ANOVA *p ≤ 0.05, **p ≤ 0.01, ***p ≤ 0.001, ****p ≤ 0.0001.*

Treatment with the Dermastamp® did not show an increased level of IL-1α release compared to PBS. The same holds true for the combination Dermastamp® + PEG-ME (Figure 43). However, the application of Dermastamp® + Lip80-ME presented an elevated concentration, which was even significantly higher than the SDS solution.

IL-6 was chosen because of its crucial and versatile role in inflammatory processes caused by the pleiotropic property. Therefore, IL-6 is often used as a marker for local as well as systemic activation of proinflammatory cytokines [26,125].

For the secretion of IL-8 the presence of full-thickness skin is necessary, enabling the communication between keratinocytes and fibroblasts. IL-8 plays an important role in endothelial cell proliferation processes and shows increased intracellular concentrations after cell damages [126]. Dermastamp® induced superficial damages; hence it was envisaged to use an increased IL-8 level as control parameter for the skin microporation. Figure 44 displays the results of IL-6 release (diagram A) next to

the concentrations of IL-8 response (diagram B). Generally, the profiles as well as the changes of interleukins response look similar in both diagrams.

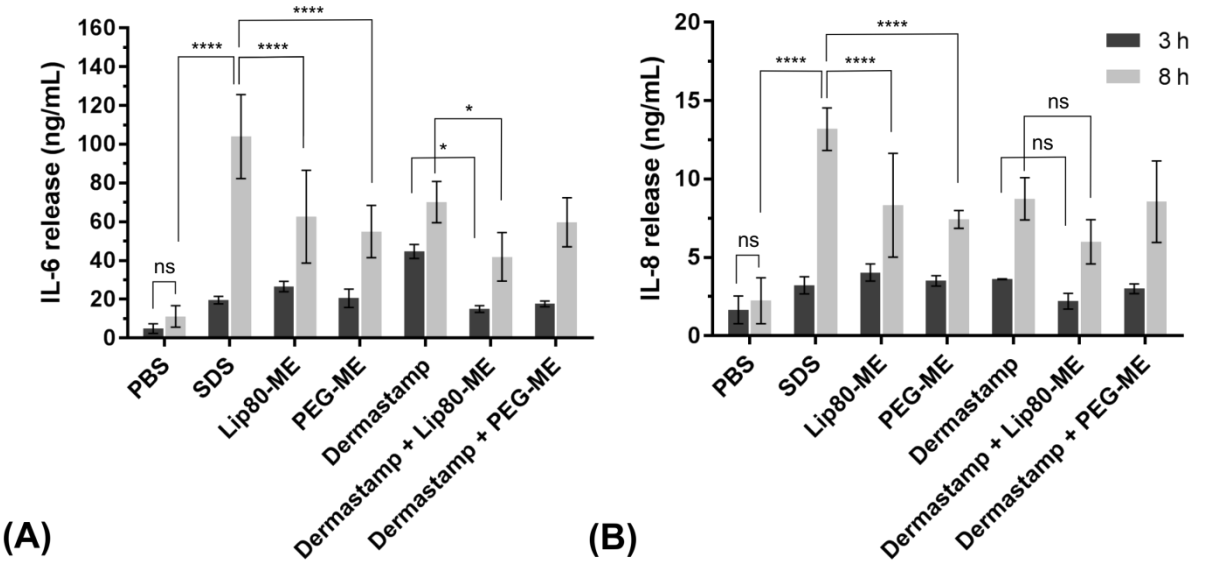

*Figure 44. Release of inflammatory biomarkers (A) IL-6 and (B) IL-8 from EFT-400 tissue into culture medium 3 h and 8 h after application. Each column presents the mean of three obtained single concentrations and error bars indicate the standard deviation. Significance levels are shown for selected groups and calculated with a two-way ANOVA as not significant (ns) $p > 0.05$, *$p \leq 0.05$, **$p \leq 0.01$, ***$p \leq 0.001$, ****$p \leq 0.0001$.*

The release of IL-6 and IL-8 upon treatment with PBS did not show a statistically significant change between 3 h and 8 h confirming stable test conditions. The application of 0.8 % SDS led to a stimulation of inflammatory processes being detected as release of IL-6 and IL-8. PBS and SDS profiles started at a similar level of IL responses (3 h), however, after 8 h exposure time IL concentrations of SDS-treated specimen increased and were statistically significant different compared to PBS. Thus, a clear induction of an inflammatory process of tested substances could be detected.

Time-dependent changes between Lip80-ME and PEG-ME regarding their tolerability on human skin were not observed (Figure 44, A and B). After 8 h both formulations resulted in increased cytokine levels compared to PBS but were significantly different to SDS.

Interestingly, both diagrams in Figure 44 show an increased cytokine response after microneedle treatment compared to the combination of needling and the application of Lip80-ME. This change was significant for the detection of IL-6, whereas IL-8 showed this effect less pronounced. PEG-based formulations did not exhibit these differences, neither after 3 h nor after 8 h exposure time.

Microneedling is harmful, but the application of ME was able to reduce the local irritating effect [39]. Presented results showed that Lip80-ME was able to reduce this effect better than PEG-ME. The weakening influence of phospholipid-based ME on the needling process which was observed for IL-6 and IL-8 (Figure 44) was not detected for IL-1α. Different sample periods and varying roles of cytokines in the inflammatory cascade might be responsible for that.

In addition to the measurement of IL-8 release the anticipated destructing effect of needle device on skin inserts was detected by analysing changes of lactate dehydrogenase (LDH) concentration in basolateral media. LDH was also quantified after 3 h and 8 h exposure time. LDH is an enzyme of cell cytosol. It catalyses the conversion of lactate to pyruvate, and *vice versa* [112]. LDH is an important parameter to control the integrity of cells: the higher the LDH concentration in medium, the more damaged is the cell [127].

The assumed initial cell damage of microneedling is presented in Figure 45. Already after 3 h the LDH level induced by Dermastamp® treatment was significantly higher than those of all other treatments. Likewise, a statistically significant increase of LDH release upon needling was observed after 8 h being even higher than the SDS level.

ME formulations did not increase LDH release compared to PBS, whereas the combination with Dermastamp® significantly increased LDH release after 8 h. However, these concentrations were not as high as in the sole use of Dermastamp®.

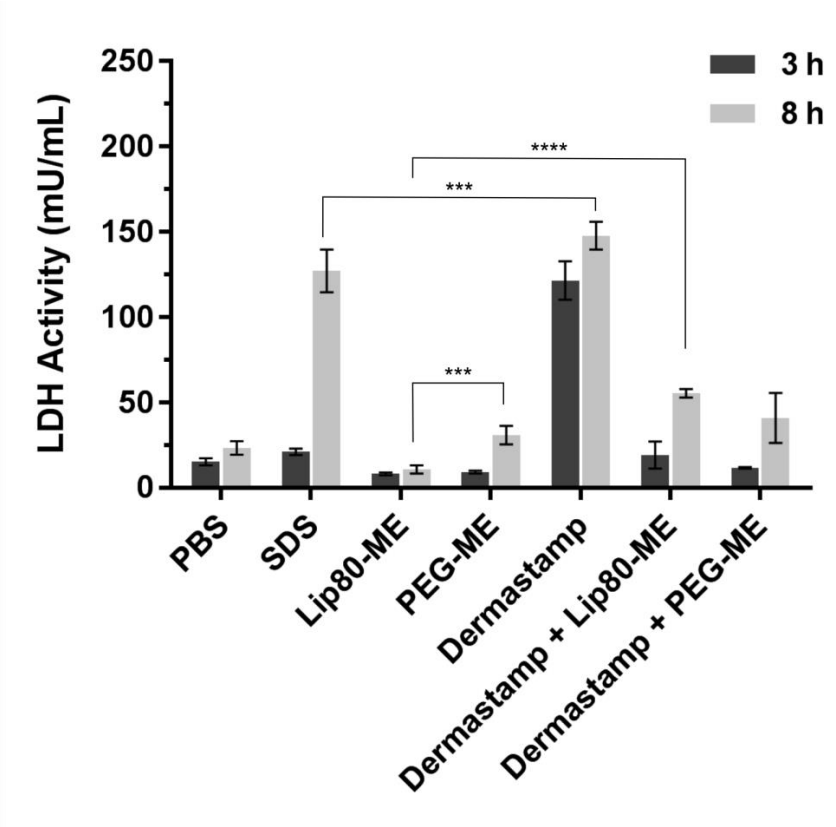

*Figure 45. Changes in LDH release after 3 h and 8 h detected as mean of LDH activity in mU/mL. Error bars indicate the standard deviation of three obtained single concentrations. Significance levels are shown for selected groups and calculated with a one-way ANOVA as *p ≤ 0.05, **p ≤ 0.01, ***p ≤ 0.001, ****p ≤ 0.0001.*

The already assumed weakening effect of Lip80-ME in Figure 44 could be confirmed by the results of the LDH assay in Figure 45. Despite the observed differences between the cytokine levels of samples treated with the needle device + microemulsion formulations (Figure 44), no statistically significant differences were measured with respect to the LDH release. In case of an application without Dermastamp®, PEG-ME showed a significantly higher LDH level compared to Lip80-ME. PEG-based ME system presented a slight tendency to have a more destructive effect on skin tissue than Lip80-ME.

4.3.2 Histological Examinations

To confirm and complete the immunological results with morphological changes, histological examinations were performed. Figure 46 depicts a characteristic image of a microneedle channel formed by Dermastamp® into Epiderm™ FT skin model.

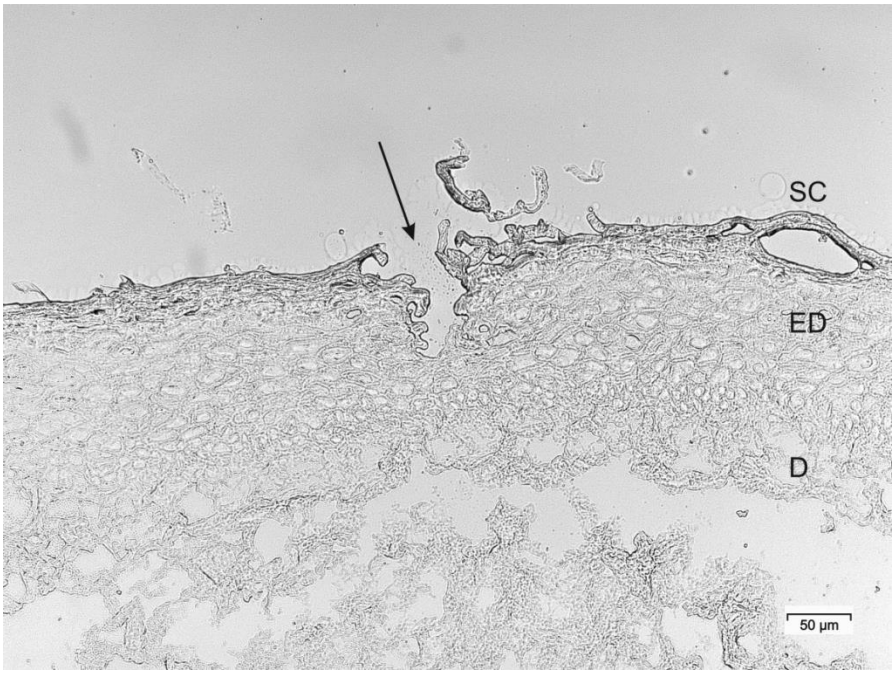

Figure 46. Histological cryo-section of EpiDerm™ FT after piercing 10 x with Dermastamp®. The arrow points at one formed microchannel. Upper layers of epidermis (ED), especially the stratum corneum (SC) are disrupted. It is apparent that the microchannel is wider at the top and tapers towards deeper epidermal layers, but is not deep enough to penetrate to dermis layers (D) lying underneath. (Scale bar = 50 µm)

The presented channel depth was approximately 100 µm. The conical shape of the needles and a cutting thickness of 5 µm made it difficult to find a complete channel section. SC, the outermost layer of skin was strongly disrupted and the microchannel, formed like a cylinder, tapered towards deeper skin layers (chapter 4.2).

Figure 47 presents H & E stained histological cross-sections of Epiderm™ FT. Epidermal layers were coloured purplish blue and were well distinguished from the pink stained dermal area.

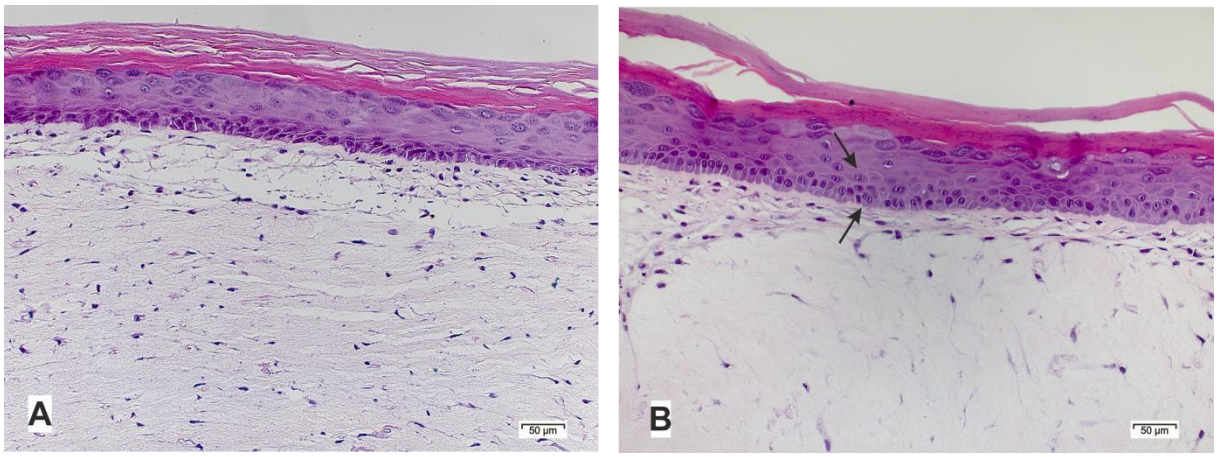

Figure 47. Histopathological examination of EpiDerm™ FT skin model after 8 h exposure of (A) PBS as mild and (B) 0.8 % SDS as irritating substance. Two arrows in (B) point at mitotically active cells in epidermis. (Scale bar = 50 µm)

Skin samples of PBS and 0.8 % SDS treatment are presented next to each other in Figure 47, images A and B. After the application of PBS all layers of epidermis as well as of dermis were normally structured and unobtrusive (Figure 47, A). However, the treatment with 0.8 % SDS (Figure 47, B) led to severe structural changes. SC was compressed in consequence of hyperkeratosis. In comparison to the PBS treated sample, the histological slice of SDS treated skin showed an irregular layering in the complete epidermal area. Mitotically active cells (arrows, image B) indicated high proliferation and led to pathological symptoms of hypergranulosis of the stratum granulosum as well as a compact hyperkeratosis of SC.

The effect of applied formulations in single use and in combination with the needle device is illustrated in Figure 48.

In comparison to PBS sample (Figure 47, A), the application of Lip80-ME (Figure 48, A) resulted in a slight hypergranulosis and -keratosis of epidermal layers. An enhanced detrimental effect was observed in combination with Dermastamp® where a hypergranulosis was emerging, causing thickened epidermal layers especially in the stratum granulosum and showing an intradermal blister (Figure 48, B arrow).

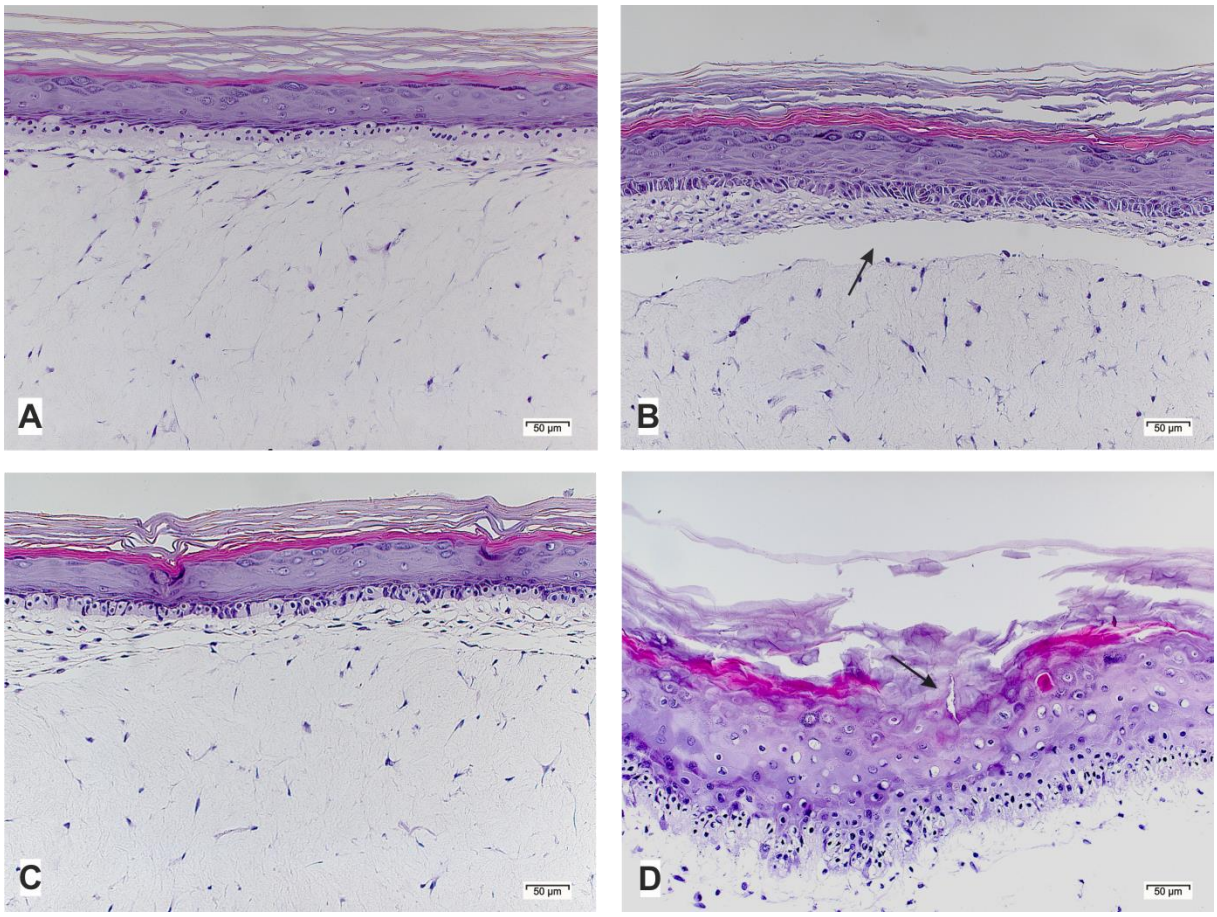

Figure 48. Histopathological examination of EpiDerm™ FT skin model after 8 h exposure of (A) Lip80-ME, (B) Dermastamp® + Lip80-ME, (C) PEG-ME and (D) Dermastamp® + PEG-ME. With Dermastamp® treated samples (B) and (D) show more distinct structural changes than (A) and (C). The arrow in picture (B) marks an intradermal blister and in image (D) a partially closed microchannel. (Scale bar = 50 µm)

The response to the treatment with reference system PEG-ME is presented in (Figure 48, C). A more thickened SC compared to Lip80-ME and a slight homogenisation of epidermal layers is shown. With regard to already observed histopathological changes of Dermastamp® + Lip80-ME (Figure 48, B), PEG-ME combined with piercing step showed an enhanced irritating effect, too (Figure 48, D). The skin perforation facilitated penetration of formulations to deeper skin layers, resulting in stronger tissue changes.

Moreover, the combination of Dermastamp® + PEG-ME resulted in a higher irritation potential compared to Dermastamp® + Lip80-ME. Image D shows a severely damaged skin with many apoptotic cells in epidermis layers. The arrow marks a necrotic area that might be a microchannel residue (Figure 48, D).

Overall, the application of PEG-ME, with or without Dermastamp® treatment, induced a more pronounced cell damage compared to Lip80-ME and confirmed the results of histological markers.

5 DISCUSSION

Formulating a protein for the dermal administration is a challenging task. On the one hand their high-molecular-weight and flexible, hydrophilic character complicate their penetration into skin; on the other hand their sensitive structure to external conditions is responsible for a short shelf-life [4]. This thesis focused on the development of a topical formulation system which facilitates the application of proteins with a high tendency of hydrolysis. Due to their instability in water bacterial collagenases are prominent examples and were used as reference. The envisaged dermal application system should ensure a high stability and a good solubility of the protein besides good spreading and penetration properties as well as a favourable tolerability on patients' skin.

To prevent enzymatic hydrolysis in an aqueous environment which is corresponding to a loss of enzymatic activity, a carrier system based on two separated phases was developed. The protein was suspended in the lipophilic-surfactant phase separated over the storage time from the aqueous phase. When both phases are mixed just before application on the skin, the protein dissolves. Hence, the contact time between protein and aqueous phase was reduced to a minimum. A dermal formulation forming spontaneously without much energy input and nonetheless giving a stable formulation was sought. Microemulsion (ME) systems were promising candidates due to their spontaneous formation at room temperature and thermodynamic stability [128]. An aqueous solution might be the easiest formulation system as it enables a quick dissolution of a protein directly before application on the skin. However, the bad spreading as well as penetration and permeation properties on skin limit their topical use [129]. Conventional topical dosage forms like creams and emulsions presented the desired properties on skin. But a long-term stability of creams and emulsions cannot be ensured without high energy input [130,131]. Therefore, MEs were the formulation systems of choice. Like emulsions or creams, MEs are composed of a surfactant/cosolvent, oil and water phase. MEs can be formed when the ratio of oil, aqueous phase and surfactants in the system is appropriate. In the present study, a composition of 35 % surfactant/cosolvent, 5 % lipophilic phase and 60 % aqueous phase allowed the formation of a ME system

(chapter 4.1.1.2). The spontaneous formation and thermodynamic stability of such systems might be explained by the low interfacial tension of the surfactant film caused by the high content of surface active components (35 %) compared to creams or emulsions [65]. Lipoid S LPC 80 (Lip80) was selected as surfactant in combination with a short chain alcohol, 2-propanol, as cosolvent, Plurol Oleique CC 497 (PO CC 497) as lipophilic phase and PBS as aqueous phase. Hoppel *et al.* (2014) emphasised the high polarity of Lip80 which improves solubility in water, enhances the self-emulsification power and the ability to form MEs [62]. Lip80 belongs to the group of phospholipids, a group of natural surfactants with favourable properties in topic formulations classified as skin-friendly and permeation enhancers [119]. It was intended to support the transport of proteins into the skin via a microneedling process. Although microneedling is minimal invasive, it raises the requirements for mild and well tolerated formulation excipients. Mild production processes and high environmental compatibility along with low irritation potential on the skin are frequently named reasons for the utilisation of Lip80 in this thesis [60]. Unfortunately, quite a number of nonionic surfactants raise skin irritations, especially in the chronical treatment, thus they were inappropriate candidates for the ME system [117]. Short chain alcohols like 2-propanol, are suitable cosolvents in combination with phospholipids [62]. They make the aqueous phase less hydrophilic, enhance the solubility of the phospholipid, shift its HLB to a higher value and enable a spontaneous microemulsification [128].

Short chain alcohols are used as cosolvents due to their affinity to both oil and aqueous phase. Likewise, they support the reduction of interfacial tension, which is mainly effected by the surfactant, by increasing the fluidity of the interface. Due to these properties short chain alcohols are commonly referred to as cosurfactants [117]. 2-propanol formed the largest ME areas in comparison to other tested alcohols such as propylene glycol and ethanol in ternary diagrams (chapter 4.1.1.1). Propylene glycol and ethanol only formed small ME areas, preferably with a high content of lipophilic phase. For the purposes of this thesis, a high content of aqueous phase (PBS) was necessary to ensure a complete dissolution of at least 1 % model enzyme. The combination of 2-propanol and PO CC 497 stabilised the largest ME area with the highest PBS content (chapter 4.1.1.2, Figure 21). During formulation development it was observed, that the choice of lipophilic component had a

considerable influence on ME formation. The ability to stabilise especially hydrophilic MEs (high content of PBS) utilising Lip80/2-propanol as surfactant/cosolvent rose with increasing hydrophilicity of the chosen oil. This relation is given by an increasing HLB value, leading to the following order: Labrafac™ Lipophile WL 1349 (HLB = 1) < Labrafac™ PG (HLB = 2) < PO CC 497 (HLB = 6).

Reducing the amount of lipophilic phase from 10 % to 5 % increased the incorporated PBS concentration in MEs even more. The influence of the oil phase on microemulsification process was explained by Warisnoicharoen *et al.* (2000) [132]. They described a mechanism in which the hydrophilic groups of oil were interspersed in the region of surfactant head group [132]. Therefore, it can be assumed that the mentioned PO CC 497 supported the formation of hydrophilic ME best, due to its highest hydrophilicity.

The final choice to apply PO CC 497 as lipophilic phase and 2-propanol as cosolvent has been made after preparing a reference ME system with a similar ME area compared to MEs based on Lip80. For the reference system, all components and their ratios were identical to the phospholipid ME, with exception to the surfactants. The high suitability of nonionic surfactants to form MEs was confirmed by the application of Polysorbate 80 and Kolliphor® EL in the reference ME. Nonionic surfactants are widely used in ME formulations and among them especially ethoxylated sorbitan esters (Polysorbates) and sorbitan fatty acid esters (Span®) [65,131]. Whether a single surfactant or in combination with further surface-active components will enable a spontaneous ME formation, depends on various tests (chapter 4.1.1.3, Figure 22). Already the exchange of the surfactants (Lip80 and Polysorbate 80/Kolliphor® EL) or different lipophilic components caused considerably changed ME areas and demonstrated the variability of these systems. The utilisation of 5 % PO CC 497 and Polysorbate 80, Kolliphor® EL/2-propanol formed MEs with a high content of PBS as obtained with Lip80, too. Both ME systems allowed the formation of hydrophilic ME systems with 60 % PBS which was necessary to dissolve 1 % of the model enzyme.

MEs are described as optically isotropic, transparent or slightly opalescent systems of low viscosity [116]. Lip80 based ME (Lip80-ME) and Polysorbate 80, Kolliphor® EL based ME (PEG) were optically transparent systems with a low viscosity, whereas

Lip80-ME was slightly opalescent due to the Lip80. Multiple light scattering (MLS) was utilised to differentiate whether it is an optical transparent ME or a turbid macroemulsion system. MLS is not reported for ME characterisation in literature yet. It is, however, a promising technique to support the first visual inspection of a ME with measured data. The high transmission values of protein-free ME formulations indicated clear transparent systems (chapter 4.1.2.1, Figure 26). Continuing measurements of the systems over 24 h confirmed a stable optical transparency. Regarding the application of MEs on skin during tolerability studies the assurance of formulation stability is absolutely essential. Tolerability studies on human skin were performed over 24 h, hence the stability of MEs were tested over this envisage period.

In literature, two types of microemulsion structures are differentiated which are most likely to be formed depending on the composition: bicontinuous ME and droplet-like structured ME (classified as oil-in-water, O/W and water-in oil, W/O) [117,129,130]. It can be assumed that the amount of 60 % hydrophilic phase in the prepared ME induced O/W-ME. Alternatively, the system could also be divided into a surfactant/cosurfactant domain (35 %) with partly incorporated oil droplets (5 %) besides a large PBS domain resulting in a bicontinuous ME. However, it is also emphasised that MEs do not consist of static phases, they are rather characterised by a highly dynamic microstructure undergoing continuous and spontaneous fluctuations [130,133]. This special structure and their special way of formation make an appropriate physicochemical characterisation of MEs a challenging task. The inner structure of produced colloidal dispersion was analysed via dynamic light scattering (DLS). To calculate the distribution of droplet sizes, parameters like dynamic viscosity (mPa*s) or density were determined. As already mentioned Lip80-ME and PEG-ME were of low viscosity in comparison to PBS or the viscous lipophilic phase PO CC 497 (chapter 4.1.2.2, Table 2). According to Karasulu *et al.* (2008) one problem associated with the topical use of MEs is their fluidity [115]. Gasco *et al.* (1991) addressed this problem with the development of a ME for the topical application of azelaic acid [134]. They used Carbopol® 934 as gelling agent to increase the viscosity of an O/W-ME system.

Crucial within the setting of this project was the applicability of MEs on the artificial skin surface in the transwell system. The volume of PEG-ME and Lip80-ME with a low viscosity needed to be adjusted to avoid an overflowing of the formulation applied onto the skin in the inserts into the basolateral medium. If a larger volume of this MEs on skin is envisaged, e.g. to ensure an evenly distribution or to achieve a higher protein dose, the addition of thickening agents might be necessary. In examined Lip80-ME and PEG-ME the utilisation of Carbopol® 934 is no option because of possible ionic interactions between the negatively charged Carbopol® 934 and cations in PBS which can induce a protein destabilisation. A more reasonable idea would be, e.g. derivates of cellulose ethers, gelatine or guar-based polymers. In all investigations described in this thesis, MEs were used without any thickening agents. DLS measurements were performed with protein-free MEs. Data of droplet size distribution by DLS are popular parameters in scientific research for the characterisation of ME systems. Although, the utilisation of DLS in this study demonstrated reproducible and stable droplet size distributions over 24 h, these investigations were an approach to point out the limitations of this technique detecting "characteristic" droplet sizes of a ME (Appendix, chapter 8.3).

Lip80-ME and PEG-ME showed a bimodal distribution, with a first signal at a droplet size of approximately 1 nm followed by a second signal of lower intensity of 20 nm (PEG-ME) or 57 nm (Lip80-ME) (chapter 4.1.2.2, Figure 28). Goddeeris *et al.* (2006) identified a signal of surfactant micelles of 11 nm in a 1 % aqueous dilution of 80 % Tween® 80 (Polysorbate 80) and 20 % ethanol [135]. Regarding this experience, the second signal of PEG-ME may be assigned to surfactant micelles of Polysorbate 80 and Kolliphor® EL. The second signal of Lip80-ME can most likely be attributed to phospholipid micelles, whereas the signal is weaker compared to the signal of PEG-ME. It is assumed that these differences are owing to mixed micelles created by Polysorbate 80 and Kolliphor® EL next to the micelles of Lip80. The first signals at 1 nm may be caused by the large hydrophilic phases of the ME structures. These data must be analysed with high caution because the measured droplet sizes are near the detection limit of 0.3 nm of the chosen setup. In literature, ME droplets are typically stated in a range of 10 to 140 nm [92,115]. A comparison to the reported droplet sizes in literature appeared to be difficult. One reason might be the common approach to reduce interparticle interactions via the dilution of original ME which is an

incorrect procedure due to changes in microstructure such as droplet disappearance. The second reason might be the observed bimodality of PEG-ME and Lip80-ME made the calculated z-average diameters based on cumulant analysis inaccurate [130,135]. In this thesis, MEs were examined undiluted. The use of concentrated systems could then again increase the probability of particle interactions and lead to an enhancement of the diffusion coefficient via repulsion effects. It may result in an underestimation of the measured droplet sizes because of incorrect calculations [130]. The theory of DLS is based on the Stokes-Einstein equation and is related to spherical systems [92]. MEs have dynamic, fluctuating droplets which contradicts this underlying assumption. Anyway, DLS measurements of colloidal dispersions such as MEs are challenging, thus it is necessary to confirm and complement the obtained results with findings from other methods. There are various techniques presented and controversially discussed in literature. Most often applied are for example static light scattering, small angle X-ray scattering, small angle neutron scattering or transmission electron microscopy [131,135,136]. Mentioned techniques might be interesting to scientific approaches in characterising the microstructure of developed MEs but of minor importance in this study. Following investigations focused on the potential of MEs as delivery vehicles for the model protein and the tolerability on human skin.

Calculations of the z-average diameter and corresponding distribution curves are intensity based and hence very sensitive to the presence of large particles. It was envisaged to use this property to detect changes in "size distribution" after the drug loading process in MEs. The incorporation of water-soluble catalase as model enzyme in the MEs showed a third peak with an increased particle size of approximately 400 nm. An increased intensity was detected for the hydrophilic phase signal at 1 nm whereas the signal of 20 nm (PEG-ME) and 57 nm (Lip80-ME) decreased. Interestingly, measurement repetitions of protein-loaded formulations presented fluctuations of dissolved catalase peaks, while the signals of ME structures were uniform and reproducible (chapter 4.1.2.2, Figure 29). The observed fluctuations might be caused by structural changes of dissolved protein in the MEs. The development of a stable protein formulation was a main target of this study because destabilisations of protein structure often result in a deactivation as well as

loss of therapeutic activity. Therefore, it was necessary to control and complement the results of DLS analysis with more detailed protein stability analyses.

The successful formulation of a protein depends on a thorough understanding of its physicochemical and biological characteristics. Several external factors such as pH, temperature and interactions with excipients may influence protein activity and 3D structure. Changes in activity of an enzyme can be measured via degradation processes of a specific substrate. Formulation development with collagenase was the initial objective of this thesis. In general, a collagenase activity assay is based on the conversion of labelled collagen (substrate) [137]. Active collagenase attacks the helical region of the molecule and collagen degradation can be detected [20]. The experimental setup and the experiment itself are expensive and time-consuming which led to an substitution of collagenase with the model enzyme catalase [21]. Catalase degrades H_2O_2, allowing a fast, easy to measure (UV photometrical) and reproducible reaction (chapter 3.2.5).

The activity of an enzyme highly depends on the conformational stability. Therefore, SEC and nanoDSF were performed to study MEs` effect on protein stability, specifically on conformational and colloidal changes as well as protein activity. Enzyme activity, R_t and T_m of a stable catalase solution at pH 7.0, 25 °C were set as control. Decreasing the pH to 3.5 resulted in an instant loss of catalase activity (chapter 4.1.3.1, Figure 30). SEC curves underlined this trend showing a considerable loss of signal intensity of catalase monomer (chapter 4.1.3.2, Figure 34). During the activity assay, it was observed that the enzyme precipitated caused by unfolding and denaturation processes. Precipitated parts of protein remained on the SEC column, reduced the concentration of detectable catalase monomer, and decreased the enzyme activity. Furthermore, the SEC diagram of enzyme solution at pH 3.5 depicted peaks that eluted later than the monomer and might be assigned to peptide fragments. These conformational changes were confirmed by nanoDSF analysis showing almost unchanged fluorescence signals and a missing T_m value of the treated sample (chapter 4.1.3.3, Figure 37). In addition to the effect of decreased pH on protein conformation, changes of colloidal stability were measured as increased backscattering intensities. The higher amount of positive charges change the ionic strengths of various functional groups of amino acids [53]. Internal forces

holding the native catalase structure got lost and the protein unfolded, inducing an inactivation. An acidic pH can accelerate hydrolytic reactions. It is reported, that non-enzymatic fragmentation is usually triggered by hydrolysis of peptide bonds, releasing polypeptides of lower molecular weight than the intact protein [55].

Catalase is a quite heat stable enzyme having a T_m at 56 °C (chapter 4.1.3.3, Figure 37) [79]. This was confirmed by the detection of a low loss of enzymatic activity (30 % in 15 min) at 50 °C (chapter 4.1.3.1, Figure 30). A thermal denaturation with a more pronounced unfolding of protein structure was measured at 60 °C. SEC analysis underlined this stronger loss of conformational stability at higher temperature showing a stronger reduced intensity of catalase monomer and a more pronounced additional peak at a later R_t (chapter 4.1.3.2, Figure 34). Switala *et al.* (2002) confirmed this behaviour of catalase as they detected 50 % inactivation at 65 °C over 30 s [79]. The mentioned pH and temperature stress tests of catalase were performed to prove the suitability and sensitivity of selected methods detecting inactivation and corresponding structural changes. The gained experiences were used to evaluate the enzyme status within the MEs. It was especially challenging in SEC measurements because excipients of MEs showed a strong absorption at 280 nm (chapter 4.1.3.2, Figure 35). However, no signals of excipients interfered with the activity assays and nanoDSF analyses. The reason might be the high specificity of both techniques. Whereas the activity assay of a protein relies on the degradation of a specific substrate, nanoDSF measurements based on the intrinsic fluorescence which cannot be found within the excipients´ structure. Interestingly, the protein-free ME systems presented deviating SEC profiles compared to those performed with pure excipients. Lip80-ME placebo eluted as one peak separated from the catalase monomer signal. Unlike the uniform SEC profile of Lip80-ME, PEG-ME eluted as two peaks, simultaneously to the catalase peak. This was a main drawback analysing PEG-ME because the overlapping signals concealed intensity variations as well as formations of new peaks caused by structural changes. With increasing incubation time, constant alterations of SEC signal indicated modifications of enzyme such as aggregates in PEG-ME (chapter 4.1.3.2, Figure 36). Protein aggregates have a higher molecular weight than the native structure, thus they eluted earlier than the catalase peak. Fluorescence intensity curves of nanoDSF measurements confirmed these results showing an unfolded enzyme directly after the preparation of PEG-ME

(0 h). Backscattering values increased over time indicating colloidal instabilities as they were detected in the SEC curves, too (chapter 4.1.3.3, Figure 39). The loss of conformational and colloidal stability of the model enzyme led to a remaining activity of approximately 20 % after 24 h (chapter 4.1.3.1, Figure 32). Catalase dissolved in Lip80-ME showed a preservation of more than 60 % activity after 24 h (chapter 4.1.3.1, Figure 31). SEC curves and backscattering data presented only a slight aggregation tendency. The slight time-dependent decrease of activity indicated conformational changes like partially unfolded protein molecules which are prone to aggregation, too. Nevertheless, a comparison between enzyme stability in PEG-ME to Lip80-ME demonstrated a superior stability of model enzyme in the phospholipid based formulation.

But why are catalase inactivation and accordingly limitations of therapeutic activity more pronounced in PEG-ME than in Lip80-ME?

The reason for that can be attributed to the different emulsifying systems, as all further excipients were identical. For the preparation of PEG-ME a high concentration of 8.75 % Polysorbate 80 and 8.75 % Kolliphor® EL was applied. In general, nonionic surfactants are added to protein solutions to prevent aggregation and unwanted adsorption, typically used in the range 0.0003 % to 0.3 % [138]. This high concentration of overall 17.5 % PEGylated surfactants can counteract the stabilising effect by accelerating aggregation via the exclusion of water molecules. PEG structures have the property to form hydrogen bonds and to exclude water molecules via a steric mechanism from the protein surrounding. They can also interfere with hydrogen bonds of the proteins` secondary structure inducing an unfolding [139,140]. Chi *et al.* (2003) reported the effect of nonionic surfactants to preferentially bind to unfolded states of protein, resulting in a decrease of native protein stability and in an increase of aggregation behaviour [53]. Furthermore, the authors state that Polysorbate 80 may contain peroxides which can oxidise sensitive proteins. It is conceivable that amino acids within catalase which have a phenolic ring system, e.g. tryptophan and tyrosine, are particularly prone to release electrons. Oxidised amino acids result in modifications of the protein domain. Until now, it is not completely understood to what extent internal electron resources can balance these damages and how strong they influence the structure as well as activity of

the enzyme [139,141,142]. Lip80-ME is stabilised by a phospholipid with the same content of 17.5 %. In literature, the effect of natural phospholipids on proteins is difficult to assess due to their inhomogeneous structure with varying fatty acid compositions. The composition of phospholipids provides an opportunity for hydrophobic as well as polar (e.g. electrostatic) interactions [4,143]. However, the initial high inactivation and changes of conformational and colloidal stability make PEG-ME unsuitable as vehicle system for catalase. Lip80-ME might be a suitable vehicle system for catalase presenting lower interactions and consequently a higher activity.

To classify the type of present protein destabilisations, e.g. size of aggregates, optimisations of performed SEC analysis would be needed. These investigations could include the use of columns with a smaller pore size increasing the resolution of peaks as well as further molecular weight calculations. Additionally, investigations such as circular dichroism, X-ray crystallography or NMR may also give residue-specific information about the destabilised protein structure. However, at first it would be necessary to find a method in which the protein can be separated from the ME formulation to avoid disturbing signals. The photometric catalase activity assay and nanoDSF measurements were insensitive to formulation ingredients and hence more eligible. They offered accurate analysis of protein stability besides protein aggregation and were crucial for the interpretation of SEC profiles.

Requirements for the desired dermal formulation system were a high stability of model enzyme besides a mild tolerability on human skin. The tolerability studies focused on the interaction of pure Lip80-ME in comparison to PEG-ME with human skin models. These studies were performed with protein-free MEs. However, the application process was performed as it would be necessary for a protein-loaded ME. Hence, special requirements had to be considered. The penetration of catalase into the skin is limited by the high molecular weight. Passive methods like optimising the formulation cannot improve the stratum corneum (SC) penetration to the necessary extent, thus active procedures like microneedling have to be used (chapter 2.1.2) [10].

Three commercially available microneedle devices (Dermaroller®, eDermastamp® and Dermastamp®) were tested regarding their ability to overcome the SC barrier.

The ability of these devices to create pores through the SC was demonstrated by the detection of pores via light microscopy (as cross-section) and SEM (as top view). SEM pictures were performed with epidermis sheets, whereas the channel depth was measured with full-thickness human skin. The depth of created pores varied between 50 µm for Dermaroller®, 60 µm for Dermastamp® and 120 µm for eDermastamp®. It was determined that with increasing channel depth likewise the diameter of micropores increased. The observed trend in the microscopic images could be confirmed by the results of TEWL measurements. eDermastamp® which created the biggest channel depth and largest channel diameter, showed likewise the most elevated TEWL values (chapter 4.2.2, Figure 42) A possible explanation is that longer needles penetrate deeper through the SC and enter the underlying dermal tissue resulting in an increased hydration of SC [144]. Needle shape as well as needle size of these devices were identical, therefore the different ways of application might be the reason for deviating results. The measurement of TEWL is a well-established method to assess the integrity of the skin barrier *in vivo*, while the transfer to *in vitro* performances with microneedles is limited [108]. On the one hand, the sensitivity to micropunctures of the applied open-chamber Tewameter® device has to be considered [145]. On the other hand, the punctures may be sealed due to cutaneous swelling and result in shallow channel depths [108,146]. Further aspects affecting microchannel depth and, likewise with this TEWL changes are skins` elasticity, application force and person-to-person variability [6]. Badran *et al.* (2009) detected a reduced pore size in full-thickness human skin 2 h after Dermaroller® treatment [104]. The authors emphasised the risk of an overestimation of about 20 % due to the usage of separated epidermis for perforation and determination of pore sizes [104].

In this study, an attempt to control these aspects and enable a comparable evaluation has been made. The experimental setup was validated regarding its ability to produce predictive values: Comparison to a reference device (cannula) showing a maximum destruction, repeated measurements and similar hydrated full-thickness skin samples (e.g. similar TEWL values of untreated skin) were used. A main advantage of the eDermastamp® is the automatically driven piercing step, which reduces the reliance on application force and the person-to-person variability. Finally, the decisive factor to choose the Dermastamp® instead of eDermastamp® was the

limited size and application area of 3D-skin in the transwell system. The transferability of the Dermastamp® performance from full-thickness human cadaver skin to 3D-skin model was controlled via its ability to create microchannels. An elevated channel depth of 100 µm in the transwell system compared to 60 µm in human skin was measured. This result can be explained by the reduced mechanical barrier properties of 3D-skin next to *ex vivo* human adult skin [147,148]. It indicates a major weakness of reconstructed skin models which should be considered in order to avoid an overestimation of results in comparison to the *in vivo* situation.

Lip80-ME was designed for the topical application and therefore needs to be non-irritating on the human skin. In this thesis, the focus was set on the examination of the effect of Dermastamp® + Lip80-ME next to Dermastamp® + reference ME (PEG-ME) on human skin. Historically, the irritation potential of topical products was investigated in animal models for safety assessment followed by *in vivo* studies with healthy volunteers [122]. The Draize rabbit primary dermal irritation test was routinely used for the preclinical determination of skin irritational potentials [149]. The relevance of animal irritancy data to the human situation is questionable and can lead to misinterpretations [122,148]. Animal tests are ethically not justifiable for this research utilisation. Furthermore, there are several possibilities to replace them. One promising alternative are human *in vitro* skin models which were first developed in the early 1990`s and gained importance with the adoption in general guidelines as COLIPA, 76/768/EEC, ICH S2 (R1) and OECD 431/439 [85,150–154]. They mimic the human skin to a high extent. A variety of reconstructed human skin models are on the market allowing various applications like skin corrosion or irritation tests (chapter 0). In addition, they enable the investigation of pathological effects (e.g. skin cancer) as well as physiological effects (e.g. wound healing) [85]. Commercially available skin models have a highly reproducible tissue quality. On the contrary, there are some drawbacks, as missing skin appendages (sweat glands, hair channels), the indirect endpoint estimation (immunological response instead of erythema/oedema manifestation) and the already mentioned impaired barrier properties, as well [147]. Lip80-ME and the reference ME (PEG-ME) were applied on a commercially available model, Epiderm™ FT 400. This full-thickness skin tissue, which matches the *in vivo* situation closely, was selected to examine the release of immunological markers [155].

Acute and chronic skin irritations are local and reversible inflammatory responses of normal living skin to external stimulants [122]. Skin irritation is a complex phenomenon that involves resident epidermal cells, dermal fibroblasts, endothelial cells and invading leukocytes. They all communicate with each other via cytokines and lipid mediators. Various parameters (IL-1α, IL-6, IL-8 release; cytotoxicity and skin morphology) reflecting irritancy and were examined in this study with Epiderm™ FT. To evaluate the level of irritation, ME samples were compared to a negative and positive control. According to manufacturers' protocol, PBS pH 7.0 was applied without any further treatment as a negative control [109]. SDS is commonly used in tolerability studies as positive control due to its ability to induce a contact dermatitis. Pre-investigations demonstrated a strong destruction of skin tissue after the treatment with ≥ 1 % SDS solution. Therefore, a 0.8 % solution of SDS was used as a positive control in this setup showing an irritant potential with a moderate cell destruction [122,156]. All examined immunological markers (IL-1α, IL-6, IL-8 and LDH) presented a significant difference between the negative and positive control. Pathohistologic examinations confirmed these results and concurrently the suitability of the chosen setup to distinguish between mild and irritating substances.

The primary function of keratinocytes is to provide structural integrity and barrier function of the epidermis. They become a key part of the initiation and perpetuation of skin inflammation and immunological reactions by the release of cytokines [26]. IL-1α is constitutively produced by keratinocytes and stimulates its own release as well as the production and release of secondary cytokines (e.g. IL-6, IL-8). IL-8 is secreted especially after mechanically induced cell damage while IL-6 is secreted after exposure to chemical *noxae*. According to the experiences of other authors, it is possible to differentiate between a mechanically or chemically induced irritation, if both markers are assessed [126]. The combination of MEs with Dermastamp® did not increase the release of secondary cytokines compared to the sole application of ME (chapter 4.3.1, Figure 44). IL-6 showed reduced concentration levels when the microneedle device was applied with the MEs compared to applying the microneedle device only. This weakening effect of MEs after microneedling was observed to be significant just after Lip80-ME was applied. Concentration profiles of IL-8 presented a similar trend, however, the interleukine release of Dermastamp® compared to Dermastamp® + MEs was not significantly different. IL-1α concentrations of

Dermastamp® and Dermastamp® + PEG-ME were on a similar low level comparable to those of the PBS sample (chapter 4.3.1, Figure 43). Their IL-1α concentration was reduced in comparison to the levels of solely applied MEs. In contrast, the combination of Dermastamp® + Lip80-ME showed significantly increased IL-1α concentrations compared to those achieved by applying the SDS solution. This development contradicts the observed weakening effect of Lip80-ME on the microneedling process in IL-6 and IL-8 profiles and underlines the weakening effect of PEG-ME. One explanation might be the initialising function of IL-1α in an inflammation process. IL-1α release increases directly after an irritating stimulation [157]. During an ongoing inflammation process the release of IL-1α decreases again caused by a negative feedback mechanism. This inhibition is stimulated, *inter alia*, by secondary cytokines like IL-6 [18,39]. IL-6 is an important regulating cytokine effecting pro- and anti-inflammatory reactions. It stimulates the synthesis of IL-1-receptor antagonist (IL-1-ra) which competitively inhibits IL-1 receptor and thus reduces the secretion as well as the inflammatory effect of IL-1α. With respect to the presented results, a lower negative feedback for Dermastamp® + Lip80-ME can be assumed because of a lower secondary cytokine release, consequently resulting in higher IL-1α levels.

It was envisaged to control the tolerability of application systems on human skin over a prolonged contact time which induced extreme conditions. The manufacturer of skin models recommended 24 h as the maximum exposure time for a good performance in tolerability studies. An evaluation of media samples (IL-6 and IL-8) after 24 h exposure time was performed but led to incorrect sample concentrations and missing reference values of the SDS sample. Due to the already mentioned detrimental effect of SDS solution the permeability of skin tissue increased over time and facilitated the contact between sample and basolateral medium. SDS reduced the number of active cells and interfered with the detection of immunological markers. During 24 h exposure time, MEs were not removed from the tissue surface. The formulations got also in contact with the basolateral media, interfered with the cytokine assays and induced decreased concentrations. However, IL-1α was not detected in the basolateral media, this cytokine was detected after tissue lysis. As it is a destructive procedure this assay was performed at the end of tolerability studies, thus after 24 h. It is conceivable, that the delayed examinations after 24 h of IL-1α

instead of 8 h for IL-6 and IL-8 supported the detection of negative feedback reactions.

A differentiation with the results of secondary cytokines between chemically and mechanically induced skin damages was not possible due to similar concentration profiles of IL-6 and IL-8. This led to the assumption, that the observations from literature did not fit to the present model or the chosen settings e.g. measuring time was unsuitable [124,126]. Besides the detection of IL-8, one parameter for cell damage is the integrity of cell membranes. LDH is a stable cytoplasmic enzyme present in all living cells. It is released into basolateral cell culture media upon damage of the plasma membrane [127]. As it was expected, the microneedling process showed the highest LDH concentration (chapter 4.3.1, Figure 45). According to the observed weakening effect of Dermastamp® + PEG-ME and Dermastamp® + Lip80-ME (IL-6, IL-8 and IL-1α), the LDH release was significantly decreased compared to the solely applied device as well. With the performance of histological examinations, it was possible to detect and proof the previously assumed distinctive properties between Lip80-ME and PEG-ME on human skin (chapter 4.3.2, Figure 47 and Figure 48). While the tissue of Dermastamp® + Lip80-ME was slightly irritated, the damage following the application of Dermastamp® + PEG-ME was tremendous. Skin layers of Dermastamp® + PEG-ME treated sample were strongly homogenised, exhibiting numerous apoptotic cells.

A comparison between histological and immunologic analyses leads to the question: How are destroyed and apoptotic cells able to release cytokines?

It is impossible and for this reason induced false negative results for the combination of Dermastamp® + PEG-ME. The common property of ME formulations to reduce the irritating effect after microneedle treatment is only correct for the phospholipid-based ME. Detected IL-6, Il-8 and IL-1α levels of Dermastamp® + PEG-ME are reduced because of destructed as well as dead cells that are not able to release cytokines. The reduced LDH concentration following Dermastamp® + PEG-ME application despite the high number of damaged cells can be explained by the test procedure. ME formulations were not removed during the 24 h measuring time. With elapsing time, the cellular leakage increased and PEG-ME got into contact with the basolateral medium. It is reported in literature that surfactants (PEG-ME includes

17.5 % of nonionic surfactants) are able to interact with the enzyme and degrade its function [127,158]. This may be led to the faulty contemplation of a low LDH release. Lip80-ME did not get into contact with the basolateral medium because of an intact skin structure and did not reduce the LDH concentration. The induced weakening effect of Lip80-ME on microneedling process can most likely be attributed to the used phospholipid. It is a biological surfactant and a major component of membrane lipids [60]. Regarding to this property it is conceivable that Lip80 can stabilise damaged cell membranes and likewise reduce the immunological reaction.

Lip80-ME demonstrated superior protein stability and favourable properties on human skin. It can be used as an attractive topical vehicle system to reach a therapeutic protein concentration in certain skin layers or in the blood circulation. The large amount of surface active substances and the additive of a short chain alcohol have a penetration enhancing effect via decreasing the resistance of upper skin layers. The high content of an aqueous phase might be able to enhance the hydration effect of the stratum corneum and likewise the percutaneous absorption of the protein. The transport of protein through the skin might also be enhanced by the similarity between phospholipid structures and the barrier layers of the skin [65,117,129]. Nonetheless, it is necessary to support the transport of a protein through the SC via a microneedling step or a comparable technique. In this thesis, the application of the needle device increased the penetration of each test formulation into the skin. In addition, Lip80-ME presented the special characteristic of a weakening effect on skin tissue after an induced damage.

6 CONCLUSION

The presented work highlights the challenges accompanying the development and characterisation of a dermal protein delivery system. For the first time a phospholipid-based ME was applied and evaluated after a microneedling step on a reconstructed human skin model.

The first aim of this thesis was the development of a formulation system, which enables the dermal application of an enzyme with a hydrolytic sensitivity. A phospholipid based pre-ME concentrate was found to be most suitable as it reduces the contact time between the enzyme and hydrophilic phase. The enzyme is suspended in the lipophilic-surfactant phase, separated from the hydrophilic phase. Just before application on the skin both phases are mixed to form the final ME. Lipoid S LPC 80 (Lip80), a phospholipid, facilitated a spontaneous formation of a stable ME.

Lip80-ME demonstrated a superior stability of the model enzyme compared to a PEGylated reference ME system (Polysorbate 80 and Kolliphor® EL). Directly after preparing the final PEGylated ME, the dissolved enzyme showed strong conformational changes as well as changes in the colloidal stability associated with a significant loss of activity. Lip80-ME presented no considerable interactions with the model enzyme and is therefore ideally suited as vehicle system for proteins. In general, the dissolution of a protein is a critical processing step, especially in an aqueous environment [159]. The current study used catalase as model enzyme (instead of collagenase), but the pre-formulated Lip80-ME concentrate might be a promising vehicle system for other proteins as well.

Detecting the protein stability within a formulation is more challenging than within a simple composed buffered solution due to various possibly interfering excipients. In this thesis, the utilised enzyme activity assay and nanoDSF measurements led to conclusive results independent of interfering excipients. Thus, the direct determination of protein stability of complex systems without further purifications could be demonstrated. These approaches can be transferred to stability examinations for other protein formulations.

The second aim of this thesis was the enhancement of protein transport into human skin via a suitable microneedle device. Dermastamp® was chosen over two other commercially available microneedle devices because it is the most efficient, reproducible, and applicable device in studies with the utilised human skin model.

Finally, the combination of Lip80-ME and Dermastamp® was examined on reconstructed human skin equivalents to predict the *in vivo* tolerability. These skin tolerability studies were performed in comparison to the PEGylated reference formulation. The effects of MEs and Dermastamp® on skin tissue was analysed by the detection of inflammatory markers and pathohistological investigations. These examinations demonstrated the ability of phospholipid based ME to decrease the irritation effect caused by the microneedle device. Furthermore, its reaction on skin was milder compared to the detrimental effect of the reference formulation (PEG-ME). These observations underlined the importance of pathohistological examinations next to immunological assays and their complementary functions. Nevertheless, the elevated permeability of reconstructed skin relative to native human skin must be considered for both methods to avoid an overestimation of observed results [148]. Until now, skin equivalents cannot completely replace *in vivo* studies, but they are important to assess the tolerability in first screening steps of chemicals as well as early states of formulation development. The possibility of a new application for human skin models besides their versatile applicability was presented.

This thesis presented new scientific findings in the field of dermal drug delivery and revealed approaches for additional investigations. Further tests (e.g. with a special focus on the weakening effect of Lip80-ME after skin disruption) could be used to analyse the correlation between the phospholipid composition like the amount of MAPL and DAPL. Additional experiments with 3D-skin equivalents, including wound healing studies, can be utilised to characterise the nature and likewise the effectiveness of the observed weakening effect. The therapeutic activity of phospholipids in addition to their emulsifying properties would open the way for new and innovative fields of application.

However, the nonirritating potential of phospholipid ME as anticipated at the beginning could not be unconfirmed. The longer the exposure time, the higher the

immunological response of Lip80-ME compared to PBS. Further investigations can focus on the irritating/immune-activating potential to elucidate whether the formulation is suitable for dermal vaccination. It is conceivable that the ME may act as vehicle system for the antigen and simultaneously as an immune adjuvant supporting the immunisation. Arya *et al.* (2015) and Shakya *et al.* (2015) emphasised the effectiveness of dermal vaccination in combination with a microneedle device. These authors showed that microneedles are suitable for cutaneous allergen specific immunotherapy and that this method is more effective than common subcutaneous injections [160,161]. Treatment with microneedles has several advantages such as the self-application of reproducible amounts of drugs without medical assistance, painless application on a large surface area and no scar formation. This would be especially important in developing countries or in the treatment of children [17,160]. Dermal vaccination is a promising and challenging research area with great need for innovative application systems. A phospholipid-based ME combined with a microneedle device is a new method for a simple and easily produced system in comparison to the current research methods that employ complex microneedle coating processes [33].

Lip80-ME is a promising vehicle system for dermal protein delivery. Targeted studies, including biopharmaceutics and pharmacological effects, will be part of continuing research.

7 REFERENCES

[1] M. Ratnaparkhi, S. Chaudhari, V. Pandya, Peptide and Proteins in Pharmaceuticals, International Journal of Current Pharmaceutical Research 2 (2011) 1–9.

[2] M. Morishita, N.A. Peppas, Is the oral route possible for peptide and protein drug delivery?, Drug discovery today 11 (2006) 905–910.

[3] T. Weil, The growing significance of peptide therapeutics, 2014, www.gesundheitsindustrie-bw.de/en/article/news/the-growing-significance-of-peptide-therapeutics/, accessed 7 April 2017.

[4] S. Frokjaer, D.E. Otzen, Protein drug stability: a formulation challenge, Nature reviews. Drug discovery 4 (2005) 298–306.

[5] H.A.E. Benson, S. Namjoshi, Proteins and peptides: Strategies for delivery to and across the skin, Journal of Pharmaceutical Sciences 97 (2008) 3591–3610.

[6] H. Kalluri, C.S. Kolli, A.K. Banga, Characterization of microchannels created by metal microneedles: formation and closure, American Association of Pharmaceutical Scientists 13 (2011) 473–481.

[7] S. Katikaneni, Transdermal delivery of biopharmaceuticals: dream or reality?, Therapeutic delivery 6 (2015) 1109–1116.

[8] C.A. Kornick, J. Santiago-Palma, N. Moryl, R. Payne, E.A.M.T. Obbens, Benefit-Risk Assessment of Transdermal Fentanyl for the Treatment of Chronic Pain, Drug Safety 26 (2003) 951–973.

[9] T. Jarupanich, S. Lamlertkittikul, V. Chandeying, Efficacy, safety and acceptability of a seven-day, transdermal estradiol patch for estrogen replacement therapy, Journal of the Medical Association of Thailand 86 (2003) 836–845.

[10] T.-M. Tuan-Mahmood, M.T. McCrudden, B.M. Torrisi, E. McAlister, M.J. Garland, T.R.R. Singh, R.F. Donnelly, Microneedles for intradermal and transdermal drug delivery, European Journal of Pharmaceutical Sciences 50 (2013) 623–637.

[11] M.B. Brown, G.P. Martin, S.A. Jones, F.K. Akomeah, Dermal and Transdermal Drug Delivery Systems: Current and Future Prospects, Drug Delivery 13 (2006) 175–187.

[12] TEVA Pharmaceuticals, Important prescribing information: Urgent – ZECUITY® (Sumaptriptan iontophoretic transdermal system) suspension of marketing (2016).

[13] The Medicines Company, Risk Evaluation and Mitigation Strategy (REMS): NDA 21338 IONSYS® (fentanyl iontophoretic transdermal system) (2015).

[14] Zosano Pharma, Our Technology-Transdermal Drug Delivery. Ready For Relief? Ready. Set. Apply., 2016, www.zosanopharma.com/technology.

[15] W. Martanto, S.P. Davis, N.R. Holiday, J. Wang, H.S. Gill, M.R. Prausnitz, Transdermal Delivery of Insulin Using Microneedles in Vivo, Pharmaceutical Research 21 (2004) 947–952.

[16] F. Cosman, N.E. Lane, M.A. Bolognese, J.R. Zanchetta, P.A. Garcia-Hernandez, K. Sees, J.A. Matriano, K. Gaumer, P.E. Daddona, Effect of transdermal teriparatide administration on bone mineral density in postmenopausal women, The Journal of Clinical Endocrinology and Metabolism 95 (2010) 151–158.

[17] S. Marshall, L.J. Sahm, A.C. Moore, Microneedle technology for immunisation: Perception, acceptability and suitability for paediatric use, Vaccine 34 (2016) 723–734.

[18] M.R. Prausnitz, J.A. Mikszta, M. Cormier, A.K. Andrianov, Microneedle-based vaccines, Current topics in microbiology and immunology 333 (2009) 369–393.

[19] C.S. Kolli, Microneedles: bench to bedside, Therapeutic delivery 6 (2015) 1081–1088.

[20] Worthington Biochemical Corporation, Worthington enzyme manual: Collagenase (2015).

[21] Genaxxon Bioscience, Collagenase: Clostridiopeptidase A from Clostridium histolyticum 01062010 (2017).

[22] Sigma Aldrich, Product Information: Collagenase, Crude, from Clostridium histolyticum (2014).

[23] Worthington Biochemical Corporation, Worthington enzyme manual: Catalase (2015).

[24] L. Bernhofer, S. Barkovic, Y. Appa, K. Martin, IL-1α and IL-1ra secretion from epidermal equivalents and the prediction of the irritation potential of mild soap and surfactant-based consumer products, Toxicology in vitro 13 (1999) 231–239.

[25] L. Bernhofer, M. Seiberg, K. Martin, The Influence of the Response of Skin Equivalent Systems to Topically Applied Consumer Products by Epithelial-Mesenchymal Interactions, Toxicology in vitro 13 (1999) 219–229.

[26] T. Welss, D.A. Basketter, K.R. Schröder, In vitro skin irritation: facts and future. State of the art review of mechanisms and models, Toxicology in vitro 18 (2004) 231–243.

[27] C. DeBenedictis, S. Joubeh, G. Zhang, M. Barria, R.F. Ghohestani, Immune functions of the skin, Clinics in dermatology 19 (2001) 573–585.

[28] P. Di Meglio, G.K. Perera, F.O. Nestle, The multitasking organ: recent insights into skin immune function, Immunity 35 (2011) 857–869.

[29] R.F. Donnelly, T.R.R. Singh, Novel delivery systems for transdermal and intradermal drug delivery, John Wiley & Sons, Inc, West Sussex, England, 2015.

[30] J.W. Wiechers, The barrier function of the skin in relation to percutaneous absorption of drugs, Pharmaceutisch Weekblad Scientific Edition 11 (1989) 185–198.

[31] D.J. Tobin, Biochemistry of human skin--our brain on the outside, Chemical Society reviews 35 (2006) 52–67.

[32] R.L. Bronaugh, H.I. Maibach, Percutaneous absorption: Drugs-cosmetics-mechanisms--methodology, 3rd ed., rev. and expanded. ed., Dekker, New York, 1999.

[33] H.S. Gill, J. Soderholm, M.R. Prausnitz, M. Sallberg, Cutaneous vaccination using microneedles coated with hepatitis C DNA vaccine, Gene therapy 17 (2010) 811–814.

[34] A.C. Williams, B.W. Barry, Skin absorption enhancers, Critical reviews in therapeutic drug carrier systems 9 (1992) 305–353.

[35] C. Bangert, P.M. Brunner, G. Stingl, Immune functions of the skin, Clinics in dermatology 29 (2011) 360–376.

[36] K.L. Audus, T.J. Raub, Biologial barriers to protein delivery, Plenum Press, New York, 1993.

[37] M.R. Prausnitz, R. Langer, Transdermal drug delivery, Nature Biotechnology 26 (2008) 1261–1268.

[38] A.C. Williams, B.W. Barry, Penetration enhancers, Advanced Drug Delivery Reviews 64 (2012) 128–137.

[39] M.R. Prausnitz, Microneedles for transdermal drug delivery, Advanced Drug Delivery Reviews 56 (2004) 581–587.

[40] Z. Ding, F.J. Verbaan, M. Bivas-Benita, L. Bungener, A. Huckriede, D.J. van den Berg, G. Kersten, J.A. Bouwstra, Microneedle arrays for the transcutaneous immunization of diphtheria and influenza in BALB/c mice, Journal of Controlled Release 136 (2009) 71–78.

[41] M. Cormier, B. Johnson, M. Ameri, K. Nyam, L. Libiran, D.D. Zhang, P. Daddona, Transdermal delivery of desmopressin using a coated microneedle array patch system, Journal of Controlled Release 97 (2004) 503–511.

[42] J.A. Matriano, M. Cormier, J. Johnson, W.A. Young, M. Buttery, K. Nyam, P.E. Daddona, Macroflux® Microprojection Array Patch Technology: A New and Efficient Approach for Intracutaneous Immunization, Pharmaceutical Research 19 (2002) 63–70.

[43] H.S. Gill, M.R. Prausnitz, Coating formulations for microneedles, Pharmaceutical Research 24 (2007) 1369–1380.

[44] J.-H. Park, M.G. Allen, M.R. Prausnitz, Biodegradable polymer microneedles: Fabrication, mechanics and transdermal drug delivery, Journal of Controlled Release 104 (2005) 51–66.

[45] G. Li, A. Badkar, H. Kalluri, A.K. Banga, Microchannels created by sugar and metal microneedles: characterization by microscopy, macromolecular flux and other techniques, Journal of Pharmaceutical Sciences 99 (2010) 1931–1941.

[46] H. Kalluri, A.K. Banga, Transdermal delivery of proteins, American Association of Pharmaceutical Scientists 12 (2011) 431–441.

[47] J.W. Lee, J.-H. Park, M.R. Prausnitz, Dissolving microneedles for transdermal drug delivery, Biomaterials 29 (2008) 2113–2124.

[48] W. Martanto, J.S. Moore, T. Couse, M.R. Prausnitz, Mechanism of fluid infusion during microneedle insertion and retraction, Journal of Controlled Release 112 (2006) 357–361.

[49] S.P. Davis, W. Martanto, M.G. Allen, M.R. Prausnitz, Hollow metal microneedles for insulin delivery to diabetic rats, IEEE transactions on bio-medical engineering 52 (2005) 909–915.

[50] R.F. Donnelly, T.R.R. Singh, M.M. Tunney, Morrow, Desmond I. J., P.A. McCarron, C. O'Mahony, A.D. Woolfson, Microneedle arrays allow lower microbial penetration than hypodermic needles in vitro, Pharmaceutical Research 26 (2009) 2513–2522.

[51] F. Franks, Internal Structure and Organization: Relationship to Function, in: F. Franks (Ed.), Protein Biotechnology, Humana Press, Totowa, NJ, 1993, 91–133.

[52] K.P. Murphy, Protein Structure, Stability, and Folding, Humana Press Inc, Totowa, NJ, 2001.

[53] E.Y. Chi, S. Krishnan, T.W. Randolph, J.F. Carpenter, Physical Stability of Proteins in Aqueous Solution: Physical Stability of Proteins in Aqueous Solution: Mechanism and Driving Forces in Nonnative Protein Aggregation, Pharmaceutical Research 20 (2003) 1325–1336.

[54] M.C. Manning, D.K. Chou, B.M. Murphy, R.W. Payne, D.S. Katayama, Stability of protein pharmaceuticals: An update, Pharmaceutical Research 27 (2010) 544–575.

[55] N.M. Ritter, J. Patel, R. Kothari, R. Tunga, B.S. Tunga, Stability Considerations for Biopharmaceuticals: Overview of Protein and Peptide Degradation Pathways, BioProcess International (2011) 20.

[56] M.E.M. Cromwell, E. Hilario, F. Jacobson, Protein aggregation and bioprocessing, American Association of Pharmaceutical Scientists 8 (2006) E572-9.

[57] B.A. Shirley, Protein stability and folding: Theory and practice, Humana Press, Totowa (N.J.), op. 1997.

[58] D.K. Chou, R. Krishnamurthy, T.W. Randolph, J.F. Carpenter, M.C. Manning, Effects of Tween 20 and Tween 80 on the stability of Albutropin during agitation, Journal of Pharmaceutical Sciences 94 (2005) 1368–1381.

[59] K. Holmberg, Natural surfactants, Current Opinion in Colloid & Interface Science 6 (2001) 148–159.

[60] P. van Hoogevest, A. Wendel, The use of natural and synthetic phospholipids as pharmaceutical excipients, European Journal of Lipid Science and Technology 116 (2014) 1088–1107.

[61] USP, Monographs: United States Pharmacopoeia, 39 ed., 2016.

[62] M. Hoppel, H. Ettl, E. Holper, C. Valenta, Influence of the composition of monoacyl phosphatidylcholine based microemulsions on the dermal delivery of flufenamic acid, International Journal of Pharmaceutics 475 (2014) 156–162.

[63] S. Zalipsky, Chemistry of polyethylene glycol conjugates with biologically active molecules, Advanced Drug Delivery Reviews 16 (1995) 157–182.

[64] BASF, Technical information on Kolliphor EL (2012).

[65] A. Kogan, N. Garti, Microemulsions as transdermal drug delivery vehicles, Advances in Colloid and Interface Science 123-126 (2006) 369–385.

[66] BASF, Technical information on Kolliphor PS 80 (2016).

[67] Gattefossé, Customer Information: Lipid Excipients for Topical Drug Delivery (2014).

[68] Gattefossé, Technical Data Sheet: Plurol Oleique® CC 497 (2010).

[69] Gattefossé, Product Infomration Pharmaceuticals: Labrafac™ Lipophile WL 1349 (2014).

[70] Gattefossé, Product Information Pharmaceuticals: Labrafac™ PG (2014).

[71] Gattefossé, Regulatory, Tox and Safety Overview: Geleol™ Mono and Diglycerides NF, Peceol™, Maisine™ 35-1, Geleol™ FPF (2014).

[72] Gattefossé, Regulatory, Tox and Safety Overview: Labrafac™ PG (2011).

[73] Gattefossé, Regulatory, Tox and Safety Overview: Plurol Oleique® CC 497 (2012).

[74] Gattefossé, Regulatory, Tox and Safety Overview: Labrafac™ Lipophile WL 1349 (2014).

[75] A. Deisseroth, A.L. Dounce, Catalase: Physical and Chemical Properties, Mechanism of Catalysis, and Physiological Role, Physiological Reviews 50 (1970).

[76] B.K. Vainshtein, W.R. Melik-Adamyan, V.V. Barynin, A.A. Vagin, A.I. Grebenko, Three-dimensional structure of the enzyme catalase, Nature 293 (1981) 411–412.

[77] S. Prajapati, V. Bhakuni, Alkaline unfolding and salt-induced folding of bovine liver catalase at high pH, European Journal of Biochemistry 255 (1998) 178–184.

[78] A. Diaz, P.C. Loewen, I. Fita, X. Carpena, Thirty years of heme catalases structural biology, Archives of Biochemistry and Biophysics 525 (2012) 102–110.

[79] J. Switala, P.C. Loewen, Diversity of properties among catalases, Archives of Biochemistry and Biophysics 401 (2002) 145–154.

[80] Protein Data Bank in Europe-, The crystal structure of bovine liver catalase without NADPH, 2017, www.ebi.ac.uk, accessed 1 February 2017.

[81] T. Samejima, M. Kamata, K. Shibata, Dissociation of bovine liver catalase at low pH, Journal of Biochemistry 51 (1962) 181–187.

[82] B. Chance, Effect of pH upon the reaction kinetics of the enzyme-substrate compounds of catalase, Journal of Biological Chemistry 194 (1951) 471–481.

[83] Dermaroller GmbH, User information: The original Dermaroller for medical micro needling, 2016, www.original-dermaroller.de.

[84] D. Fischer, Rückfragen zu Dermaroller Mustern. Email, 2014.

[85] B. de Wever, D. Petersohn, K.R. Mewes, Overview of human three-dimensional (3D) skin models Overview of human three-dimensional (3D) skin models used for dermal toxicity assessment Part 1, Household and Personal Care Today 1 (2013) 18–22.

[86] MatTek Corporation, Data sheet of EpiDerm FT (2016).

[87] MatTek Corporation, EpidermFT™: User Information-Technology, 2017, www.mattek.com/products/epidermft/, accessed 16 May 2017.

[88] M. Bachelor, Further information about 3D-skin model. email, 2015.

[89] MatTek Corporation, In Vitro EpiDerm Skin Irritation Test (EPI-200-SIT): For use with MatTek Corporation`s Reconstructed Human Epidermal Model EpiDerm, 2014.

[90] Formulaction SAS, User manual: Turbiscan LAB 2.1.0.52 (2014).

[91] W.I. Goldburg, Dynamic light scattering, American Journal of Physics 67 (1999) 1152–1160.

[92] Malvern Instruments, Zeta Nano User Manual 1 (2013).

[93] L. Martin, S. Schwarz, D. Breitspeicher, Application Note Nanotemper - Thermal unfolding.

[94] F. Bleffert, V. Misetic, M. Jerabek, Application Note Nanotemper-Thermal stability of membrane-bound proteins (2016).

[95] Nanotemper technologies, Prometheus Series: Product Information (2016).

[96] F. Söltl, J. Derix, D. Breitsprecher, Application Note Nanotemper-Unfolding and Aggregation of mAbs (2016).

[97] B.J. Spix, M. Veurink, Application Note Nanotemper - Chemical and thermal unfolding.

[98] P. Baaske, S. Duhr, System und Verfahren für ein abdichtungsfreies Temperieren von Kapillaren, DE102014018535 A1 (2016).

[99] S. Fekete, A. Beck, J.L. Veuthey, D. Guillarme, Theory and practice of size exclusion chromatography for the analysis of protein aggregates, Journal of pharmaceutical and biomedical analysis 101 (2014) 161–173.

[100] H.G. Barth, C. Jackson, B.E. Boyes, Size Exclusion Chromatography, Analytical Chemistry 66 (1994) 595–620.

[101] P. Hong, S. Koza, E.S. Bouvier, Size-Exclusion Chromatography for the Analysis of Protein Biotherapeutics and their Aggregates, Journal of liquid chromatography & related technologies 35 (2012) 2923–2950.

[102] R.D. Ricker, L.A. Sandoval, Fast, reproducible size-exclusion chromatography of biological macromolecules, Journal of Chromatography A 743 (1996) 43–50.

[103] Sigma Aldrich, Technical Documents: Enzymatic Assay of Catalase (EC 1.11.1.6) (2015).

[104] M.M. Badran, J. Kuntsche, A. Fahr, Skin penetration enhancement by a microneedle device (Dermaroller®) in vitro: Dependency on needle size and applied formulation, European Journal of Pharmaceutical Sciences 36 (2009) 511–523.

[105] W. Kempf, Dermatopathologie, Steinkopff Verlag Darmstadt, Darmstadt, 2007.

[106] A.H. Fischer, K.A. Jacobson, J. Rose, R. Zeller, Cryosectioning tissues, Cold Spring Harbor Protocols 2008 (2008) pdb.prot4991.

[107] Courage+Khazaka electronic GmbH, Information and Operating Instruction for the Software MPA: The Tewameter TM 300 (2014).

[108] J. Pinnagoda, R.A. Tupkek, T. Agner, J. Serup, Guidelines for transepidermal water loss (TEWL) measurement. A Report from the Standardization Group of the European Society of Contact Dermatitis, Contact Dermatitis 22 (1990) 164–178.

[109] MatTek Corporation, EpiDerm Full Thickness 400 (EFT-400): User Protocol (2016).

[110] BioLegend, Human IL-6: ELISA MAX Deluxe Sets (2015).

[111] BioLegend, Human IL-8: ELISA MAX Deluxe Sets (2015).

[112] Sigma Aldrich, Product Information: Lactate Dehydrogenase Activity Assay Kit (2016).

[113] R. Mallampati, R.R. Patlolla, S. Agarwal, R.J. Babu, P. Hayden, M. Klausner, M.S. Singh, Evaluation of EpiDerm full thickness-300 (EFT-300) as an in vitro model for skin irritation: studies on aliphatic hydrocarbons, Toxicology in vitro 24 (2010) 669–676.

[114] BioLegend, Human IL-1α: ELISA MAX Deluxe Sets (2015).

[115] H.Y. Karasulu, Microemulsions as novel drug carriers: the formation, stability, applications and toxicity, Expert Opinion on Drug Delivery 5 (2008) 119–135.

[116] I. Danielsson, B. Lindman, The definition of microemulsion, Colloids and Surfaces 3 (1981) 391–392.

[117] M.J. Lawrence, G.D. Rees, Microemulsion-based media as novel drug delivery systems, Advanced Drug Delivery Reviews 64 (2012) 175–193.

[118] J.C. Schwarz, V. Klang, M. Hoppel, D. Mahrhauser, C. Valenta, Natural microemulsions: Formulation design and skin interaction, European Journal of Pharmaceutics and Biopharmaceutics 81 (2012) 557–562.

[119] D. Paolino, C.A. Ventura, S. Nisticò, G. Puglisi, M. Fresta, Lecithin microemulsions for the topical administration of ketoprofen: percutaneous adsorption through human skin and in vivo human skin tolerability, International Journal of Pharmaceutics 244 (2002) 21–31.

[120] Sigma Aldrich, Product Information: Catalase from bovine liver, lyophilized powder, 2,000-5,000 units/mg protein (2017).

[121] R. Aboofazeli, M.J. Lawrence, Investigations into the formation and characterization of phospholipid microemulsions. I. Pseudo-ternary phase diagrams of systems containing water-lecithin-alcohol-isopropyl myristate, International Journal of Pharmaceutics 93 (1993) 161–175.

[122] F. de Brugerolle, V. Picarles, S. Chibout, M. Kolopp, J. Medina, P. Burtin, M.E. Ebelin, S. Osborne, F.K. Mayer, A. Spake, M. Rosdy, B. de Wever, R.A. Ettlin, A. Cordier, Predictivity of an in vitro model for acute and chronic skin irritation (SkinEthic) applied to the testing of topical vehicles, Cell biology and toxicology 15 (1999) 121–135.

[123] I.R. Williams, T.S. Kupper, Immunity at the surface: Homeostatic mechanisms of the skin immune system, Life Sciences 58 (1996) 1485–1507.

[124] A. Coquette, N. Berna, A. Vandenbosch, M. Rosdy, B. de Wever, Y. Poumay, Analysis of interleukin-1α (IL-1α) and interleukin-8 (IL-8) expression and release in in vitro reconstructed human epidermis for the prediction of in vivo skin irritation and/or sensitization, Toxicology in vitro 17 (2003) 311–321.

[125] B.E. Barton, IL-6: insights into novel biological activities, Clinical immunology and immunopathology 85 (1997) 16–20.

[126] A. Li, S. Dubey, M.L. Varney, B.J. Dave, R.K. Singh, IL-8 Directly Enhanced Endothelial Cell Survival, Proliferation, and Matrix Metalloproteinases Production and Regulated Angiogenesis, The Journal of Immunology 170 (2003) 3369–3376.

[127] R. Scherliess, The MTT assay as tool to evaluate and compare excipient toxicity in vitro on respiratory epithelial cells, International Journal of Pharmaceutics 411 (2011) 98–105.

[128] A. Cilek, N. Celebi, F. Tirnaksiz, Lecithin-based microemulsion of a peptide for oral administration: preparation, characterization, and physical stability of the formulation, Drug Delivery 13 (2006) 19–24.

[129] P. Boonme, Applications of microemulsions in cosmetics, Journal of Cosmetic Dermatology 6 (2007) 223–228.

[130] P. Santos, A.C. Watkinson, J. Hadgraft, M.E. Lane, Application of microemulsions in dermal and transdermal drug delivery, Skin Pharmacology and Physiology 21 (2008) 246–259.

[131] S. Heuschkel, A. Goebel, R.H.H. Neubert, Microemulsions--modern colloidal carrier for dermal and transdermal drug delivery, Journal of Pharmaceutical Sciences 97 (2008) 603–631.

[132] W. Warisnoicharoen, A.B. Lansley, M.J. Lawrence, Nonionic oil-in-water microemulsions: The effect of oil type on phase behaviour, International Journal of Pharmaceutics 198 (2000) 7–27.

[133] A.C. Lam, R.S. Schechter, The theory of diffusion in microemulsion, Journal of Colloid and Interface Science 120 (1987) 56–63.

[134] M.R. Gasco, M. Gallarate, F. Pattarino, In vitro permeation of azelaic acid from viscosized microemulsions, International Journal of Pharmaceutics 69 (1991) 193–196.

[135] C. Goddeeris, F. Cuppo, H. Reynaers, W.G. Bouwman, G. van den Mooter, Light scattering measurements on microemulsions: estimation of droplet sizes, International Journal of Pharmaceutics 312 (2006) 187–195.

[136] T. Sottmann, C. Stubenrauch, Microemulsions: Background, New Concepts, Applications, Perspectives: Phase behaviour, interfacial tension and microstructure of microemulsions, Wiley (2009) 1–47.

[137] M.T. Gisslow, B.C. McBride, A rapid sensitive collagenase assay, Analytical Biochemistry 68 (1975) 70–78.

[138] S. Ohtake, Y. Kita, T. Arakawa, Interactions of formulation excipients with proteins in solution and in the dried state, Advanced Drug Delivery Reviews 63 (2011) 1053–1073.

[139] T.J. Kamerzell, R. Esfandiary, S.B. Joshi, C.R. Middaugh, D.B. Volkin, Protein-excipient interactions: Mechanisms and biophysical characterization applied to protein formulation development, Advanced Drug Delivery Reviews 63 (2011) 1118–1159.

[140] I.L. Shulgin, E. Ruckenstein, Preferential hydration and solubility of proteins in aqueous solutions of polyethylene glycol, Biophysical chemistry 120 (2006) 188–198.

[141] P. Nicholls, I. Fita, P.C. Loewen, Enzymology and structure of catalases, Advances in Inorganic Chemistry 51 (2000) 51–106.

[142] P. Nicholls, G.R. Schonbaum, I. Boyer, P.D. Lardy, H. Myrback, The enzymes, Academic Press 8 (1963) 147–225.

[143] T. Cserháti, M. Szögyi, Interaction of phospholipids with proteins and peptides. New advances 1990, International Journal of Biochemistry 24 (1992) 525–537.

[144] P.J. Caspers, In vivo skin characterization by confocal Raman microspectroscopy, University Rotterdam, 2003.

[145] E. Elmahjoubi, Y. Frum, G.M. Eccleston, S.C. Wilkinson, V.M. Meidan, Transepidermal water loss for probing full-thickness skin barrier function: correlation with tritiated water flux, sensitivity to punctures and diverse surfactant exposures, Toxicology in vitro 23 (2009) 1429–1435.

[146] F. Netzlaff, K.-H. Kostka, C.-M. Lehr, U.F. Schaefer, TEWL measurements as a routine method for evaluating the integrity of epidermis sheets in static Franz type diffusion cells in vitro. Limitations shown by transport data testing, European Journal of Pharmaceutics and Biopharmaceutics 63 (2006) 44–50.

[147] Dr. Helena Kandarova, Drug Delivery to Human Skin: In vitro skin models in pharmaceutical research and industry, 4th Galenus Workshop, Saarbrücken, 2015.

[148] F. Netzlaff, C.-M. Lehr, P.W. Wertz, U.F. Schaefer, The human epidermis models EpiSkin, SkinEthic and EpiDerm: An evaluation of morphology and their suitability for testing phototoxicity, irritancy, corrosivity, and substance transport, European Journal of Pharmaceutics and Biopharmaceutics 60 (2005) 167–178.

[149] J.H. Draize, G. Woodard, H.O. Calvery, Methods for the study of irritation and toxicity of substances applied topically to the skin and mucous membranes, Journal of Pharmacology and Experimental Therapeutics 82 (1944) 377–390.

[150] COLIPA, Cosmetic Ingredients: Guidlines for Percutaneous Absorption/Penetration, Brüssel, 1995.

[151] EU Cosmetics Directive, 76/768/EEC 7th Amendment (2003).

[152] European Medicines Agency, ICH guideline S2 (R1) on genotoxicity testing and data interpretation for pharmaceuticals intended for human use: ICH S2(R1), 2012.

[153] OECD, Test No. 439: In Vitro Skin Irritation - Reconstructed Human Epidermis Test Method (2004).

[154] OECD, Test No. 431: In Vitro Skin Corrosion: Human Skin Model Test (2004).

[155] M. Nakamura, T. Rikimaru, T. Yano, K.G. Moore, P.J. Pula, B.H. Schofield, A.M. Dannenberg, Full-Thickness Human Skin Explants for Testing the Toxicitiy of Topically Applied Chemicals, Journal of Investigative Dermatology 95 (1990) 325–332.

[156] T. Hunziker, C.U. Brand, A. Kapp, E.R. Waelti, L.R. Braathen, Increased levels of inflammatory cytokines in human skin lymph derived from sodium lauryl sulphate-induced contact dermatitis, British Journal of Dermatology 127 (1992) 254–257.

[157] C.A. Dinarello, Interleukin-1, interleukin-1 receptors and interleukin-1 receptor antagonist, International Reviews of Immunology 16 (1998) 457–499.

[158] J. Weyermann, D. Lochmann, A. Zimmer, A practical note on the use of cytotoxicity assays, International Journal of Pharmaceutics 288 (2005) 369–376.

[159] P.V. Iyer, L. Ananthanarayan, Enzyme stability and stabilization—Aqueous and non-aqueous environment, Process Biochemistry 43 (2008) 1019–1032.

[160] J. Arya, M.R. Prausnitz, Microneedle patches for vaccination in developing countries, Journal of Controlled Release 240 (2016) 135–141.

[161] A.K. Shakya, H.S. Gill, A comparative study of microneedle-based cutaneous immunization with other conventional routes to assess feasibility of microneedles for allergy immunotherapy, Vaccine 33 (2015) 4060–4064.

8 APPENDIX

8.1 Buffers

8.1.1 50 mM Phosphate Buffered Saline pH 7.0

Ingredients

K_2HPO_4 x $3H_2O$ (Sigma Aldrich Chemie GmbH, Steinheim, Germany)	11.42 g/L

8.1.2 50 mM Phosphate Buffered Saline pH 7.0; Modified

Ingredients

K_2HPO_4 x $3H_2O$ (Sigma Aldrich Chemie GmbH, Steinheim, Germany)	11.42 g/L
L-arginine hydrochloride (Sigma Aldrich Chemie GmbH, Steinheim, Germany)	42.13 g/L

8.1.3 Tissue Lysis Buffer

Ingredients

$MgCl_2$ (Sigma Aldrich, Saint Louis, US)	15 mmol/L
HEPES (dry powder)	50 mmol/L
NaCl (Sigma Aldrich, Saint Louis, US)	150 mmol/L
Urea (Sigma Aldrich, Saint Louis, US)	8 mol/L
Triton X-100 (Merck KGaA, Darmstadt, Germany)	0.1 % (m/m)

Add one SigmaFast Inhibitor Cocktail Tablet (Sigma Aldrich, Saint Louis, US) to 20 mL lysis buffer.
500 µL of the final mixture is able to inhibit 0.5 g tissue (calculated with manufacturer`s protocol).

8.2 Size Exclusion Chromatography-Method

Stationary Phase:	PSS PROTEEMA analytical 300 Å, 5 µm
Mobile Phase:	50 mM phosphate buffered saline pH 7.0; modified add 0.05 % (m/m) NaN_3 pH adjusted with 1 M HCl
Flow Rate:	0.7 mL/min
Injection Volume:	50 µL
Detection Wavelength:	280 nm
Detection Sensitivity:	0.02

8.3 Dynamic Light Scattering-Stability Analysis

	0 h		24 h	
	z-average	**PDI**	**z-average**	**PDI**
Lip80-ME	1.20	0.29	1.15	0.26
PEG-ME	1.40	0.50	1.43	0.50

DANKSAGUNG

Mit Fertigstellung und Abgabe dieser Arbeit endet eine wunderschöne und unvergessliche Zeit in Kiel und insbesondere auch am Pharmazeutischen Institut. Diese Zeit wurde geprägt durch viele wunderbare Menschen, den ich gern aus tiefstem Herzen danken möchte.

Zunächst gilt mein besonderer Dank meinem Doktorvater, Herrn Prof. Dr. Steckel, der es bereits verstand mich als „Hiwi“ für die Pharmazeutische Technologie zu begeistern und mich bis hin zur Promotion unterstützt und gefördert hat.

Das Verfassen und Stellen eines Forschungsantrages zur finanziellen Unterstützung dieser Arbeit war ein großer und wichtiger Schritt. Dabei möchte ich mich besonders bei Frau PD Dr. Scherließ für die Übernahme der Projektleitung und für die wissenschaftliche Unterstützung bedanken. Ein besonderer Dank gilt dabei auch dem Phospholipid Research Center und Herrn Dr. van Hoogevest, die diese Unterstützung gewährten.

Einen großen Teil meiner praktischen Arbeit fertigte ich in der Dermatologie in Kiel unter der Betreuung von Prof. Dr. Proksch an. Ich danke Ihnen und Ihren Mitarbeitern für die sowohl praktische als auch theoretische Unterstützung und die stets herzliche Atmosphäre. Das Arbeiten in Ihrem Arbeitskreis bereitete mir besonders Freude durch die Zusammenarbeit mit Frau Neumann, die durch ihre positive und interessierte Art mich stets motivierte und mir das histologische Schneiden sowie Färben mit einer stoischen Geduld beibrachte - einen besonderen Dank dafür!

Des Weiteren möchte ich Herrn Fischer von Dermastamp® GmbH und Herrn Dr. Quadflieg von Gattefossè für die freundliche Unterstützung und Förderung durch das zur Verfügung stellen von Materialien und Hilfsstoffen danken.

Liebe TA´s (Regina K., Hanna, Rüdiger, Simone, Anna und Maren) ihr seid das Herzstück dieser Abteilung und habt mir, wann immer es euch möglich war, tatkräftig zur Seite gestanden. Gerade in Fragen zu nasschemischen Nachweisen oder analytischen Problemen (z.B. HPLC-Validierungen) konnte man von dir, liebe Maren, sehr viel lernen und immer auf deine Unterstützung zählen. Ich werde auch gern an unseren gemeinsamen Ausflug mit dem Tandem zurückdenken. Ein besonderer

Dank geht an Regina K. und Hanna die mich besonders bei der Auswertung der Verträglichkeitsstudien unterstützt haben. Liebe Hanna wie viele ELISA´s und damit Proben wir am Ende angefertigt und untersucht haben, weiß ich leider nicht, aber was ich weiß ist, dass es ohne dich nicht so viel Spaß gemacht hätte – wie war es doch schön mit dir in der Zellkultur und dieser großartige blaue Stuhl!

Wie schön waren doch die gemeinsamen und vielseitigen Erlebnisse und Gespräche mit dir, lieber Rüdi. Von Kunst bis Schweinebauch, es gab keine Tabuthemen und nichts in dem du mich nicht unterstützt hättest.

Nicht nur im Praktikum oder „beim Forschen“ waren wir füreinander da, sondern auch privat haben wir so einiges zusammen erlebt. Liebe Ann-Kathrin, Eric, Annika, Fritzi, und Judith ich danke euch für diese schöne Zeit. Besondere Ausdauer im Korrekturlesen dieser Arbeit haben Ann-Kathrin und Judith gezeigt, wobei der ab und zu in Anspruch genommene Korrekturblick von Annika ebenso beeindruckend und hilfreich war – herzlichsten Dank dafür. Ein großer Dank gilt natürlich auch allen anderen Alt- und Neukollegen ich bedanke mich bei euch für den Spaß den wir gemeinsam hatten und dass durchweg positive Arbeitsumfeld.

Bedanken möchte ich mich auch bei Detlef, Volkmar, Dirk und Kalle. Ich konnte mich während meiner gesamten Promotionszeit auf eure schnelle Hilfe in technischen und manchmal auch weniger technischen Fragen verlassen. Liebe Denissa auch dir gilt mein besonderer Dank für deine Geduld und Unterstützung in so manchem lückenhaft ausgefülltem Antrag, du hast immer den Durchblick behalten.

Schließlich möchte ich mich von ganzem Herzen bei meinem Mann für seine stetige und unermüdliche Geduld bedanken. In jeder Situation hast du einen kühlen Kopf bewahrt und für jedes „Problem“ hattest du eine Lösung parat.

Meiner Familie möchte ich für ihr Verständnis und den Rückhalt danken. Insbesondere meinen Großeltern Edith und Albin gilt mein herzlichster Dank für ihre unerlässliche Unterstützung – ihr seid meine großen Vorbilder!